

88 p.

Three-Dimensional Turbulent Boundary Layer Flow over a Spinning Cylinder

David M. Driver and Sheshagiri K. Hebbar

(NASA-TM-102240) THREE-DIMENSIONAL
TURBULENT BOUNDARY LAYER FLOW OVER
A SPINNING CYLINDER (Diskette
Supplement) (NASA) 88 p

N93-24533

Unclas

G3/34 0159800

December 1991



National Aeronautics and
Space Administration

Three-Dimensional Turbulent Boundary Layer Flow over a Spinning Cylinder

David M. Driver
Ames Research Center, Moffett Field, California

Sheshagiri K. Hebbar
Naval Postgraduate School, Monterey, California

December 1991



National Aeronautics and
Space Administration

Ames Research Center
Moffett Field, California 94035-1000

SUMMARY

Two sets of experiments are reported for a three-dimensional turbulent boundary-layer flow over a spinning cylinder, with and without a pressure gradient, which was produced by a forward-facing-step obstruction. Additional measurements are reported for two-dimensional flow over the same cylinder (nonspinning), with and without a pressure gradient. The data are presented in tables. The cylinder, which is axially aligned with the flow, contains three sections: an upstream stationary section, a central spinning section (where the flow develops a lateral component), and a downstream stationary section (where the flow's lateral component decays). Measurements were acquired primarily on the downstream stationary section and include all 3 components of mean velocity, all 6 Reynolds stresses, and 10 triple-velocity-product correlations. Surface pressure and skin friction were also measured. The data indicate that Reynolds shear stress is not simply proportional to mean-flow strain rate and that significant anisotropies develop in eddy viscosities. Also, the streamwise pressure gradient is seen to alter streamwise velocity and Reynolds stress without significantly affecting transverse velocity and Reynolds stress. Calculations using a Reynolds-stress-equation model predict the mean flow reasonably well.

NOMENCLATURE

C_{f_x}	axial (streamwise) skin-friction coefficient, $\tau_{w_x}/\frac{1}{2}\rho_o U_o^2$
C_{f_z}	circumferential (transverse) skin-friction coefficient, $\tau_{w_z}/\frac{1}{2}\rho_o U_o^2$
C_p	pressure coefficient, $(P - P_o)/\frac{1}{2}\rho_o U_o^2$
H	step height, 2.54 cm
k	turbulent kinetic energy, $(\overline{u^2} + \overline{v^2} + \overline{w^2})/2$
l	mixing length, $\sqrt[4]{\overline{uv^2} + \overline{vw^2}}/\sqrt{(\partial U/\partial r)^2 + (\partial W/\partial r - W/r)^2}$
l_o	Prandtl mixing length
P	static pressure
Q	resultant velocity vector
R	radius of cylindrical model
Re_θ	momentum thickness Reynolds number, $U_o\theta/\nu$
r	radial distance from centerline of cylinder
U_o	upstream free-stream velocity (used in normalization of data), nominally 36.5 m/s
U, V, W	mean velocity components in x, y , and z directions, respectively
u_τ	friction velocity, $\sqrt{\tau_w/\rho}$
u, v, w	fluctuating velocity components in x, y , and z directions, respectively
$\overline{u^2}, \overline{v^2}, \overline{w^2}$	mean-square velocity fluctuations in x, y , and z directions, respectively
$\overline{uv}, \overline{vw}, \overline{uw}$	turbulent velocity fluctuation correlations
$\overline{u^3}, \overline{uv^2}, \overline{uw^2},$ $\overline{vu^2}, \overline{v^3}, \overline{vw^2},$ $\overline{wu^2}, \overline{wv^2}, \overline{w^3},$ \overline{uvw}	turbulent triple-velocity-product correlation
\overline{vk}	turbulent triple-velocity-product correlation, $(\overline{vu^2} + \overline{v^3} + \overline{vw^2})/2$

W_s	transverse (circumferential) velocity of the rotating cylinder's surface (spinning section), nominally 36.5 m/s
x_s	separation location
x, y, z	coordinate system representing axial, normal, and circumferential distances from the downstream end of spinning cylinder (see fig. 1)
y^+	nondimensional distance from the wall, yu_τ/ν
β	skew angle of horizontal velocity vector relative to free stream
δ	local boundary-layer thickness
ε	dissipation rate of kinetic energy
ν	molecular kinematic viscosity of air, nominally 0.000015 m ² /s
ν_t	eddy viscosity
ρ	air density, nominally 1.2 kg/m ³
τ_w	total wall shear stress
τ_{wx}, τ_{wz}	axial (streamwise) and circumferential (transverse) wall shear stresses, respectively
ω	specific dissipation rate of turbulence kinetic energy, $\varepsilon/0.09k$

Subscripts

w	wall conditions
o	upstream free-stream conditions at $x = -12.7$ mm

INTRODUCTION

Successful aerodynamic simulations of flight vehicles require careful treatment of the turbulence that is generated along the vehicle surfaces because faulty simulation of the turbulence can produce inaccurate predictions of drag, stall characteristics, shock location, etc. Direct numerical simulations that solve for all small-scale motions of turbulence using the fundamental equations of motion require prohibitively large computational memories and times; therefore, turbulence models are used to simplify the computation while capturing the important flow physics necessary for engineering accuracy. Useful turbulence models are being developed to describe a wide range of two-dimensional flows. In contrast, relatively little work has been done on three-dimensional turbulence modeling (refs. 1 and 2). Expecting a turbulence model developed for two-dimensional flow to adequately describe three-dimensional flow may be unreasonable. Well-planned experiments using new instrumentation are needed to guide such an effort.

In practice, three-dimensional flows usually arise from transverse pressure gradients, such as those that occur on swept wings, on rotating turbines, or in curved ducts. Likewise, most experiments use a transverse pressure gradient to generate a crossflow, making it difficult to study viscous effects independently (refs. 2-6).

An innovative experiment devised to study a three-dimensional boundary layer that had no pressure gradient was done by Furuya, Nakamura, and Kawachi (ref. 7). They studied the growth of crossflow produced by a spinning cylinder aligned with a uniform flow. Bissonette and Mellor (ref. 8) and Lohmann (ref. 9) later reported turbulence measurements from similar experiments, suggesting that turbulent shear stresses may not be simply proportional to the mean-flow strain (via scalar eddy viscosity), as is often

assumed. Instead, eddy viscosity appeared to be anisotropic (i.e., $-\overline{uv}/(\partial U/\partial y) \neq -\overline{vw}/(\partial W/\partial r - W/r)$). In a further experimental and computational study, Higuchi and Rubesin studied the decay of crossflow on a stationary section of cylinder immediately downstream of a spinning section (refs. 10 and 11). In their computational study, Higuchi and Rubesin showed that models that accounted for anisotropy of eddy viscosity predicted crossflow better than those that used scalar eddy viscosity (refs. 10 and 11). However, sizable discrepancies remained between the measurements and the calculations; these discrepancies were thought to be caused by the pressure rate-of-strain model. Higuchi and Rubesin were able to make direct measurements of skin friction in an effort to find a law of the wall in three-dimensional flow. Mean flow-field measurements were reported, but no turbulence measurements were obtained. A review of spinning-cylinder flows is given by Nakamura and Yamashita (ref. 12).

The current report presents tabulated data for flow-field measurements in a relaxing, three-dimensional turbulent boundary layer and represents a continuation of the work presented by Higuchi and Rubesin in reference 10. The primary purpose of the current report is to present tables of data for the analysis that was reported in reference 13. A newly developed three-component laser Doppler velocimeter (LDV) was used to measure 3 components of mean velocity, all 6 Reynolds stresses, and 10 triple products. Values of eddy viscosity, turbulence production, convection, diffusion, dissipation (balance-of-kinetic-energy equation), and pressure strain (balance-of-stress equation) were extracted from the data and reported in reference 13. Various turbulence models for eddy viscosity, stress diffusion, pressure rate-of-strain, and anisotropy of Reynolds stresses were tested using the data and were also reported in reference 13. In the current report, calculations using a Reynolds-stress-equation model are compared with the data.

In a second set of experiments the effects of an adverse pressure gradient, produced by a forward-facing-step obstruction, were studied. The results are discussed in the second half of the current report. Combinations of extra rates of strain do not always result in a linear combination of effects from the individual strains. The spinning case with the forward-facing step contains a combination of extra rates of strain caused by pressure gradient ($\partial U/\partial x$), transverse shear ($\partial W/\partial y$), and curvature (W/r), making the flow more challenging for turbulence models. This flow is similar to the flow studied by Furuya, Nakamura, Yamashita, and Ishii, who imposed a mild adverse pressure gradient on their spinning-cylinder flow (ref. 14). Also, the spinning step flow case resembles the swept forward-facing-step flow studied by Johnston, in which the Reynolds stresses were found to develop slowly compared to the mean-flow strain-rate field (ref. 15). In the second half of the current report, measurements for the spinning case with a forward-facing-step obstruction are presented along with tables of data. A detailed analysis of this data is presented in reference 16.

EXPERIMENT

The first set of experiments was conducted in a 31- by 31-cm low-speed wind tunnel with a 14.0-cm-diameter cylinder running the length of the tunnel along the tunnel centerline (fig. 1(a)). The x -direction was aligned with the cylinder's axis and the y -direction was normal to the cylinder's surface. The tunnel walls were deflected slightly to compensate for boundary-layer growth and to produce a zero pressure gradient. The cylinder was divided into three sections. One section (91.4 cm long) rotated, producing a lateral flow in the boundary layer. One section upstream of this spinning section and one downstream remained stationary; data were taken on the downstream stationary section. The gap

between the spinning and downstream stationary sections was closed to within 0.0254 cm, and the two sections were equal in diameter (14 cm) to within ± 0.02 cm (the spinning section was smaller in radius than the stationary section, by 0.01 cm ($y^+ = 10$)). The abrupt change in boundary conditions from the spinning section to the downstream stationary section produced a significant mean-flow strain on the turbulence field—it was the turbulence’s response to this sudden application of strain that these experiments were designed to study. A three-component LDV (described in app. A) was used to measure mean and fluctuating velocities.

A second set of experiments was conducted on a stationary section of cylinder with a forward-facing-step obstruction (a circular sleeve with step height $H = 2.54$ cm) mounted on it (fig. 1(b)). This was done to study the effects of an adverse pressure gradient on the boundary layer. The step experiment contained a combination of extra rates of strain caused by pressure gradient ($\partial U/\partial x$), transverse shear ($\partial W/\partial y$), and curvature (W/r), making the flow challenging for turbulence models. (Curvature effects are described in detail in app. B.) The forward-facing step was located $6.06H$ downstream of the junction between the spinning and stationary sections so as to locate the steep pressure rise on the stationary section just downstream of the cylinder’s junction. Locating the step at $x/H = 6.06$ left the flow at the end of spin relatively uncontaminated by a pressure gradient, while the pressure gradient grew immediately downstream (a region where transverse flow was rapidly evolving). Measurements were performed primarily on the stationary sections where the boundary layer was relaxing from the sudden change in boundary conditions (cessation of spin); the combined effects of pressure gradient and transverse strain were studied.

Four experimental test cases were studied:

1. Zero $\partial P/\partial x$ with cylinder spinning ($W_s = U_o = 36.5$ m/sec), referred to as 3-D flat-plate flow
2. Zero $\partial P/\partial x$ with cylinder stationary ($W_s = 0$ and $U_o = 36.5$ m/sec), referred to as 2-D flat-plate flow
3. Step with cylinder spinning ($W_s = U_o = 36.5$ m/sec), referred to as 3-D step flow
4. Step with cylinder stationary ($W_s = 0$ and $U_o = 36.5$ m/sec), referred to as 2-D step flow

Test conditions were based on an upstream reference velocity (U_o) of 36.5 m/sec and on atmospheric pressure and temperature. The boundary-layer thickness (δ_o) near the end of the spinning section was 2.8 cm, with a momentum-thickness Reynolds number (Re_θ) of 6900. For the nonspinning cases, $\delta_o = 1.8$ cm and $Re_\theta = 4500$.

Measurement Uncertainties

Surface-flow measurements were reported in a previous study by Hebbar and Driver (ref. 17). The coefficient of pressure (reproduced in table C1 of app. C for completeness) is believed to be accurate to ± 0.005 . The coefficient of surface-skin friction was measured with a fence gauge (ref. 10) whose uncertainties were $\pm 10\%$.

Flow-field measurements were made using a three-component LDV to obtain the three mean-flow components and all six Reynolds stresses (see app. A for details). The flow-field measurements were complimented with a conventional two-component LDV in flow locations near the step where access by the three-component system was not possible. Uncertainties in U , V , and W were estimated to be $\pm 2\%$. Uncertainties in $\overline{u^2}$, $\overline{v^2}$, and $\overline{w^2}$ were estimated to be $\pm 8\%$, $\pm 8\%$, and $\pm 15\%$, respectively, while uncertainties in \overline{uv} , \overline{vw} , and \overline{uw} were estimated to fall in the range of -10 to $+25\%$. The weighted uncertainty reflects the belief that shear stresses measured by the three-component LDV are systematically low in the inner portion of the boundary layer, because of multiple seed particles in the measurement volume (see app. A for a discussion). The uncertainties quoted here include the amount by which the stresses are believed to be low. Triple-velocity-product correlations (e.g., \overline{uvk}) are also expected to be measured low by 10 to 20%, and uncertainties that include this bias are estimated to be -20 to $+30\%$. The two-component LDV does not suffer from this complication and uncertainties in \overline{uv} are $\pm 10\%$.

Reynolds-averaged statistics were computed with and without a velocity-bias correction. To correct for possible velocity biases, a weight function $F_{w_i} = \frac{\frac{1}{n} \sum_{j=1}^n \sqrt{U_j^2 + V_j^2 + W_j^2 + \epsilon_Q}}{\sqrt{U_i^2 + V_i^2 + W_i^2 + \epsilon_Q}}$ was multiplied by the quantity of interest before averaging (i.e., $\overline{T} = \frac{1}{n} \sum_{i=1}^n T_i F_{w_i}$). An upper bound on the weight is provided by the term ϵ_Q in the weight function, where $\epsilon_Q = 0.0001 U_o^2$. Differences between the "uncorrected" data ($F_{w_i} = 1$) and the "corrected" data are minimal except in the vicinity of zero mean flow. Consequently, "uncorrected" data were used in the results and discussion section of this report and are reported in the data tables in appendix C. However, both "corrected" and "uncorrected" data are reported and stored on the floppy disk attached to the inside back cover of this report, so that when future research on velocity bias is available an informed decision can be made as to which of the data sets to use.

Flow-Field Quality

The momentum integral equations were balanced to check the overall quality of the flow field and the self-consistency of the measurements. The momentum integral equations for zero pressure gradient and axial symmetry reduce to

$$\frac{C_{f_x}}{2} = \tau_{wx} / \rho_o U_o^2 = d\theta_{xx} / dx$$

and

$$\frac{C_{f_z}}{2} = \tau_{wz} / \rho_o U_o^2 = -d\theta_{xz} / dx$$

where

$$\theta_{xx} = \int_0^\delta (U/U_o)(1 - U/U_o)(1 + y/R) dy$$

and

$$\theta_{xz} = \int_0^\delta (U/U_o)(W/W_s)(1 + y/R)^2 dy$$

Integrating these equations in x removes the need to differentiate the momentum thickness. Figure 2 shows the measured distribution of momentum thickness (based on skin friction) for the axial and

transverse directions of the zero pressure gradient case. The agreement of $\pm 7\%$ between measured and inferred distributions of momentum thickness indicates the high level of self-consistency of the data and the good axisymmetry of the flow. For the case with the step, simple integral momentum balances were not possible because variations in static pressure in the normal direction were not measured.

COMPUTATIONS

Calculations were performed using a boundary-layer solver that assumed a uniform pressure distribution in the y -direction (ref. 18). The pressure distribution was prescribed in the calculations using the surface static-pressure distribution measured in the experiment. The assumption that pressure is uniform in the y -direction is not a good one for the step flow but is tolerable in the inner layer of the boundary layer. This assumption was necessary because of the lack of a Navier-Stokes equation solver.

The calculations employed a Launder, Reece, and Rodi (LRR) Reynolds-stress-equation (RSE) turbulence model (ref. 19) with the Wilcox and Rubesin ω^2 length-scale equation ($\omega = \varepsilon/0.09k$) (ref. 20). In addition, computations were performed with a $k - \omega^2$ model and a Prandtl mixing-length model, although these results will not be shown.

The computations started at $0.1\delta_o$ upstream of the junction, with experimentally measured values of mean velocities and all six Reynolds stresses; a starting procedure developed by Rubesin et al. was used (Rubesin, M. W.; Higuchi, H.; Olsen, M. E.; and Viegas, J. R.: A Reexamination of the Behavior of a Transversely Shear-Strained Turbulent Boundary Layer, to be published). Starting the calculations with experimental data ensured that downstream differences between the calculations and experiment were caused by the model assumptions and not by the initial conditions.

RESULTS FOR ZERO PRESSURE GRADIENT

The flow field was surveyed with many profiles (13) so that mean and turbulence quantities could be differentiated in both the streamwise and normal directions. Although the data shown in the figures are only a fraction of those acquired, all of the data are reported in the data tables in appendix C. Derivatives were obtained by fitting piecewise least-square curves (quadratic and cubic) to the data. Uncertainties in differentiated quantities were determined by an n th order uncertainty analysis and are indicated by error bars on the figures.

The key to understanding this flow is realizing the existence of at least two distinctly different flow zones: (1) an interaction zone where the fluid responds to the new boundary condition (cessation of spin), and (2) an undisturbed, outer, boundary-layer zone where the flow continues in equilibrium. Figure 1(a) shows the approximate edge of the interaction zone as implied by the measurements.

Skin-Friction and Surface-Flow Angle

The skin-friction distribution, measured by the surface fence gauge, is shown in figure 3(a). The axial skin friction is about 6% lower than earlier measurements by Higuchi and Rubesin (ref. 10), probably because of a slightly thicker boundary layer in this study (the inlet was rebuilt between

studies). The transverse skin friction agrees very well with Higuchi and Rubesin's earlier measurements. As Higuchi and Rubesin noted, the transverse-wall shear stress decays exponentially, and the axial-wall shear stress decays slowly and similarly to that of a two-dimensional boundary layer. Calculations of skin friction with the RSE model (fig. 3(a)) agree well with the measured values, although the axial component appears overpredicted, probably because of modeling deficiencies.

The surface-flow-angle distribution, measured by the fence gauge and by surface oil-flow patterns, can be seen in figure 3(b). These measured angles compare very well with angles previously measured by Higuchi and Rubesin (ref. 10). Downstream, the flow near the surface changes direction rapidly from 90° (upstream) to nearly 0° (two-dimensional) downstream.

Flow Field

Mean and fluctuating flow-field measurements were made with the three-component LDV. A few profiles of time-averaged streamwise and crossflow components of velocity (U and W) are shown in figures 4(a) and 4(b), respectively. The symbol size represents a conservative estimate of the experimental uncertainty. A sketch of the model in figure 4 shows the x -location corresponding to each profile. In figure 4(b), strong crossflow velocities can be seen on the spinning cylinder upstream of the junction. Nearest the wall at $y^+ = 40$, the value of W is only 33% of its wall value, indicating that most of the turning is done below $y^+ = 40$. Downstream of the junction, the transverse component of velocity quickly decays near the wall, while away from the wall transverse velocity continues unaffected. The streamwise component of velocity for the most part continues unchanged except near the wall, where small accelerations can be seen (see fig. 4(a)). Calculations of the mean velocities compare well with the measured values, although the calculated W has its maximum slightly farther out in the flow than the W measured experimentally.

A polar velocity plot (W vs. U), shown in figure 5, reveals that the flow in the boundary layer at the end of the spinning section is nearly collateral, $W/W_s = 1 - U/U_e$. This is a desirable initial condition, indicating that the flow has reached equilibrium. Downstream of the spinning section, the velocities in the U - W plane develop the familiar triangular shape. The apex of the triangle decreases with distance downstream. Near the wall, on the slow-speed side of the triangle, the measured direction of the surface shear stress extrapolates nicely to the mean velocity measurements near the wall—this is a region of nearly constant flow angle. The outer part of the boundary layer (beyond the local maximum in W) remains undisturbed by the relaxation process.

Measurements and calculations of axial shear stress (\overline{uv}) are graphed in figure 6(a). The measured values compare reasonably well with the stress inferred from integrating the mean x -momentum equation (using C_{f_x} at the wall as a starting point). The nonzero stress found by the inferred method at the edge of the boundary layer can be attributed to the accumulation of differentiation uncertainties, and differences in the two profiles near the wall reflect inaccuracies in the measurement technique; these inaccuracies are discussed in appendix A. The axial component of shear stress shown in figure 6(a) develops similarly to that of a two-dimensional boundary layer, with one exception revealed by both profiles: a local minimum in shear stress appears in the inner portion of the boundary layer, indicating a region of flow acceleration. Calculations with the RSE model generally overpredict the shear, showing

a sharp maximum near the wall where the measured data have a minimum. This may explain why skin friction is overpredicted.

Transverse shear stress (\overline{vw}), graphed in figure 6(b), initially behaves like the axial shear stress (\overline{uw}); this is an expected characteristic of collateral flow. Yet downstream of the junction, the transverse shear reverses sign near the wall, responding to the direction reversal of the transverse skin friction. The interaction region ($\partial\overline{vw}/\partial y > 0$ for the inner boundary layer) grows with distance in x . Further downstream, this component of shear stress decays as the boundary layer relaxes back to a two-dimensional flow. Also shown are the stresses inferred from integrating the differential transverse momentum equation. The good agreement between the two profiles of shear stress demonstrates the high level of self-consistency of the data. Calculations using the RSE model (also shown) agree extremely well.

Profiles of kinetic energy $k = (\overline{u^2} + \overline{v^2} + \overline{w^2})/2$, shown in figure 7(a), exhibit a boundary-layer shape with high levels of kinetic energy near the wall where turbulence is predominantly produced. The kinetic energy decays to a lower level downstream of the junction, where energy is not produced by spin. In the outer part of the boundary layer, calculations using the RSE model compare very well with measurements, but closer to the wall computed kinetic energy decays to values lower than those observed experimentally.

Figure 7(b) shows measured values of the turbulent triple-velocity-product correlation $\overline{vk} = (\overline{vu^2} + \overline{v^3} + \overline{vw^2})/2$. This correlation is a measure of the turbulent diffusion of kinetic energy in the y -direction. A positive sign indicates that turbulent mixing is carrying kinetic energy away from the wall, and negative means transport toward the wall. Consistent with the gradient-diffusion turbulence-model assumption, \overline{vk} is largest where gradients of k are most severe. All 10 turbulent triple-velocity products were measured (although not shown), and their behavior is similar to that of the \overline{vk} triple-velocity product.

An estimate of terms in the transverse momentum equation is shown in figure 8 for a station at $x/\delta_o = 1.7$. The measured rate of change of transverse momentum, DW/Dt , nearly equals the forces produced by turbulent Reynolds stress, $(-1/r^2)[d(r^2\overline{vw})/dr]$. Other forces resulting from normal stresses and molecular viscosity are negligible and not shown here. The figure shows that crossflow momentum near the wall is lost because frictional forces resist the flow. Conversely, in the outer part of the boundary layer, the crossflow continues to accelerate as a result of residual shear-stress forces pulling the fluid in the direction of rotation. This balance demonstrates the high level of self-consistency and differentiability of the data and provides confidence for balancing other turbulent transport equations.

In the prediction of turbulent flow, the Reynolds stress is often assumed to be proportional to the mean-flow strain rate (the constant of proportionality is the eddy viscosity, ν_t) as follows:

$$\begin{aligned} -\overline{uw} &= \nu_{t_x} \partial U / \partial y \\ -\overline{vw} &= \nu_{t_z} (\partial W / \partial y - W / r) \end{aligned}$$

where ν_{t_x} and ν_{t_z} are determined by a turbulence model. Many models assume (prescribe) that eddy viscosity is a scalar that is independent of direction ($\nu_{t_z} = \nu_{t_x}$), thus simplifying computations. To check this assumption, components of eddy viscosity were determined from the data (using the relationships above) at locations $-5\delta_o$ upstream and $+3.3\delta_o$ downstream of the junction (see fig. 9). At the upstream station the two components of eddy viscosity are virtually equal to each other (isotropic condition). At

the downstream station the viscosities differ by a factor of three or four. This illustrates the nonisotropic nature of eddy viscosity and indicates the need for a full Reynolds-stress turbulence model. Also shown are two prominent models for scalar eddy viscosity. The Jones-Launder model ($\nu_{tx} = \nu_{tz} = 0.09k^2/\epsilon$, using experimentally determined values for k and ϵ) works well for modeling the ν_{tx} component of eddy viscosity (ref. 21), but the Cebeci model,

$$\nu_{tx} = \nu_{tz} = \begin{cases} 0.0168 \int_0^\delta (1 + y/R)[Q_e - Q(y)]dy/[1 + (y/\delta)^6] & \text{outer layer} \\ (0.4y)^2 \partial Q / \partial y & \text{inner layer} \end{cases}$$

rather severely underpredicts ν_{tx} (ref. 22). Neither is capable of simulating ν_{tx} . The Cebeci model does not include curvature correction terms. Including curvature correction terms is expected to improve the agreement at the upstream station (see app. B).

Additional analysis is performed on the data and is reported in reference 13, analysis that involves testing of various pressure-strain turbulence models and models for diffusion.

RESULTS FOR PRESSURE-GRADIENT FLOW

Additional measurements were made for the forward-facing-step geometry. Two forward-facing-step cases were studied, one of no spin (referred to as 2-D step flow) and another with spin rate $W_s = U_o$ (referred to as 3-D step flow). This section will describe the measurements, which are tabulated in appendix C. These measurements are analyzed in reference 16.

Streamlines and Pressure

Stream-function contours obtained from velocity measurements show the general features of the forward-facing-step flows (fig. 10). Flow divergence from the wall is seen as far forward as $5H$ ahead of the step. Boundary-layer detachment is seen at $0.7H$ ahead of the step in the 3-D case (fig. 10(a)) and $0.8H$ in the 2-D case (fig. 10(b)). Both cases indicate that reattachment occurs on the face of the step. One difference between the two cases is the size and shape of the separation bubble; a somewhat thinner bubble is seen in the 3-D case. This difference is thought to be due to differences in the upstream U -velocity distribution, rather than to differences in the turbulence. Stream-function contours appear smooth, even at the interface between 3-D and 2-D LDV measurement stations (at $x/H = 4.4$ and 4.5 , respectively) shown in figure 10(a), indicating good self-consistency of the data. Measurements at 14 streamwise stations were used to determine the stream-function contours for the 3-D step flow, and 10 stations were used for the 2-D step flow.

Surface pressure increases rapidly with proximity to the step (fig. 11). There are only slight differences between the 2-D and 3-D cases. Normal pressure gradients exist in this flow and pressure is not uniform through the boundary layer. At distances farther from the wall the pressure distribution will look different.

Surface skin-friction measurements are reported in reference 17 and are not shown here.

Flow Field

Velocity measurements of the 3-D (spinning) cases with and without a pressure gradient are shown in figure 12(a) for $x/H = 4.4$, which is $1.66H$ upstream of the step and $0.96H$ upstream of separation. The pressure gradient is clearly seen to retard the streamwise velocity, while the transverse velocity appears to be only negligibly affected by the streamwise pressure gradient.

Shear stresses appear to be unaffected by the pressure gradient at this location (fig. 12(b)). Furuya, Nakamura, Yamashita, and Ishii similarly found minimal changes in the transverse mean flow and the Reynolds stress, because of an increasing adverse pressure gradient on their spinning cylinder flow (ref. 14).

Perhaps the most striking feature is the local minimum in \overline{uv} shear stress seen 0.2δ from the wall. Two-component LDV measurements were performed farther downstream where three-component measurements were not possible (because of optical restraints), and this local minimum was seen to persist downstream. This local minimum in \overline{uv} shear stress is seen in the zero-pressure-gradient flow as well. Similarly, Bradshaw and Pontikos saw a global, rather than local, reduction of shear stress in their "infinite" swept wing flow—they associated this reduction with transverse strain effects (ref. 6). Some of the reduction seen here is due to transverse strain effects, but a large share of the reduction is due to the flow adjusting to a new wall boundary condition ($W_s = 0$) that carries with it a lower level of wall shear and a thus a lower level of turbulence production.

Calculations of the time-averaged velocity field for the pressure-gradient case, shown in figure 12(a), compare well with the measurements in the near-wall region. Away from the wall, lower velocities are predicted because of the solver's lack of a normal momentum equation and the erroneous assumption that the normal pressure gradient is zero. Comparisons between the measurements and the calculations should be limited to the inner portion of the boundary layer for this reason.

Calculations of the streamwise component of Reynolds shear stress, seen in figure 12(b), fail to predict the local minimum in shear stress seen in the experiment. This local minimum is not peculiar to the step-induced pressure gradient, but is a characteristic of the relaxation process. To the authors' knowledge, none of the current turbulence models can predict this phenomenon.

The corresponding 2-D step flow is shown in figure 13. The velocity distribution in the 2-D step flow (fig. 13(a)) for $x/H = 4.5$, which is $1.56H$ upstream of the step, shows a larger velocity deficit than that seen in the corresponding 3-D step flow. Differences between the 2-D and 3-D streamwise velocity profiles originate upstream in the zero-pressure-gradient region of the flow. Higher velocities near the wall in the 3-D case are a result of a destabilizing rotation that enhances mixing and momentum transfer between the wall and the free stream (see app. B). The 2-D step flow did not exhibit a local minimum in Reynolds shear stress (fig. 13(b)); instead, a local maximum is seen (typical of 2-D adverse-pressure-gradient flows such as that of Simpson, Chew, and Shivaprasad (ref. 23)).

The turbulent kinetic energy of 3-D flow, in which $\partial P/\partial x = 0$, is lower downstream of the spinning section than it is on the spinning section itself (fig. 14(a)), primarily because of a loss in the $\overline{w^2}$ whose production is associated with the $\partial W/\partial y$ gradients. However, a pressure gradient increases the kinetic energy above the zero-pressure-gradient level as a result of increased $\partial U/\partial y$ gradients. This

increase in $\partial U/\partial y$ is more pronounced in the step flow than in other adverse-pressure-gradient flows (ref. 23) as a result of an accelerating free stream combining with a decelerating near-wall flow. The turbulent kinetic energy measurements for the 2-D step flow are shown in figure 15(a).

Diffusion of turbulent kinetic energy and thickening of the boundary layer is associated with the triple-velocity-product correlations \overline{vk} shown in figures 14(b) and 15(b). Positive \overline{vk} is an indication of kinetic-energy diffusion away from the wall, and negative \overline{vk} indicates diffusion toward the wall. Triple-velocity-product \overline{vk} decays downstream in the 3-D case, again primarily because of decay in $\overline{w^2}$ and in associated $\overline{vw^2}$ once active on the spinning cylinder. The adverse pressure gradient only minimally effects \overline{vk} . For the 2-D case, the adverse pressure gradient produces a change in sign (from positive to negative) of \overline{vk} in the vicinity of the wall; this is consistent with gradient-diffusion-type modeling (see fig. 15(b)). The magnitude of \overline{vk} typically is assumed (modeled) to be proportional to the gradient of kinetic energy.

The step flow is overwhelmingly dominated by pressure forces, everywhere except very close to the wall, as can be seen in figure 16(a) (3-D flow) and 16(b) (2-D flow). The terms in the x -momentum equation,

$$DU/Dt = -\frac{1}{\rho}\partial P/\partial x - \frac{1}{r}\partial(r\overline{uv})/\partial r - \partial\overline{u^2}/\partial x$$

are shown in figure 16(a); they are computed from the data, with the exception of $(1/\rho)\partial P/\partial x$, which is inferred from the balance. The pressure gradient inferred from the balance of the momentum equation extrapolates nicely to the measured wall value of the streamwise pressure gradient, shown with an arrow in figures 16(a) and 16(b). Here, streamwise momentum loss in both the 3-D and 2-D step flows is almost exclusively a result of streamwise pressure gradient. Shear-stress gradients are not significant until within $0.03H$ of the wall ($y^+ < 40$).

Additional analysis is presented for the step data in reference 16. Balances of the kinetic energy equation and of the \overline{uv} and \overline{vw} shear-stress equations are presented along with comparisons of various turbulence models.

CONCLUSIONS

Two sets of experimental data were reported and tabulated for three-dimensional flow over a spinning cylinder: (1) flow with a zero pressure gradient and (2) flow with a pressure gradient induced by a forward-facing-step obstruction. Additional measurements were reported and tabulated for two-dimensional flow over the same cylinder (nonspinning), with and without a forward-facing-step obstruction.

New turbulence measurements using a three-component laser Doppler velocimeter (LDV) were obtained and reported in tables in appendix C. The experiments were performed in an effort to better understand and model the turbulent transport processes. While some deficiencies were noted in the LDV measurements, the level of accuracy was generally high.

An abrupt change in boundary conditions is encountered when flow passes from a spinning section of cylinder to a stationary section of cylinder. The perturbation (change in boundary condition) diffuses into the turbulent boundary layer with a secondary boundary-layer-type growth—that is, the perturbation is not instantly felt throughout the boundary layer. This perturbed region of the boundary layer produces fairly strong anisotropies in the eddy viscosities (Reynolds stresses). Full Reynolds-stress transport-equation models predict this anisotropy to some extent. In both the experiment and the full Reynolds-stress-model calculations, the Reynolds shear-stress response to the change in boundary condition lags the response of the mean flow field. Calculations using a Reynolds-stress-equation turbulence model generally agree well with the data.

Streamwise shear stress exhibits a local minimum in both the zero- and adverse-pressure-gradient flow, possibly caused in part by transverse strain effects like those seen in the “infinite” swept wing of Bradshaw and Pontikos (ref. 6). Calculations fail to predict this local minimum in shear stress.

A streamwise pressure gradient was seen to affect primarily the streamwise mean flow and the streamwise Reynolds stress. The streamwise flow was shown to be predominantly pressure driven, with viscous forces becoming important only very near the wall. The pressure rise was found to occur over such a short distance that turbulent stresses were barely able to respond before the flow separated. Crossflow and transverse shear stress seemed to be insensitive to a streamwise pressure gradient, at least for this case of sudden pressure gradient.

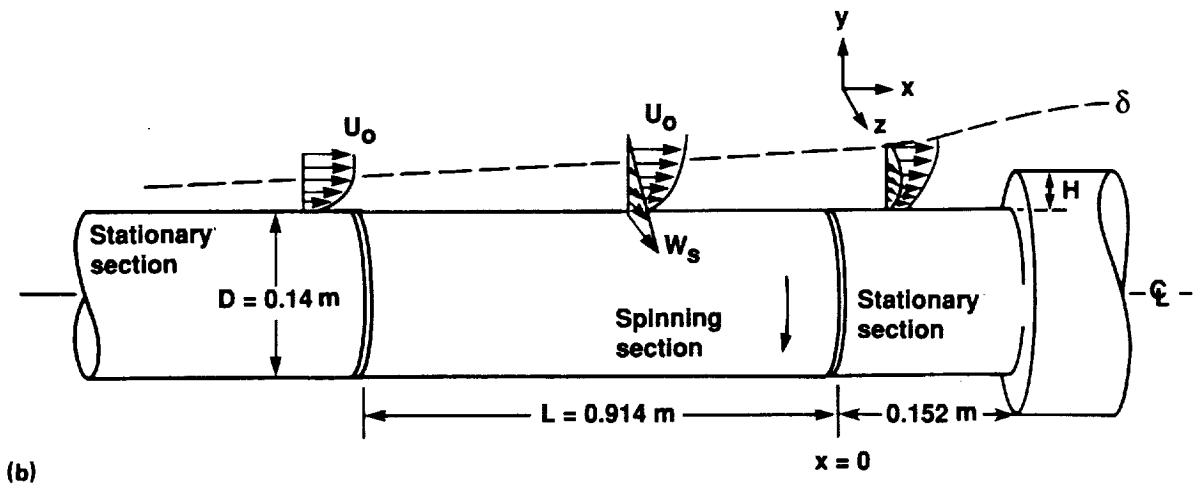
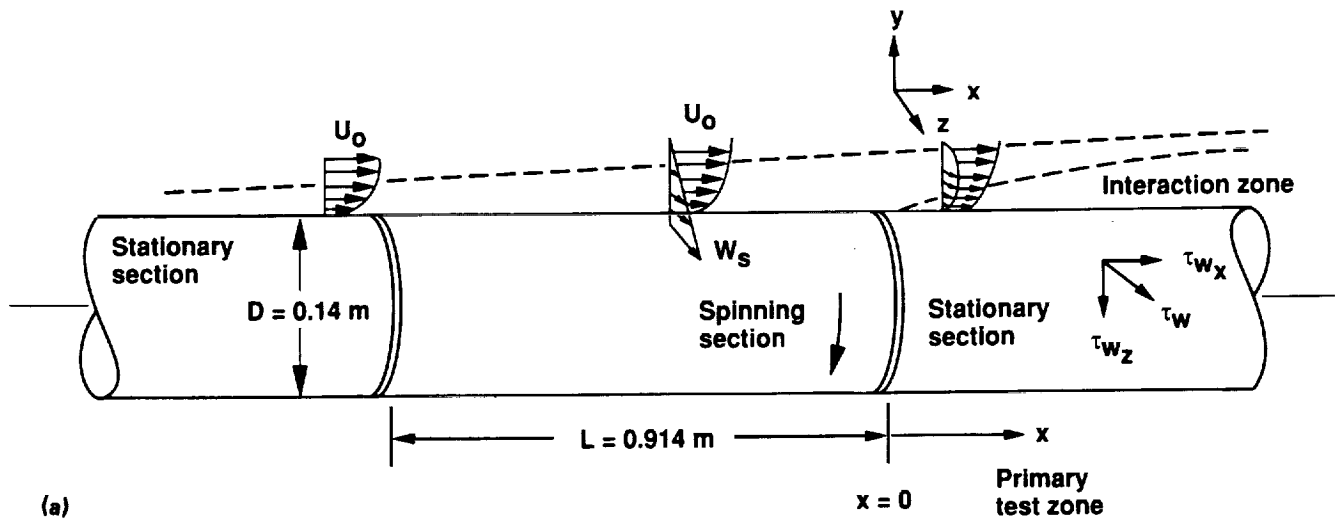


Figure 1. Test configuration and flow conditions for (a) $\partial P/\partial x = 0$ and (b) step-induced $\partial P/\partial x$; $U_o = W_s = 36.5$ m/sec, $\delta_o = 2.8$ cm ($x = 0$).

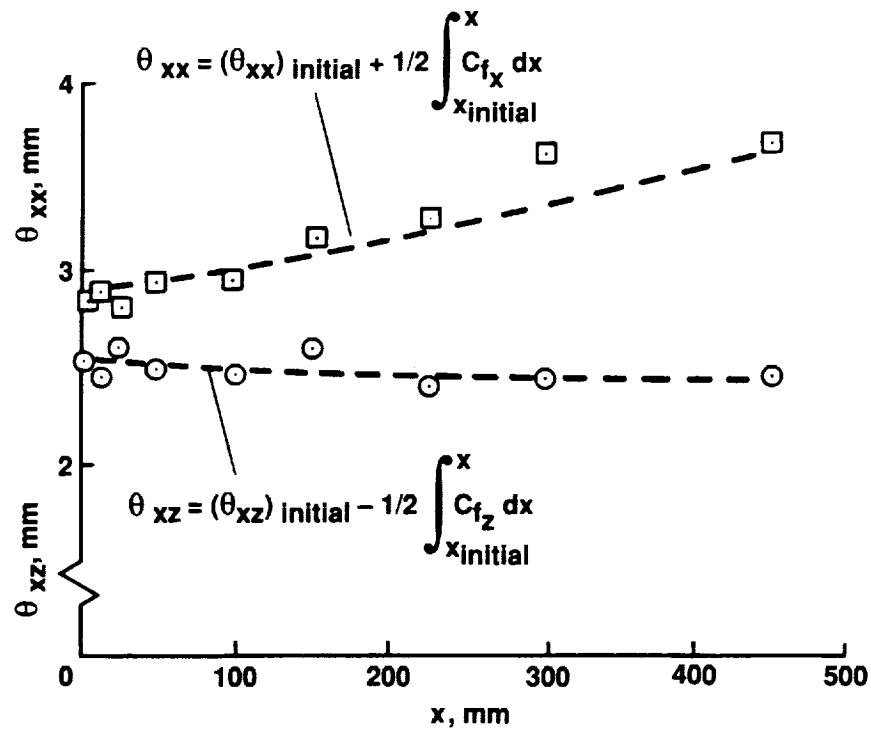


Figure 2. Integral momentum balance; $\partial P / \partial x = 0$.

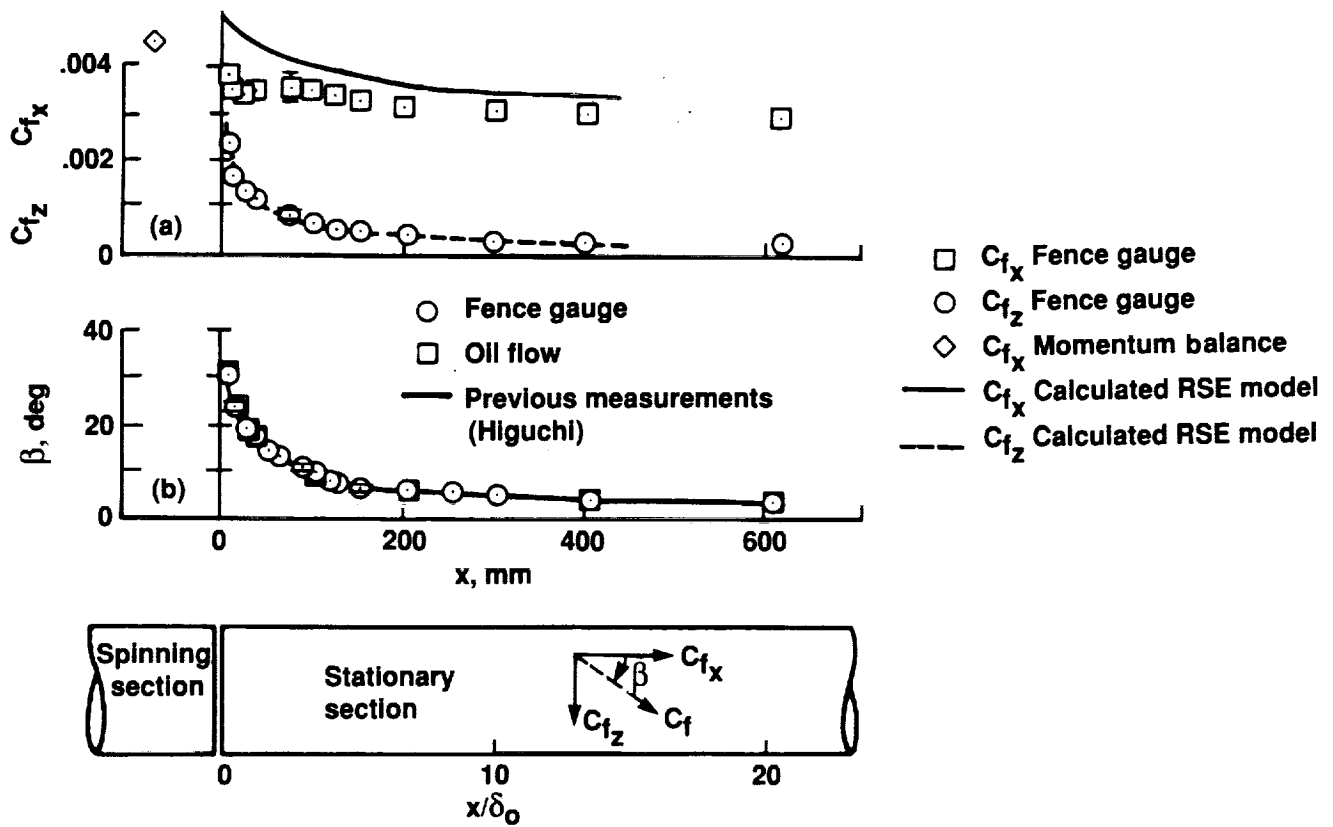


Figure 3. Distributions of (a) skin-friction and (b) surface-flow-angle; $\partial P / \partial x = 0$.

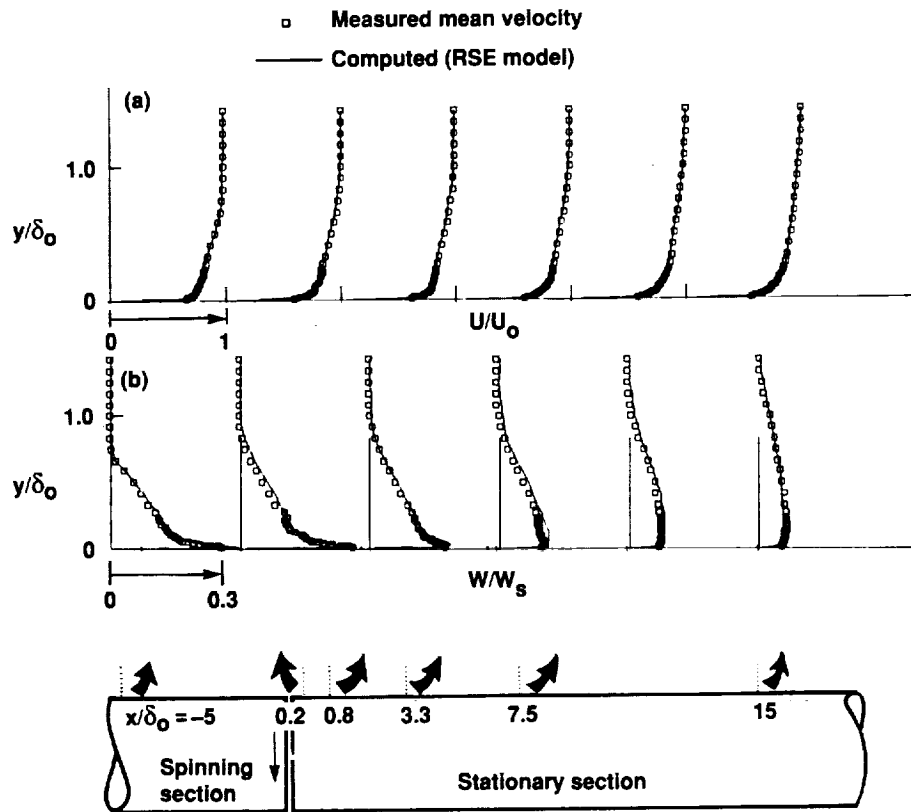


Figure 4. Mean-velocity measurements and calculations for (a) streamwise and (b) crossflow velocity components; $\partial P/\partial x = 0$.

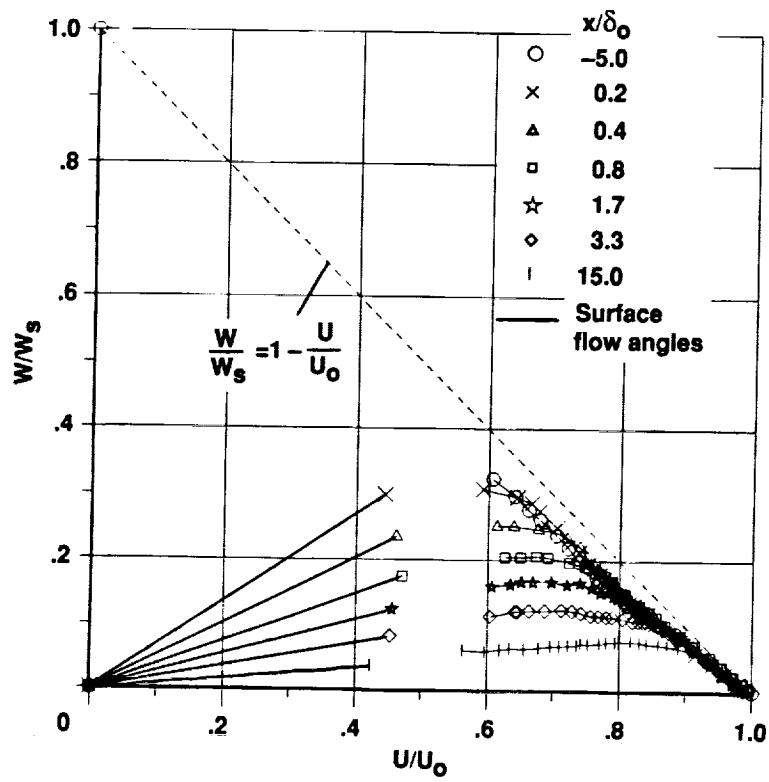


Figure 5. Polar velocity profile; $\partial P/\partial x = 0$.

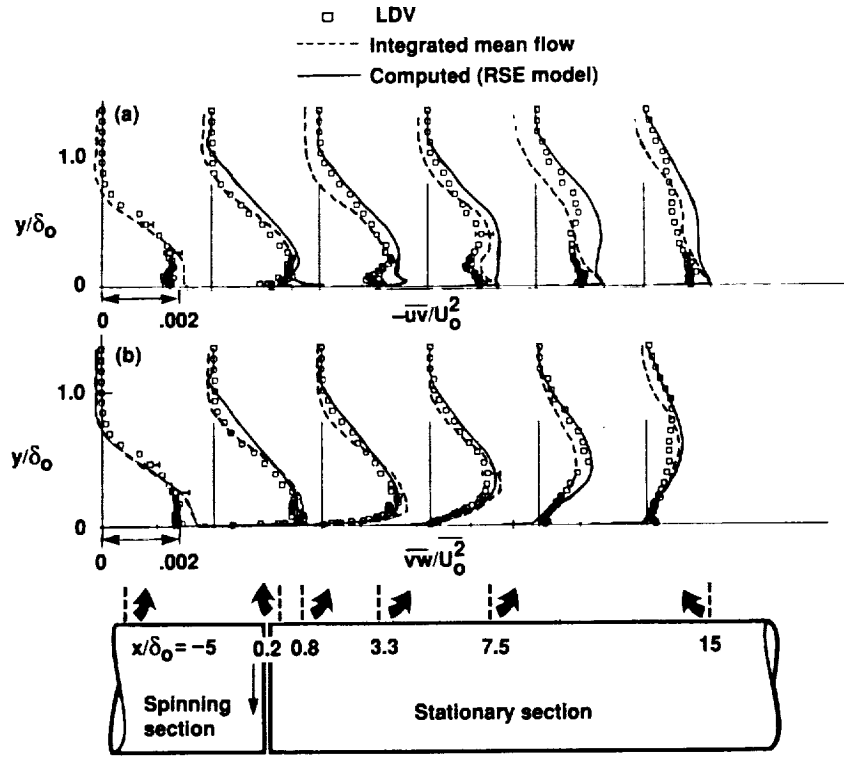


Figure 6. Reynolds shear-stress profiles, measured and calculated: (a) axial (\overline{uv}) and (b) transverse (\overline{vw}); $\partial P/\partial x = 0$.

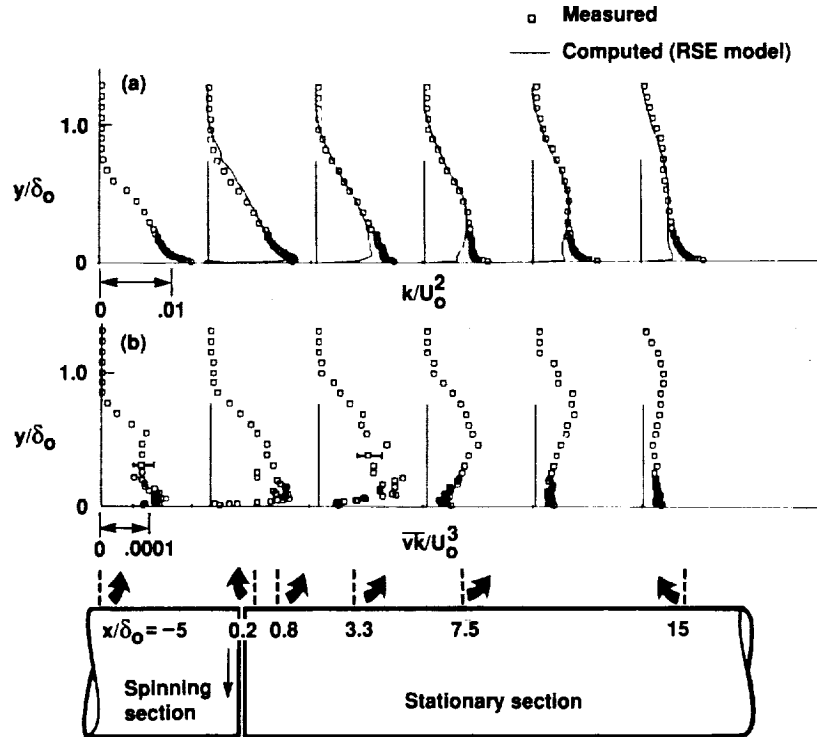


Figure 7. Profiles of (a) kinetic energy and (b) the \overline{vk} triple-velocity-product correlation; $\partial P/\partial x = 0$.

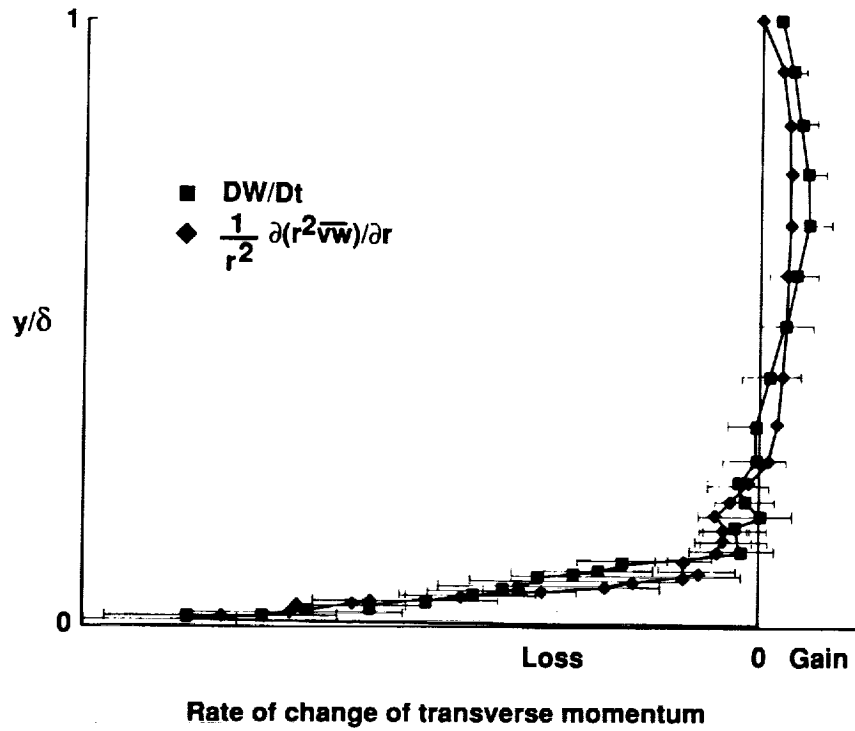


Figure 8. Terms in the transverse-momentum equation, $DW/Dt = (-1/r^2)[d(r^2 \overline{vw})/dr]$, at $x/\delta_o = 1.7$; $\partial P/\partial x = 0$.

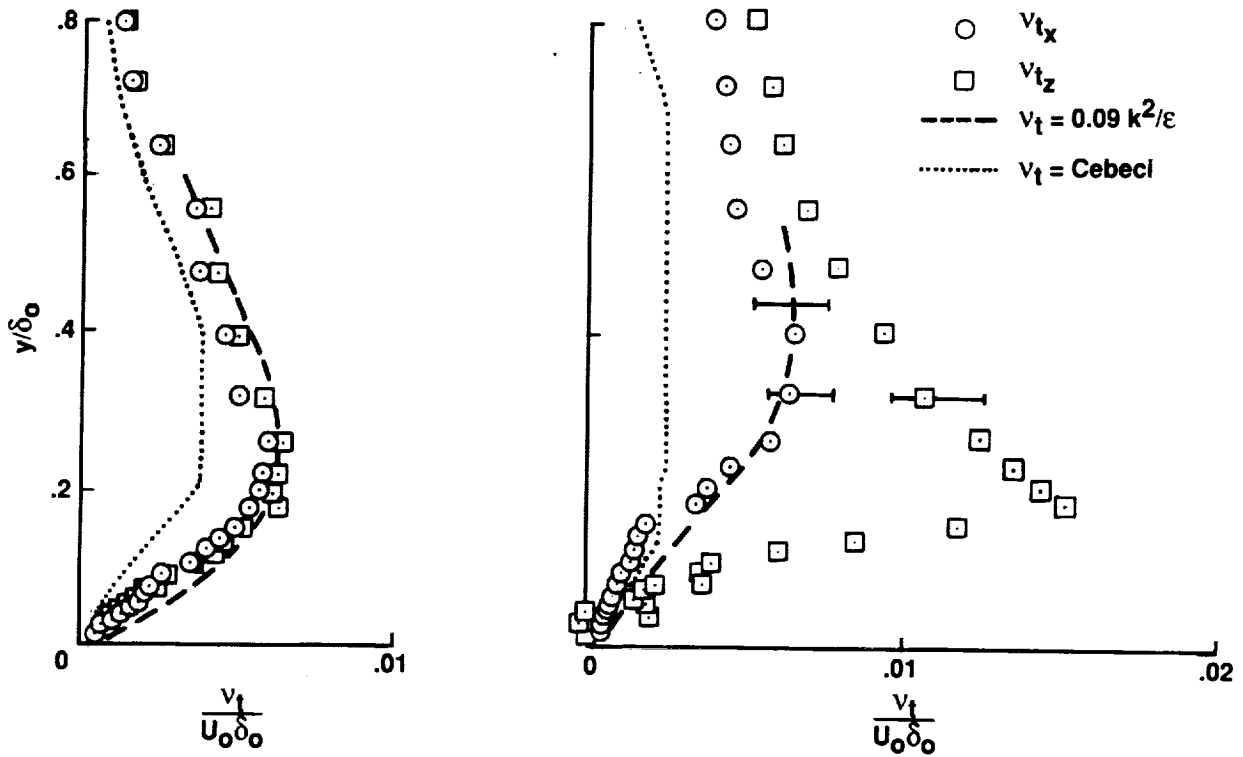


Figure 9. Turbulent eddy-viscosity components ν_{tx} and ν_{tz} ; $\partial P/\partial x = 0$. (a) $x/\delta_o = -5$. (b) $x/\delta_o = 3.3$.

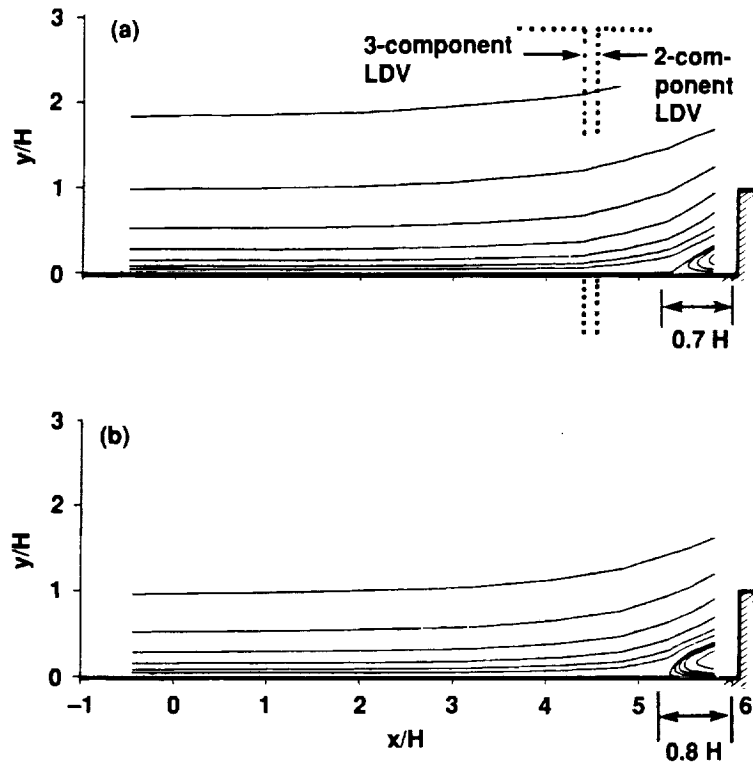


Figure 10. Stream-function contours for forward-facing-step flow. (a) Spinning case (3-D step flow). (b) Nonspinning case (2-D step flow).

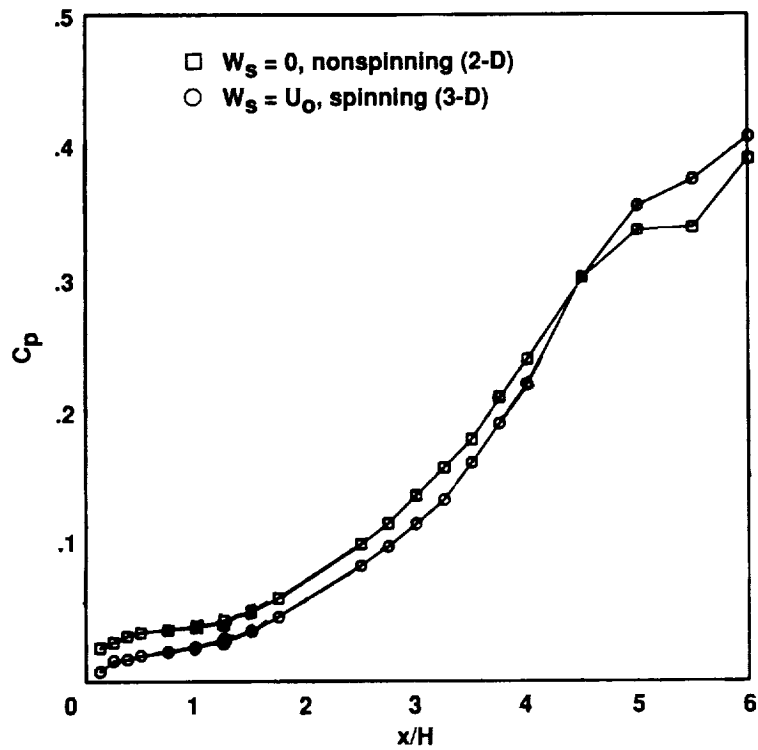


Figure 11. Pressure distribution for forward-facing-step flow, $H = 25.4$ mm.

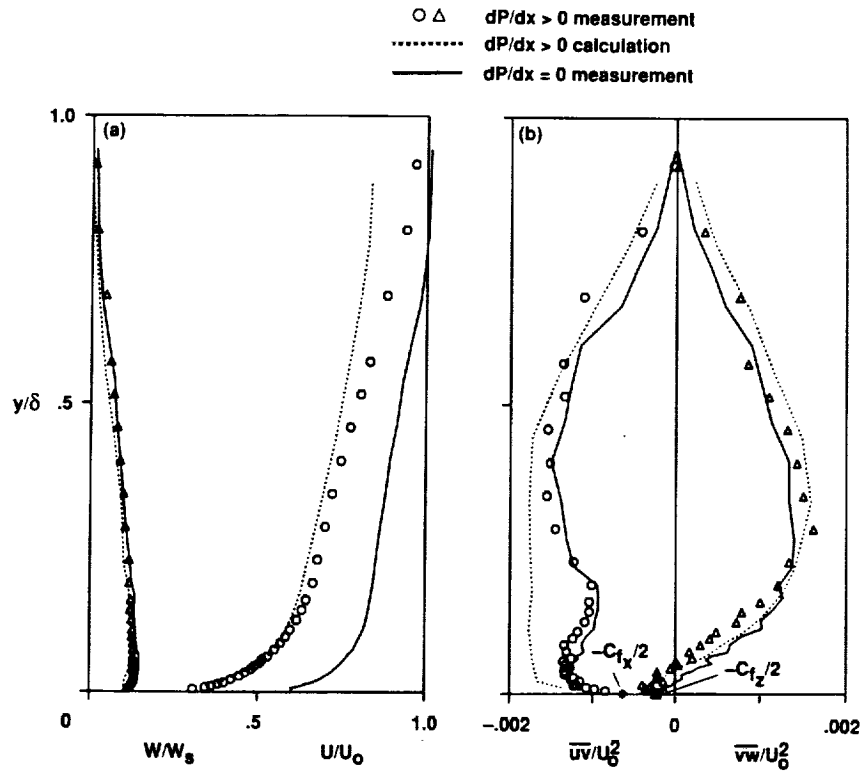


Figure 12. Three-dimensional forward-step (a) velocities and (b) stresses at $x/H = 4.4$.

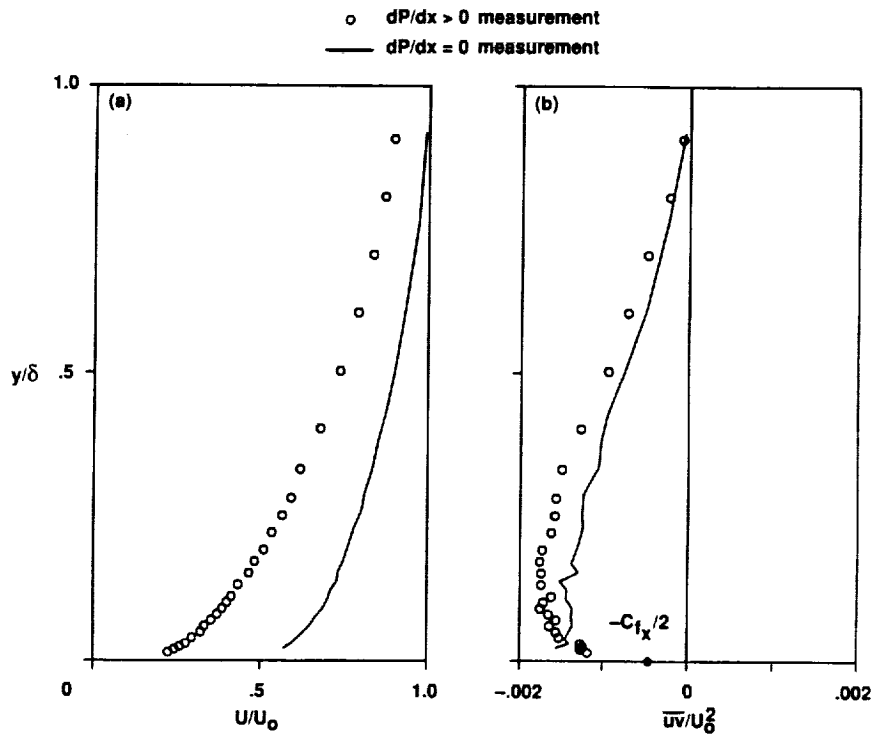


Figure 13. Two-dimensional forward-step (a) velocities and (b) stresses at $x/H = 4.5$.

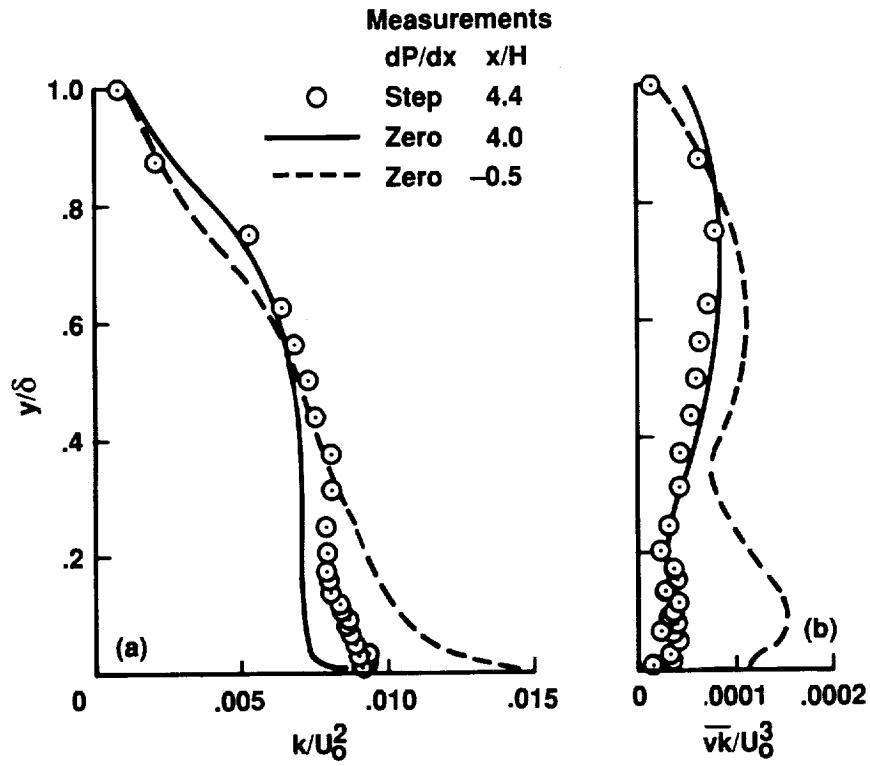


Figure 14. (a) Kinetic energy and (b) triple-velocity-product correlation measurements for 3-D flow.

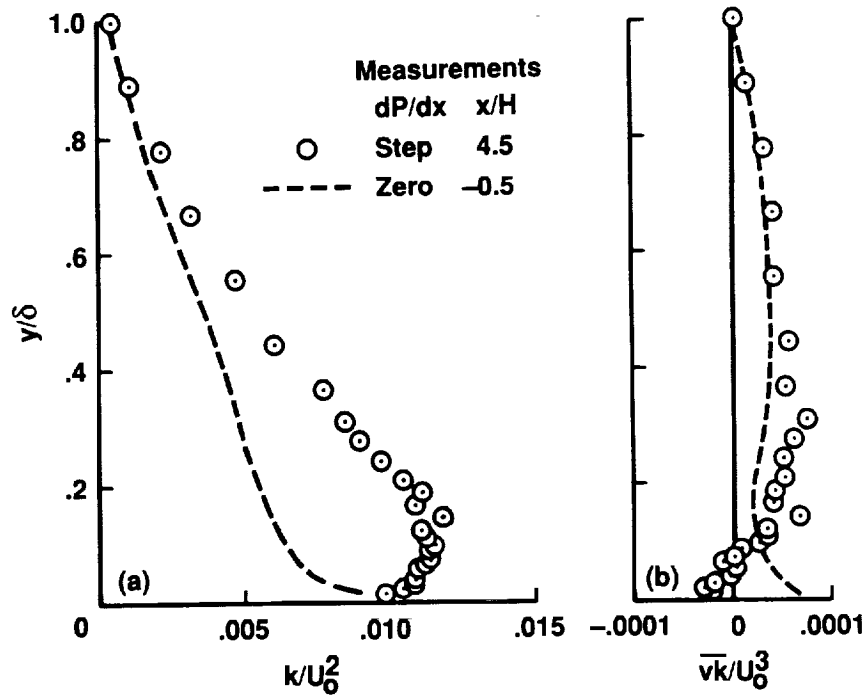


Figure 15. (a) Kinetic energy and (b) triple-velocity-product correlation measurements for 2-D flow.

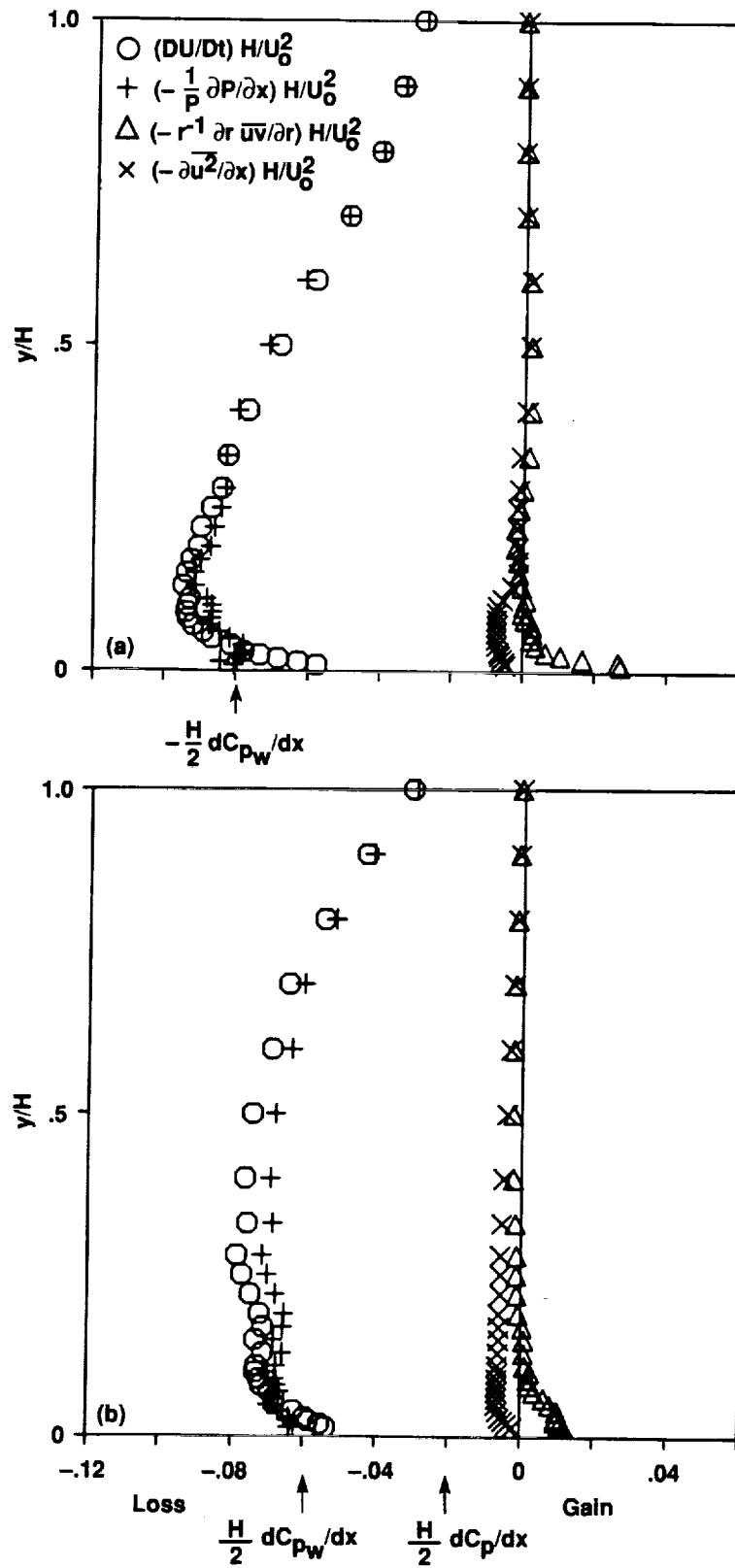


Figure 16. U -momentum equation balance: (a) 3-D step flow at $x/H = 4.4$, (b) 2-D step flow at $x/H = 4.5$.

APPENDIX A

This appendix is devoted to a discussion of the specific design and practical difficulties of conducting measurements with a three-component laser Doppler velocimeter (LDV) system. The discussion presented here is primarily intended for potential LDV users, although it is also useful for anyone trying to understand the inherent problems and uncertainties associated with three-component LDV measurements.

Several researchers have recently developed three-component LDV systems (refs. 24–27). These efforts have been primarily focused on obtaining mean velocities, without concern about turbulence measurements. Although attempts have been made to measure turbulence quantities, few results have actually been reported, and those that have been reported were for measurements done in complex flows for which there is little or no means of comparison. Recently Bell, Rodman, and Mehta compared their three-component LDV measurements directly with hot-wire measurements (ref. 28). The LDV and the hot-wire data compared within 10 to 20% on all measurements except \overline{uw} , which was different by 50%, and \overline{vw} , which was not measured with the hot-wire. The work presented here is concerned with the measurement of turbulence quantities and of uncertainties associated with these quantities.

LDV Configuration

The system (shown in fig. A1) used three differently colored beam pairs (forward scatter), nearly orthogonal, all intersecting at the same point in space. Simultaneous measurements of all three velocities were collected. Then each velocity triplet was transformed into Cartesian velocity components, and ensemble averages were calculated.

An argon ion laser generated a blue (488-nm) and a green (514.5-nm) set of beams comprising the $V - 0.0221U + 0.0043W$ (small dip angle) and the $0.883U - 0.470W$ (-28.05° direction) components of velocity, respectively. A second argon ion laser generated a violet (476.5-nm) pair of beams that measured a $0.872U + 0.489W$ ($+29.3^\circ$ direction) component of velocity. Fringe spacings were $9.090\ \mu\text{m}$, $8.711\ \mu\text{m}$, and $3.326\ \mu\text{m}$ for the green, blue, and violet beams, respectively. Bragg shifting (40 mHz) was applied to each of the three pairs of beams.

Electronic signal processing was performed with two TSI counters and one counter designed in-house (ARC-1). The resolutions of the TSI counters and the ARC-1 counter were $\pm 1.0\ \text{ns}$ and $\pm 0.8\ \text{ns}$, respectively. Sixteen fringes were counted. A logic circuit built at Ames was used to validate only velocity measurements received simultaneously ($\pm 5\ \mu\text{s}$). At each measuring station 10,000 velocity triplets were collected for use in ensemble averaging.

The flow was seeded with $0.5\text{-}\mu\text{m}$ -diameter latex particles. Seed particles were uniformly injected into the flow far upstream in the plenum chamber with density $\approx 1\ \text{particle}/\text{mm}^3$. This was somewhat sparse compared to the combined scattering-volume size of $0.2\ \text{mm}^3$ ($7\ \text{mm}$ long \times $0.2\ \text{mm}$ in diameter for blue-green and $1.5\ \text{mm} \times 0.1\ \text{mm}$ for violet).

Sources of error— The intersection of all three beam pairs at one point was critical not only for high data rates, but also for accurate measurements. When poor intersection occurred, as shown in

figure A2(a), measurements of cross correlations (\overline{uv} , \overline{vw} , \overline{uw}) went to zero. Also, misalignment (see fig. A2(b)) could cause a velocity bias in favor of particles with preferred trajectories, since simultaneity is required for the particle to traverse all three volumes.

One other potential source of error exists—multiple seeds in the measuring volume (see fig. A2(c)). Most of the time, one particle is in the scattering volume at a time, and occasionally it is at the intersection of all three volumes. Once in a while, though, one particle is in one volume while another particle is simultaneously in the other volume. These particles will be counted and validated, even though the velocity components are measured at different locations. This can cause errors in measuring fluctuating quantities if the scale of the turbulence is smaller than the distance between the particles. Evidence of this is seen in the \overline{uv} and \overline{vw} correlations; these correlations decrease with any increase in particle density. This problem is recognized by many researchers. The obvious cure seemed to be a reduction in the seed density, but even with excruciatingly sparse seed densities, stress values were still low by 10% (compared to measurements of \overline{uv} made with the two-dimensional LDV system). Another idea was to shrink the scattering volume by viewing it with apertured off-axis receiving optics. This might have worked, but we were unable to demonstrate the concept, since scattered light diminished quickly with increased distance from forward scatter. Unfortunately, the problem of multiple particles was not resolved and the data reported here are thought to be in slight error because of a small percentage of multiple-seed-particle measurements. This is thought to be systematically causing lower values of 10 to 20% in the \overline{uv} and \overline{vw} shear stresses.

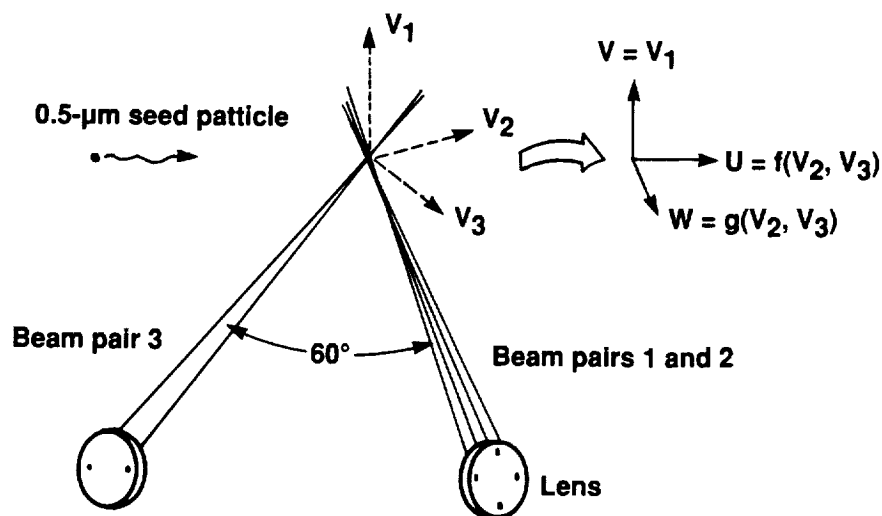
Other uncertainties arise because of statistical variation and uncertainty in measuring beam angles, but these are second-order compared to misalignment and multiple-seed-particle uncertainties.

Three-dimensional LDV measurements—Measurements with the three-component LDV system were initially made in a flat-plate boundary-layer flow (see fig. A3) and compare well with hot-wire measurements made earlier by Acharya in the same flow (ref. 29). Values of $\overline{w^2}$ stress that are inflated relative to the hot wire may be a result of multiple seed particles. Even though LDV and hot-wire measurements of \overline{uv} stress agree well, they both extrapolate to abnormally low stress values at the wall. Again, the LDV could be affected by multiple-seed-particle measurements. Shear stresses \overline{vw} and \overline{uw} are both nearly zero, as they should be in a two-dimensional boundary layer (lack of correlation will not be reflected here).

The LDV was then used in a three-dimensional swirling flow over a spinning cylinder where crossflow was strong (see fig. A4). Here W is largest near the wall, where it approaches the speed of the spinning cylinder ($W_s = U_e$). Measurements of both U and W agree well with the three-hole, pitot-probe measurements of Higuchi and Rubesin (ref. 10). The $\overline{u^2}$ and $\overline{w^2}$ turbulence intensities are nearly equal to each other, as expected (flow similarity in U and W directions). Also, the Reynolds shear stresses \overline{uv} and \overline{vw} are equal in magnitude. The peak level of Reynolds shear stress (measured using the LDV) is almost equal to the shear stress at the wall, which was determined from a momentum balance. However, the Reynolds shear stress appears to be lower (by 10 to 25%) than the surface shear stress; this is possibly due to the existence of multiple seed particles in the scattering volume.

Concluding Remarks

Simultaneous LDV measurements have potential problems that are not experienced with nonsimultaneous measurements; these problems include biasing caused by multiple seed particles. Good alignment of beams reduces some error, but multiple-seed-particle measurements remain a difficulty and contribute to reduced shear-stress values. Nevertheless, a 20% uncertainty in shear stress is acceptable for difficult measurements.

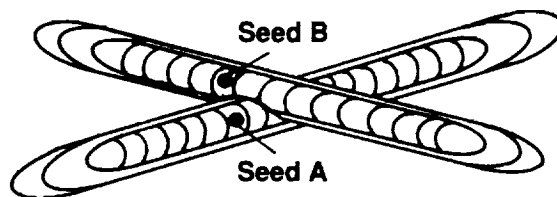


Features

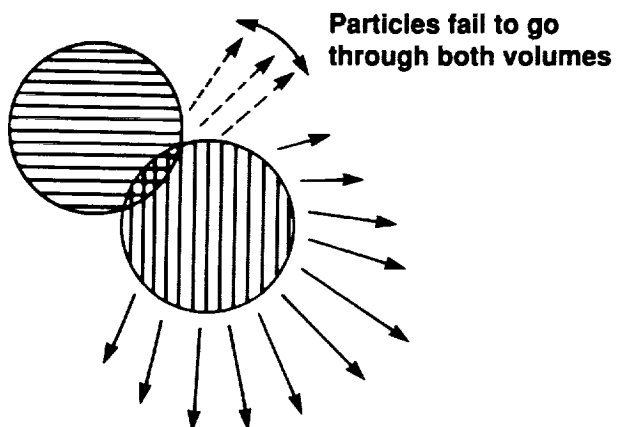
- 3-Color system
- Simultaneous measurements of each of the 3 measured velocity components
- Velocities resolved into Cartesian coordinates for each measurement

Figure A1. Three-component laser Doppler velocimeter (LDV) configuration.

(a) Side view



(b) End view



(c) Top view

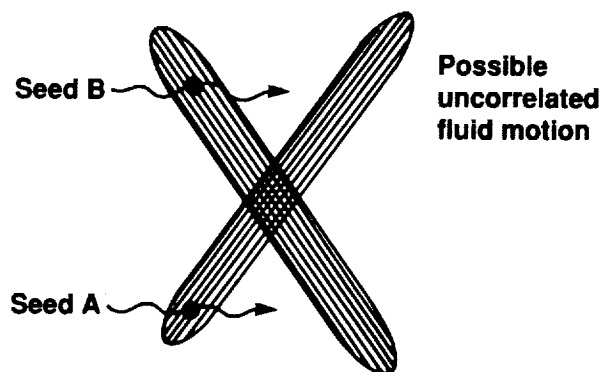


Figure A2. Sources of error with three-component LDV measurements. (a) Two-particle measurements uncorrelated because of misalignment. (b) Velocity bias caused by misalignment. (c) Multiple-particle measurements.

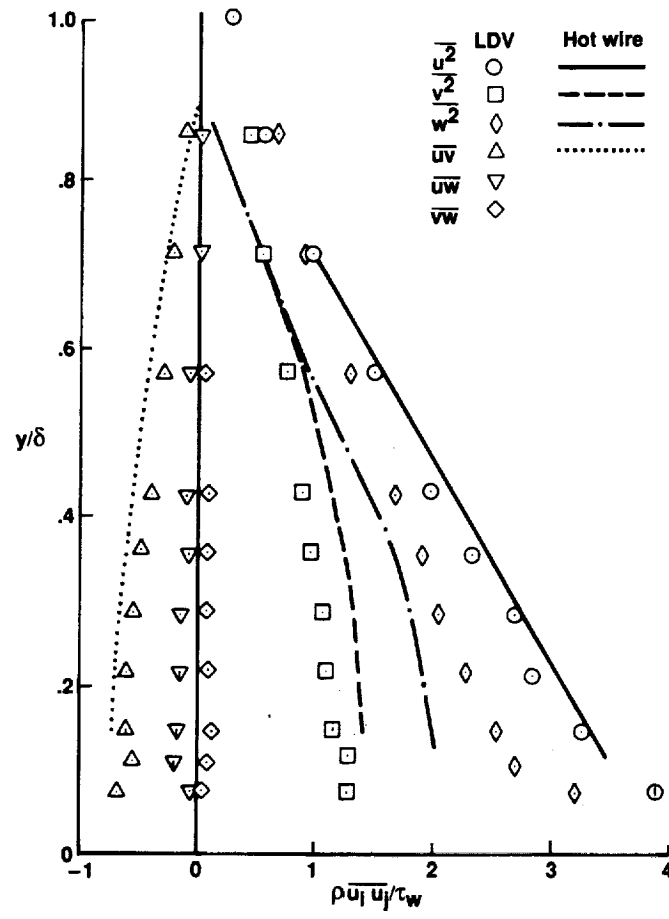


Figure A3. Flat-plate boundary-layer measurements of Reynolds-stress components.

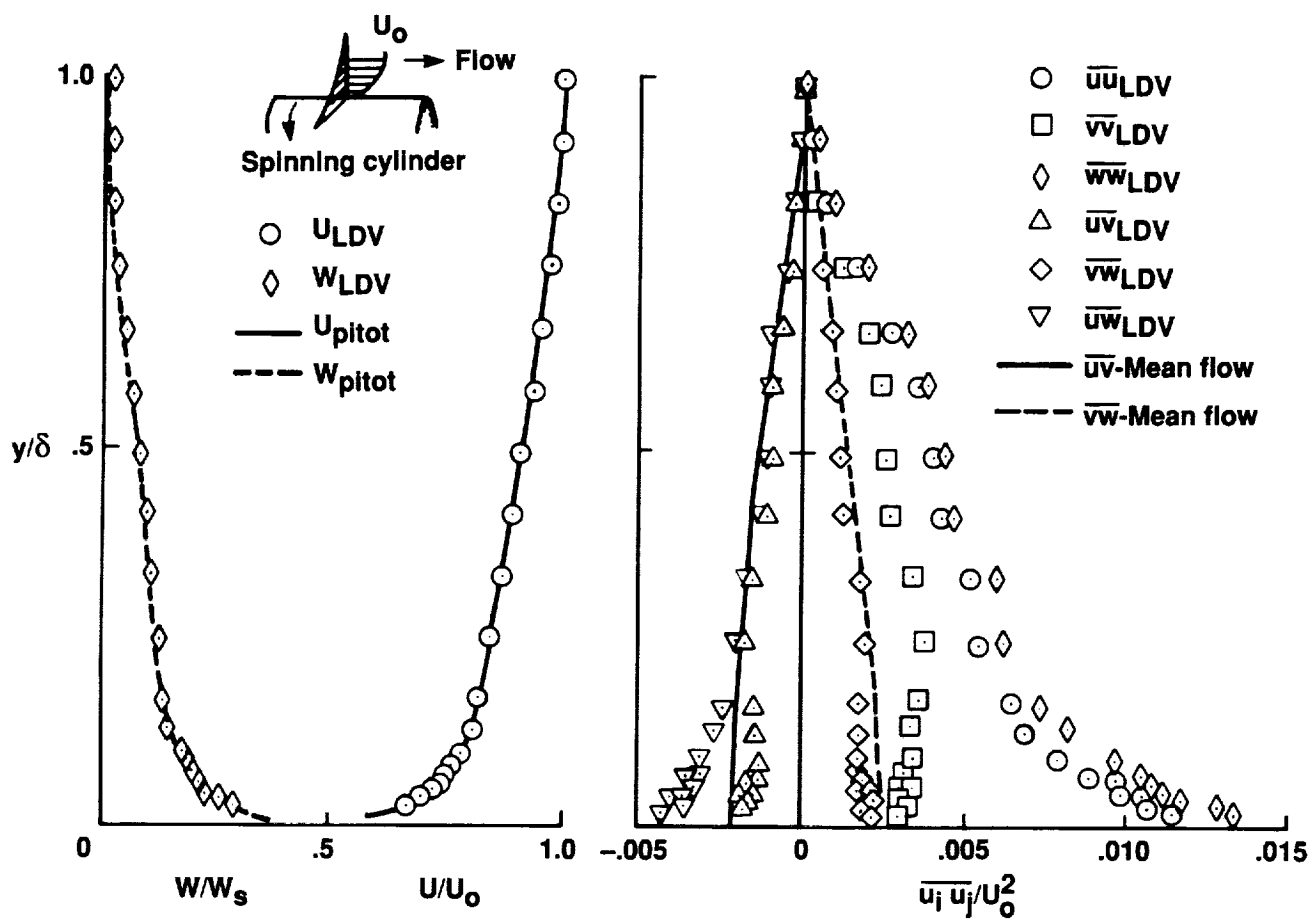


Figure A4. Three-dimensional boundary-layer measurements of Reynolds-stress components at $x = -12$ mm.

APPENDIX B

Evidence of the destabilizing effects of rotation on turbulence can be seen in the mixing length, where

$$l = \sqrt[4]{\overline{uv^2} + \overline{vw^2}} / \sqrt{(\partial U / \partial r)^2 + (\partial W / \partial r - W/r)^2}$$

In a 2-D flat-plate-type boundary layer, the mixing length appears to obey the usual $l_o = 0.41y$ scaling near the wall and $l_o = 0.09\delta$ away from the wall (see fig. B1). In the 3-D case (cylinder spinning), the mixing length is larger and seems to obey the simple scaling reported by Bradshaw (ref. 30) in which $l = l_o(1 - 7Ri)$, where

$$Ri = 2(W/r)(\partial W / \partial r + W/r) / [(\partial U / \partial r)^2 + (\partial W / \partial r - W/r)^2]$$

Physically, the way to understand the destabilizing effect of rotation is to consider a fluid element with angular momentum $\rho r W$ (see fig. B2). The fluid's orbital path around the cylinder is maintained by an inward pressure force. If the fluid is perturbed from its original orbit to a new orbit farther away (where inward pressure force is weaker and unable to hold the fluid in orbit) the fluid will travel a path that diverges from the cylinder. This essentially contributes to a thickening of the boundary layer. Conversely, fluid that is bumped inward toward the center of rotation would be drawn farther inward by a pressure gradient (which increases with proximity to the wall).

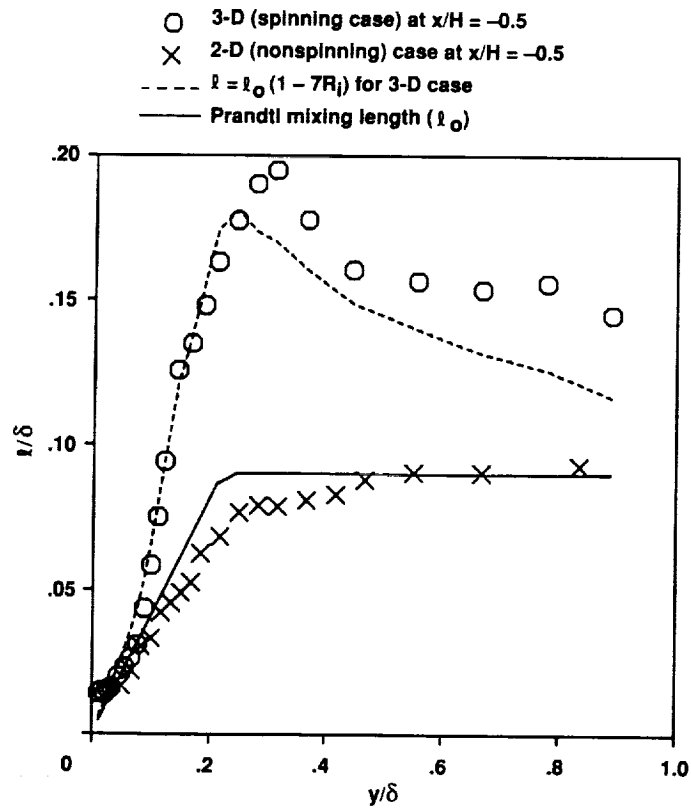


Figure B1. Mixing length distribution at $x/H = -0.5$; $\partial P/\partial x = 0$.

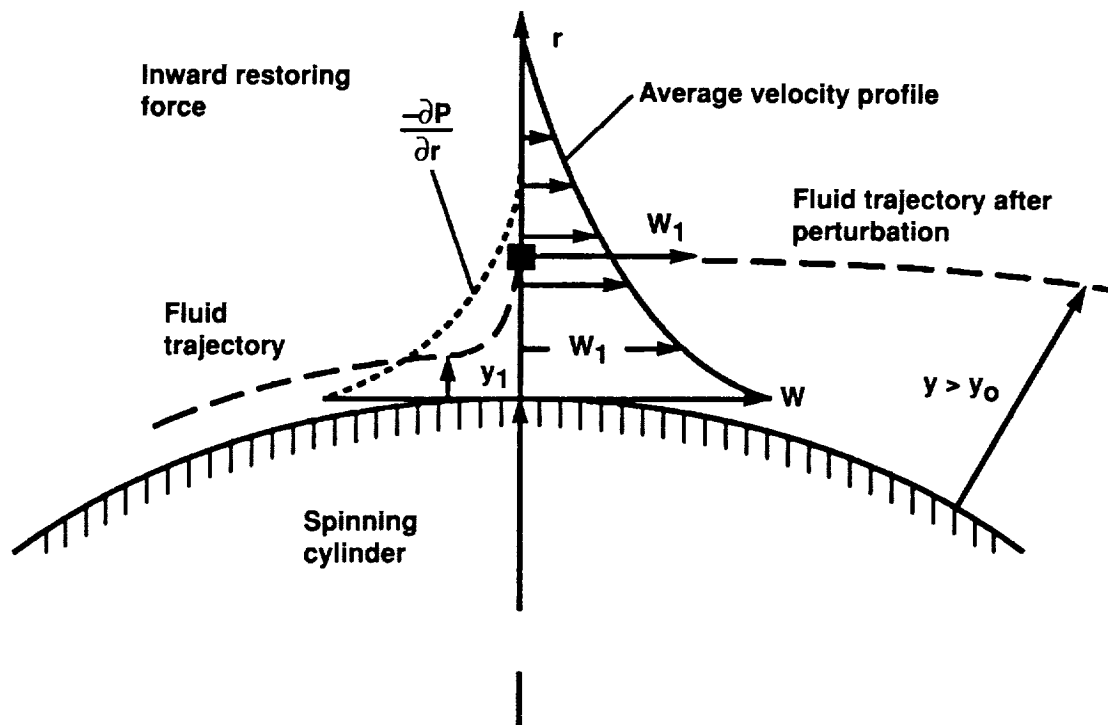


Figure B2. Curvature and rotational effects on fluid elements.

APPENDIX C

The measurements discussed in this report are tabulated in this appendix. Laser Doppler velocimeter measurements of the mean and fluctuating quantities are obtained in two ways:

1. Simple ensemble average of the 10,000 individual realizations
2. Weighted ensemble average; i.e., giving more weight to the slowly moving particles according to the method described in the Measurement Uncertainty section. This is done in the interest of removing a possible velocity bias.

Tables C5 to C9 are the simple (unweighted) ensemble averages, and tables C10 to C14 are the weighted ensemble averages. This report and references 13 and 16 use the unweighted ensemble averages in the analysis, since it is still uncertain as to how to correct for velocity bias. We recommend using the unweighted data for analysis as long as the question of velocity bias is unresolved.

List of Tables

- C1 Surface pressures distributions.
- C2 Skin-friction for zero pressure gradient.
- C3 Skin-friction for step flow model.
- C4 Surface shear stress direction, oil flow method.

Unweighted Ensemble Averages (printed and on floppy disk)

- C5 LDV measurements for zero pressure gradient with spin (case Z.S1).
- C6 LDV measurements for zero pressure gradient with spin—repeat runs (case Z.S1B).
- C7 LDV measurements for forward-facing step with spin (case S.S1).
- C8 LDV measurements for zero pressure gradient, no spin (case Z.S0).
- C9 LDV measurements for forward-facing step, no spin (case S.S0).

Weighted Ensemble Averages (on floppy disk only)

- C10 LDV measurements for zero pressure gradient with spin (case Z.S1).
- C11 LDV measurements for zero pressure gradient with spin—repeat runs (case Z.S1B).
- C12 LDV measurements for forward-facing step with spin (case S.S1).
- C13 LDV measurements for zero pressure gradient, no spin (case Z.S0).
- C14 LDV measurements for forward-facing step, no spin (case S.S0).

Table C1. Surface pressures distributions.

X(mm)	ZERO PRESSURE GRADIENT		FORWARD STEP FLOW	
	No Spin Cp	Spin Cp	No Spin Cp	Spin Cp
3.175	-0.0138	-0.0300	0.0251	0.0075
6.35	-0.0069	-0.0231	0.0295	0.0155
9.55	-0.0046	-0.0185	0.0340	0.0165
12.7	-0.0046	-0.0185	0.0367	0.0194
19.0	-0.0092	-0.0208	0.0389	0.0224
25.4	-0.0092	-0.0185	0.0409	0.0255
31.7	-0.0092	-0.0185	0.0457	0.0313
38.0	-0.0092	-0.0185	0.0525	0.0378
44.4	-0.0092	-0.0185	0.0627	0.0486
63.5	-0.0070	-0.0160	0.1031	0.0870
69.8	-0.0092	-0.0185	0.1187	0.1015
76.0	-0.0092	-0.0185	0.1396	0.1183
82.4	-0.0092	-0.0185	0.1605	0.1362
89.0	-0.0092	-0.0185	0.1817	0.1642
95.3	-0.0092	-0.0185	0.2131	0.1935
101.6	-0.0092	-0.0185	0.2418	0.2232
114.3	-0.0092	-0.0185	0.3028	0.3031
127.0	-0.0092	-0.0185	0.3385	0.3572
139.7	-0.0092	-0.0185	0.3405	0.3772
152.4	-0.0092	-0.0185	0.3923	0.4086
165.1	-0.0092	-0.0185	---	---
177.8	-0.0092	-0.0185	---	---
190.5	-0.0092	-0.0185	---	---
203.2	-0.0092	-0.0185	---	---
215.9	-0.0092	-0.0185	---	---
228.6	-0.0092	-0.0185	---	---
254.0	-0.0092	-0.0185	---	---
279.4	-0.0092	-0.0139	---	---
304.8	-0.0092	-0.0185	---	---
355.6	-0.0092	-0.0185	---	---
381.0	-0.0092	-0.0185	---	---
406.4	-0.0092	-0.0185	---	---
431.8	-0.0092	-0.0185	---	---
457.2	-0.0046	-0.0139	---	---
482.6	-0.0092	-0.0139	---	---
508.0	-0.0092	-0.0185	---	---
533.4	-0.0115	-0.0185	---	---
558.8	-0.0138	-0.0231	---	---
584.2	-0.0183	-0.0278	---	---
609.6	-0.0229	-0.0278	---	---

Table C2. Skin-friction for zero pressure gradient.

X(mm)	No Spin	With Spin		
	Cfx	Cfx	Cfz	Beta,deg
6.35	0.00350	0.00393	0.00242	31.6
12.7	0.00301	0.00359	0.00168	25.1
19.0	0.00304	0.00331	0.00138	22.6
25.4	0.00297	0.00348	0.00138	21.7
38.0	0.00309	0.00354	0.00125	19.4
76.0	0.00300	0.00362	0.00087	13.4
89.0	0.00304	0.00369	0.00075	11.5
101.6	0.00303	0.00356	0.00068	10.8
127.0	0.00303	0.00347	0.00054	8.9
152.4	0.00298	0.00332	0.00051	8.7
203.2	0.00292	0.00320	0.00041	7.3
304.8	0.00293	0.00314	0.00030	5.4
406.4	0.00297	0.00308	0.00024	4.4
508.0	0.00318	0.00331	0.00023	4.0
609.6	0.00312	0.00323	0.00019	3.4

Table C3. Skin-friction for step flow model.

X(mm)	No Spin	With Spin		
	Cfx	Cfx	Cfz	Beta,deg
6.35	0.00332	0.00366	0.00234	32.7
12.7	0.00282	0.00332	0.00172	27.4
19.0	0.00275	0.00301	0.00132	23.7
25.4	0.00274	0.00310	0.00129	22.6
38.0	0.00265	0.00317	0.00121	21.0
76.0	0.00212	0.00269	0.00081	16.7
89.0	0.00171	0.00236	0.00075	17.5
101.6	0.00117	0.00174	0.00068	21.4
127.0	0.00030	0.00036	0.00047	52.4
152.4	-0.00130	-0.00125	0.00021	-9.4

Table C4. Surface shear stress direction, oil flow method.

X(mm)	No Step Beta,deg	Step @X=154mm Beta,deg
3.175	37.5	38.5
6.35	32	33
12.7	25	27
19.0	23	25
25.4	20	23
38.0	18	20
50.8	16	17
63.5	14	15
76.0	--	18
89.0	12	21
101.6	10	25
114.3	9	40
127.0	8	60
133.3	-	90
139.7	-	-75 (reverse flow)
152.4	7	-11 (reverse flow)
203.2	6.5	--
254.0	6	--
304.8	5.5	--
406.4	4.5	--
508.0	-	--
609.6	3.5	--

Table C5. LDV measurements for zero pressure gradient with spin.

Case Z.S1			Station= 1			Date=1227.82 Time=18.49										
x=-304.8mm			Tunnel Run#= 110			Ue/Uo= 1.000										
No Bias Correction																
LR	y (mm)	U/Ue	V/Ue	W/Ue	normalized by 0.001 Uet2			Uet2	normalized by 0.0001 Uet3			Uet3				
					uu	uv	uw		uuu	uvv	uuv		uuu	uvv	uuv	
1	0.38	0.647	-0.005	0.310	10.89	2.67	13.70	-1.46	1.79	-4.49	-1.40	-0.27	-2.82	0.72	1.84	0.77
2	0.51	0.667	-0.005	0.285	9.70	2.94	12.81	-1.39	1.76	-3.73	-1.10	-0.31	-2.18	0.76	1.49	-0.77
3	0.63	0.678	-0.003	0.275	9.66	2.98	12.76	-1.45	1.83	-3.91	-1.06	-0.25	-2.36	0.66	1.12	-0.60
4	0.76	0.691	-0.004	0.260	9.61	2.87	12.07	-1.39	1.68	-3.63	-1.13	-0.30	-1.66	0.70	1.31	-0.62
5	1.02	0.712	-0.004	0.237	9.41	3.17	11.24	-1.64	1.81	-3.68	-1.35	-0.37	-1.79	0.64	1.02	-0.52
7	1.27	0.730	-0.006	0.217	8.97	3.22	10.54	-1.59	1.86	-3.62	-1.15	-0.43	-1.88	0.75	1.31	-0.57
8	1.52	0.741	-0.004	0.208	8.69	3.30	10.37	-1.62	1.94	-3.60	-1.00	-0.38	-1.74	0.83	1.51	-0.63
6	1.78	0.752	-0.005	0.195	8.45	3.39	9.89	-1.66	1.88	-3.45	-1.56	-0.41	-1.55	0.80	1.43	-0.58
9	2.03	0.763	-0.007	0.182	8.04	3.44	9.21	-1.66	1.82	-3.14	-1.72	-0.45	-1.67	0.88	1.48	-0.55
10	2.29	0.769	-0.007	0.176	8.00	3.47	9.02	-1.65	1.79	-3.19	-1.43	-0.47	-1.40	0.78	1.40	-0.58
11	2.54	0.776	-0.006	0.171	7.63	3.61	8.91	-1.71	1.86	-2.98	-1.34	-0.37	-1.23	0.54	1.09	-0.46
12	2.79	0.780	-0.006	0.162	7.43	3.58	8.75	-1.67	1.85	-3.12	-1.24	-0.49	-1.70	0.73	0.80	-0.62
14	3.30	0.786	-0.003	0.159	6.96	3.69	8.41	-1.67	1.83	-2.83	-0.90	-0.49	-1.06	0.58	1.13	-0.62
15	3.81	0.799	-0.004	0.149	7.06	3.73	7.86	-1.82	1.88	-2.64	-1.11	-0.37	-0.92	0.61	0.77	-0.55
16	4.32	0.805	-0.004	0.142	6.77	3.77	7.66	-1.83	1.85	-2.53	-1.39	-0.49	-0.89	0.62	0.78	-0.42
17	4.83	0.811	-0.002	0.137	6.71	3.87	7.56	-1.74	1.84	-2.27	-1.27	-0.34	-0.75	0.57	0.48	-0.39
18	5.59	0.826	-0.003	0.125	6.16	3.74	7.34	-1.70	1.75	-2.10	-1.01	-0.45	-0.75	0.65	0.68	-0.37
19	6.35	0.838	-0.002	0.117	6.05	3.68	6.99	-1.72	1.75	-2.06	-1.29	-0.46	-0.87	0.51	0.53	-0.35
20	7.11	0.851	-0.002	0.104	5.75	3.53	6.56	-1.64	1.53	-2.01	-1.17	-0.42	-0.81	0.47	0.73	-0.36
21	8.38	0.871	-0.001	0.091	5.26	3.14	6.15	-1.46	1.46	-1.80	-1.41	-0.48	-0.70	0.54	0.49	-0.33
22	10.16	0.902	0.001	0.066	4.46	2.74	5.30	-1.28	1.32	-1.65	-1.53	-0.51	-0.91	0.58	0.59	-0.39
23	12.70	0.940	0.002	0.039	3.51	2.06	3.59	-1.03	0.91	-1.37	-1.98	-0.60	-0.99	0.73	0.72	-0.45
24	15.24	0.973	0.001	0.016	1.67	1.33	1.98	-0.47	0.42	-0.69	-1.00	-0.33	-0.60	0.37	0.90	-0.33
25	17.78	0.992	0.000	0.002	0.57	0.77	0.81	-0.16	0.19	-0.28	-0.23	-0.11	-0.18	0.12	0.16	-0.22
26	20.32	0.999	-0.001	-0.003	0.18	0.38	0.32	-0.02	0.02	-0.10	0.00	-0.01	0.00	0.01	0.00	-0.09
27	22.86	1.000	-0.002	-0.004	0.12	0.25	0.24	0.00	0.00	-0.08	0.00	0.00	0.00	0.00	0.00	-0.09
28	25.40	1.000	-0.002	-0.004	0.09	0.22	0.22	0.00	0.00	-0.08	0.00	0.00	0.00	0.00	0.00	-0.09
29	27.94	1.001	-0.002	-0.004	0.08	0.18	0.21	0.00	0.00	-0.07	0.00	0.00	0.00	0.00	0.00	-0.09

normalized by 0.0001 Uet3			normalized by 0.0001 Uet3			normalized by 0.0001 Uet3		
uuu	uvv	uww	uuu	uvv	uww	uuu	uvv	uww
-1.40	-0.27	-2.82	0.72	0.17	1.26	1.84	0.44	3.44
-1.10	-0.31	-2.18	0.76	0.36	1.12	1.49	0.45	2.39
-1.06	-0.25	-2.36	0.66	0.38	1.08	1.31	0.51	3.12
-1.13	-0.30	-1.66	0.70	0.27	0.98	1.02	0.41	2.35
-1.35	-0.37	-1.79	0.64	0.26	1.25	1.31	0.55	2.33
-1.15	-0.43	-1.88	0.75	0.32	1.20	1.51	0.64	2.40
-1.00	-0.38	-1.74	0.83	0.35	1.30	1.43	0.55	2.81
-1.56	-0.41	-1.55	0.80	0.45	1.14	1.48	0.59	2.64
-1.72	-0.45	-1.67	0.88	0.46	1.01	1.40	0.51	2.55
-1.43	-0.47	-1.40	0.78	0.41	1.09	1.12	0.58	2.26
-1.34	-0.37	-1.23	0.54	0.50	1.07	0.80	0.70	2.42
-1.24	-0.49	-1.70	0.73	0.47	1.03	1.13	0.68	2.81
-0.90	-0.49	-1.06	0.58	0.61	0.92	0.77	0.69	2.00
-1.11	-0.37	-0.92	0.61	0.42	0.83	0.78	0.48	1.88
-1.39	-0.49	-0.89	0.62	0.58	0.91	0.48	0.61	1.75
-1.27	-0.34	-0.75	0.57	0.61	0.80	0.68	0.46	1.61
-1.01	-0.45	-0.75	0.50	0.65	0.76	0.53	0.57	1.56
-1.29	-0.46	-0.87	0.51	0.71	0.67	0.73	0.53	1.56
-1.17	-0.42	-0.81	0.47	0.55	0.66	0.49	0.50	1.37
-1.41	-0.48	-0.70	0.54	0.62	0.65	0.59	0.48	1.63
-1.53	-0.51	-0.91	0.58	0.66	0.74	0.72	0.60	1.65
-1.98	-0.60	-0.99	0.73	0.63	0.71	0.90	0.55	1.68
-1.00	-0.33	-0.60	0.37	0.45	0.41	0.49	0.30	0.98
-0.23	-0.11	-0.18	0.12	0.22	0.20	0.16	0.13	0.31
0.00	-0.01	0.00	0.01	0.05	0.02	0.00	0.01	0.00
0.00	0.00	0.00	0.00	0.01	0.01	0.00	0.00	-0.01
0.00	0.00	0.00	0.00	0.00	0.00	0.00	0.00	0.00
0.00	0.00	0.00	0.00	-0.01	0.00	0.00	0.00	-0.01

Table C5. Continued.

Case Z.S1		Station= 2		Date=1227.82		Time=19.43	
x=-152.4mm		Tunnel Run#= 111		Ue/Uo= 0.980			
No Bias Correction							
LR	y(mm)	U/Ue	V/Ue	W/Ue	uu	vv	ww
1	0.38	0.672	-0.007	0.303	11.21	2.78	13.71
2	0.51	0.683	-0.005	0.295	10.66	2.91	13.08
3	0.63	0.700	-0.005	0.276	10.81	3.06	12.61
4	0.76	0.712	-0.006	0.260	10.71	3.21	11.96
5	1.02	0.729	-0.003	0.246	10.20	3.16	11.70
6	1.27	0.745	-0.002	0.228	9.54	3.19	11.27
7	1.52	0.745	-0.003	0.211	9.06	3.18	10.79
8	1.78	0.754	-0.002	0.199	8.36	3.18	10.02
9	2.03	0.760	-0.003	0.191	8.39	3.34	9.59
10	2.29	0.768	-0.001	0.185	8.63	3.40	9.52
11	2.54	0.779	-0.002	0.177	7.70	3.36	9.24
12	2.79	0.782	0.000	0.175	7.77	3.42	9.04
13	3.30	0.789	0.000	0.165	7.34	3.70	8.63
14	3.81	0.796	0.000	0.158	7.09	3.69	8.39
15	4.32	0.804	0.000	0.152	6.71	3.92	7.99
16	4.83	0.811	0.002	0.149	6.64	3.97	7.76
17	5.59	0.822	-0.001	0.139	6.37	3.93	7.26
18	6.35	0.826	0.004	0.136	6.27	3.90	7.28
19	7.11	0.832	0.006	0.131	5.86	3.80	7.13
20	8.38	0.850	0.007	0.121	5.73	3.86	6.92
21	10.16	0.867	0.009	0.104	5.27	3.50	6.29
22	12.70	0.895	0.012	0.084	4.89	3.18	5.56
23	15.24	0.927	0.013	0.062	4.00	2.67	4.53
24	17.78	0.954	0.011	0.037	2.88	2.13	3.30
25	20.32	0.982	0.005	0.013	1.37	1.39	1.68
26	22.86	0.994	0.004	0.002	0.60	0.84	0.76
27	25.40	0.999	0.004	-0.001	0.27	0.53	0.43
28	27.94	1.000	0.002	-0.003	0.14	0.30	0.26
29	30.48	1.001	0.001	-0.003	0.10	0.23	0.22

Table C5. Continued.

Case Z.S1			Station= 3			Date=1227.82			Time=20.39											
x= -3.2mm			Tunnel Run#= 112			Ue/Uo= 0.982														
No Bias Correction																				
The y-position has been corrected by adding 2.540 to each measured y-position in this profile.																				
LR	y (mm)	U/Ue	V/Ue	W/Ue	normalized by 0.001 Uet2			normalized by 0.0001 Uet3			Uet3									
					uu	uv	uw	uuu	uvv	uww										
2	0.38	0.607	-0.007	0.333	11.78	2.97	17.92	-1.87	2.47	-5.71	-1.62	-0.29	-4.03	0.75	0.05	1.79	3.39	0.48	3.77	-1.19
3	0.51	0.640	-0.007	0.306	11.70	3.29	16.17	-1.97	2.44	-4.84	-1.84	-0.36	-3.37	0.92	0.58	1.78	2.56	0.61	3.66	-1.09
4	0.63	0.661	-0.008	0.285	11.47	3.43	15.29	-2.13	2.73	-4.88	-2.27	-0.57	-3.55	1.02	0.62	1.76	2.51	0.79	3.70	-1.02
5	0.76	0.680	-0.007	0.269	10.53	3.30	14.37	-1.88	2.25	-4.21	-1.67	-0.48	-2.86	0.96	0.55	1.62	2.14	0.70	3.34	-0.91
6	1.02	0.704	-0.006	0.246	10.31	3.52	13.39	-1.91	2.25	-3.94	-2.16	-0.63	-3.02	1.13	0.74	1.73	2.30	0.80	3.72	-1.04
7	1.27	0.721	-0.005	0.225	9.69	3.26	12.59	-1.71	2.01	-3.78	-1.94	-0.58	-2.89	0.87	0.52	1.65	1.87	0.74	3.25	-0.82
8	1.52	0.739	-0.005	0.205	9.51	3.29	11.45	-1.76	1.88	-3.43	-2.93	-0.68	-3.08	1.30	0.61	1.63	2.44	0.76	3.71	-0.98
9	1.78	0.753	-0.005	0.194	9.03	3.38	11.23	-1.75	2.10	-3.52	-2.03	-0.81	-2.66	1.17	0.62	1.74	2.15	0.94	3.86	-0.98
10	2.03	0.764	-0.007	0.180	8.42	3.27	10.02	-1.71	1.87	-3.06	-2.16	-0.80	-2.35	1.20	0.68	1.49	1.87	0.88	3.60	-0.93
11	2.29	0.769	-0.004	0.175	8.20	3.34	10.35	-1.61	1.84	-3.21	-1.78	-0.59	-2.66	1.06	0.71	1.69	1.87	0.74	3.99	-0.87
12	2.54	0.779	-0.005	0.167	8.05	3.35	10.14	-1.58	1.89	-3.02	-1.90	-0.61	-2.34	1.03	0.49	1.68	1.53	0.89	3.77	-0.86
13	2.79	0.783	-0.004	0.164	8.03	3.37	9.82	-1.69	1.91	-3.30	-2.02	-0.67	-2.55	1.11	0.66	1.78	1.92	0.86	3.84	-0.98
14	3.30	0.794	-0.004	0.157	7.41	3.54	9.33	-1.63	1.90	-3.19	-1.37	-0.68	-2.11	0.93	0.55	1.47	1.67	0.82	3.62	-0.83
15	3.81	0.800	-0.003	0.147	7.46	3.73	8.77	-1.82	1.97	-2.84	-2.04	-0.78	-1.87	1.14	0.81	1.68	1.53	0.92	3.63	-0.85
16	4.32	0.808	-0.003	0.142	6.95	3.99	8.27	-1.92	1.92	-2.63	-1.50	-0.80	-1.59	1.02	0.94	1.42	1.13	0.89	3.07	-0.84
17	4.83	0.813	-0.004	0.136	6.88	3.88	8.14	-1.77	1.96	-2.76	-1.97	-0.81	-1.70	1.11	0.74	1.54	1.41	0.93	2.85	-0.91
18	5.59	0.825	-0.004	0.130	6.42	4.04	7.66	-1.85	1.97	-2.44	-1.71	-0.77	-1.32	1.00	0.92	1.26	1.13	0.97	2.20	-0.78
19	6.35	0.831	-0.003	0.128	6.20	3.98	7.25	-1.81	1.92	-2.26	-1.33	-0.59	-0.97	0.75	0.81	1.04	0.93	0.78	1.84	-0.62
20	7.11	0.837	-0.003	0.122	6.11	4.03	7.24	-1.87	1.91	-2.11	-1.41	-0.71	-1.04	0.79	1.00	1.15	0.83	0.87	1.98	-0.60
21	8.38	0.850	-0.002	0.113	5.64	4.05	6.67	-1.82	1.88	-1.87	-1.23	-0.61	-0.78	0.68	0.99	0.87	0.68	0.73	1.44	-0.48
22	10.16	0.863	0.002	0.104	5.31	3.91	6.18	-1.64	1.77	-1.64	-0.90	-0.49	-0.53	0.49	0.82	0.64	0.52	0.59	1.07	-0.35
23	12.70	0.886	0.005	0.091	4.89	3.46	5.83	-1.49	1.60	-1.58	-1.31	-0.46	-0.58	0.54	0.78	0.69	0.64	0.60	1.15	-0.34
24	15.24	0.910	0.005	0.071	4.10	3.08	4.97	-1.33	1.40	-1.41	-1.12	-0.51	-0.61	0.52	0.81	0.64	0.57	0.59	1.30	-0.30
25	17.78	0.933	0.005	0.051	3.54	2.48	4.20	-1.06	1.05	-1.17	-1.36	-0.49	-0.69	0.55	0.67	0.65	0.52	0.52	1.49	-0.31
26	20.32	0.953	0.009	0.037	2.85	2.20	3.39	-0.89	0.94	-1.04	-1.26	-0.46	-0.61	0.54	0.73	0.68	0.65	0.55	1.46	-0.31
27	22.86	0.970	0.009	0.023	2.11	1.88	2.54	-0.70	0.80	-0.86	-1.07	-0.46	-0.64	0.46	0.68	0.62	0.59	0.48	1.28	-0.30
28	25.40	0.985	0.009	0.010	1.26	1.41	1.68	-0.44	0.51	-0.55	-0.63	-0.29	-0.43	0.33	0.57	0.48	0.40	0.35	0.91	-0.21
29	27.94	0.994	0.010	0.004	0.92	1.24	1.20	-0.34	0.39	-0.34	-0.37	-0.24	-0.26	0.25	0.54	0.37	0.24	0.29	0.65	-0.13
30	30.48	0.999	0.005	-0.003	0.35	0.71	0.55	-0.10	0.14	-0.15	-0.05	-0.06	-0.05	0.08	0.28	0.14	0.05	0.10	0.15	-0.04
31	33.02	1.001	0.000	-0.007	0.14	0.30	0.29	-0.01	0.01	-0.11	0.00	0.00	0.01	0.00	0.02	0.00	0.00	0.00	-0.01	-0.04

Table C5. Continued.

Case Z.S1			Station= 5		Date=1228.82		Time=13.12													
x= 3.2mm			Tunnel Run#= 115		Ue/Uo= 0.993															
No Bias Correction																				
LR	y(mm)	U/Ue	V/Ue	W/Ue	normalized by 0.001 Uet2			Uet3												
					uu	uv	uw													
1	0.38	0.658	0.009	0.300	10.32	4.41	14.24	-1.25	2.01	-3.89	-0.19	0.19	-1.71	0.51	2.80	0.59	1.21	0.03	1.47	-0.30
2	0.51	0.675	0.006	0.283	10.45	4.02	13.87	-1.55	2.14	-3.73	-1.22	-0.16	-1.73	0.62	1.75	0.98	1.48	0.41	2.88	-0.53
3	0.63	0.685	0.004	0.270	10.14	3.69	13.38	-1.59	2.24	-4.15	-1.77	-0.40	-2.49	0.60	0.55	1.24	1.66	0.56	3.95	-0.55
4	0.76	0.701	0.003	0.255	10.65	3.62	13.36	-1.70	2.28	-3.92	-1.89	-0.49	-2.19	0.91	0.68	1.40	1.90	0.81	2.87	-0.79
5	1.02	0.730	0.001	0.228	10.23	3.65	12.51	-1.70	2.18	-3.82	-2.59	-0.76	-2.35	0.96	0.66	1.58	2.14	0.91	3.92	-0.80
6	1.27	0.752	0.001	0.205	9.69	3.57	11.61	-1.62	1.97	-3.66	-2.18	-0.62	-2.62	1.01	0.66	1.51	2.17	0.82	4.33	-0.77
7	1.52	0.767	0.002	0.190	9.32	3.43	10.63	-1.63	1.82	-3.33	-3.34	-0.75	-3.09	1.21	0.76	1.50	2.31	0.85	4.70	-0.92
8	1.78	0.774	0.001	0.175	8.77	3.38	10.04	-1.56	1.77	-3.12	-2.60	-0.74	-2.80	1.16	0.73	1.60	2.10	0.97	4.19	-1.01
9	2.03	0.781	0.003	0.166	8.24	3.36	9.50	-1.37	1.69	-2.91	-2.39	-0.59	-2.19	1.06	0.60	1.48	1.90	0.85	3.46	-0.79
10	2.29	0.788	0.004	0.157	8.13	3.39	9.01	-1.47	1.66	-2.89	-2.41	-0.63	-2.33	1.16	0.55	1.45	2.16	0.86	3.34	-0.90
11	2.54	0.788	0.002	0.153	8.10	3.43	9.12	-1.60	1.79	-2.94	-2.16	-0.77	-2.21	1.24	0.57	1.54	2.00	0.89	3.37	-0.98
12	2.79	0.788	0.002	0.150	7.52	3.47	8.44	-1.49	1.65	-2.79	-1.74	-0.64	-1.81	0.98	0.61	1.33	1.48	0.80	3.08	-0.76
13	3.30	0.798	0.001	0.143	7.33	3.63	8.37	-1.52	1.61	-2.78	-1.79	-0.71	-1.84	0.93	0.90	1.20	1.44	0.89	3.13	-0.72
14	3.81	0.800	0.002	0.143	7.00	3.81	8.85	-1.66	1.87	-3.06	-1.64	-0.53	-1.91	0.76	0.92	1.38	1.18	0.85	3.42	-0.65
15	4.32	0.809	0.002	0.136	6.70	3.84	8.20	-1.57	1.60	-2.63	-1.43	-0.61	-1.46	0.86	0.90	1.18	1.17	0.65	2.56	-0.60
16	4.83	0.817	0.001	0.129	6.48	4.03	7.91	-1.65	1.83	-2.43	-1.54	-0.58	-1.41	0.87	1.07	1.19	1.29	0.79	2.39	-0.78
17	5.59	0.823	0.002	0.122	6.17	3.85	7.35	-1.67	1.70	-2.24	-1.43	-0.57	-1.13	0.69	0.81	0.98	1.01	0.73	2.15	-0.48
18	6.35	0.830	0.003	0.118	5.81	3.85	7.25	-1.57	1.64	-2.11	-1.15	-0.56	-0.92	0.69	0.81	0.94	0.85	0.75	1.97	-0.53
19	7.11	0.838	0.000	0.114	5.65	4.12	6.90	-1.65	1.68	-1.95	-1.13	-0.46	-0.93	0.62	1.08	0.91	0.85	0.71	1.98	-0.46
20	8.38	0.849	0.001	0.106	5.34	4.00	6.69	-1.68	1.76	-1.91	-1.07	-0.57	-0.84	0.60	1.27	0.93	0.70	0.73	1.80	-0.47
21	10.16	0.865	0.001	0.094	5.05	3.58	6.02	-1.46	1.63	-1.59	-1.09	-0.43	-0.58	0.44	0.81	0.64	0.55	0.55	1.46	-0.27
22	12.70	0.889	0.002	0.076	4.44	3.25	5.45	-1.33	1.47	-1.40	-1.04	-0.49	-0.57	0.44	0.96	0.67	0.49	0.66	1.28	-0.30
23	15.24	0.912	0.002	0.060	4.02	2.80	4.83	-1.21	1.27	-1.42	-1.34	-0.53	-0.61	0.61	0.79	0.72	0.58	0.67	1.45	-0.37
24	17.78	0.927	0.009	0.051	3.71	2.72	4.01	-1.15	1.15	-1.29	-1.37	-0.57	-0.54	0.58	0.91	0.63	0.55	0.61	1.27	-0.31
25	20.32	0.950	0.010	0.033	2.93	2.20	3.44	-0.90	0.94	-1.22	-1.30	-0.46	-0.63	0.52	0.65	0.54	0.60	0.46	1.27	-0.28
26	22.86	0.970	0.010	0.017	2.11	1.84	2.61	-0.68	0.71	-0.92	-1.11	-0.44	-0.67	0.47	0.66	0.50	0.58	0.46	1.35	-0.24
27	25.40	0.985	0.007	0.005	1.24	1.31	1.65	-0.40	0.42	-0.57	-0.62	-0.29	-0.42	0.31	0.48	0.38	0.38	0.28	0.84	-0.17
28	27.94	0.996	0.007	0.002	0.61	0.97	0.93	-0.20	0.26	-0.29	-0.20	-0.15	-0.16	0.15	0.38	0.23	0.15	0.19	0.40	-0.09
29	30.48	0.998	0.004	0.007	0.31	0.61	0.49	-0.08	0.10	-0.17	-0.05	-0.06	-0.03	0.06	0.19	0.08	0.03	0.06	0.07	-0.03
30	38.10	1.002	0.000	0.000	0.11	0.24	0.27	-0.01	0.01	-0.11	0.00	0.00	0.00	0.00	0.00	0.00	0.00	0.00	0.01	0.00

Table C5. Continued.

Case Z.S1			Station= 7		Date=1228.82		Time=16.26								
x= 12.7mm			Tunnel Run# = 117		Ue/Uo= 0.987										
No Bias Correction															
LR	y(mm)	U/Ue	V/Ue	W/Ue	normalized by 0.001 Uet2			normalized by 0.0001 Uet3							
					uu	uv	uw	uuu	uvv	uww					
1	0.38	0.615	0.000	0.252	11.00	-1.96	0.41	-0.95	-1.38	0.01	0.32	-1.17	-0.18	-2.34	0.43
2	0.51	0.640	0.001	0.251	9.74	-1.66	0.58	-1.70	-0.88	-0.10	0.06	0.44	-0.03	0.37	-0.09
3	0.63	0.676	0.000	0.248	9.40	-1.55	1.00	-2.37	-0.39	-0.09	0.26	0.37	-0.06	0.13	0.17
4	0.76	0.689	0.003	0.251	8.97	-1.36	1.13	-2.30	-0.25	-0.03	0.63	0.28	-0.04	0.48	0.55
5	1.02	0.722	0.002	0.234	8.74	-1.39	1.56	-2.59	-0.34	-0.15	-0.73	0.54	0.12	0.42	0.82
6	1.27	0.740	0.001	0.220	8.92	-1.56	1.90	-3.04	-0.85	-0.32	-1.06	0.60	0.32	0.86	0.96
7	1.52	0.751	0.000	0.205	9.01	-1.67	2.08	-3.24	-1.40	-0.42	-1.40	0.97	0.44	1.01	1.51
8	1.78	0.762	0.000	0.194	8.96	-1.78	2.10	-3.37	-1.98	-0.58	-1.88	1.06	0.62	1.34	1.51
9	2.03	0.771	0.000	0.184	8.76	-1.87	2.13	-3.52	-1.99	-0.68	-2.48	1.23	0.70	1.58	2.15
10	2.29	0.776	0.000	0.178	8.77	-1.87	2.11	-3.73	-2.17	-0.60	-2.28	1.14	0.57	1.64	2.15
11	2.54	0.786	0.000	0.170	8.42	-1.86	2.09	-3.45	-1.86	-0.62	-2.20	1.08	0.68	1.39	1.88
12	2.79	0.795	0.000	0.162	7.94	-1.87	2.01	-3.29	-2.05	-0.63	-2.22	1.07	1.03	1.57	1.98
13	3.30	0.804	-0.003	0.151	7.91	-1.85	1.93	-3.21	-2.39	-0.76	-2.23	1.20	0.58	1.70	1.89
14	3.81	0.810	-0.002	0.147	7.36	-1.91	1.97	-3.09	-1.88	-0.76	-1.76	1.21	0.81	1.40	1.55
15	4.32	0.824	-0.002	0.133	6.95	-1.71	1.75	-2.85	-1.75	-0.59	-1.60	1.08	2.97	1.31	1.51
16	4.83	0.827	-0.004	0.129	6.74	-1.67	1.83	-2.80	-1.85	-0.51	-1.65	1.00	2.10	1.44	1.33
17	5.59	0.835	-0.004	0.123	6.31	-1.79	1.88	-2.47	-1.85	-0.61	-1.25	0.77	1.41	1.31	1.06
18	6.35	0.841	-0.004	0.119	6.18	-1.91	1.88	-2.39	-1.43	-0.73	-1.10	0.87	1.01	1.16	1.01
19	7.11	0.846	-0.005	0.116	6.03	-1.92	1.95	-2.31	-1.27	-0.64	-0.82	0.73	1.13	0.94	0.80
20	8.38	0.858	-0.003	0.105	5.64	-1.75	1.70	-1.94	-1.24	-0.44	-0.72	0.64	1.05	0.85	0.61
21	10.16	0.871	-0.002	0.094	5.18	-1.67	1.70	-1.92	-1.31	-0.67	-0.79	0.74	2.03	0.88	0.77
22	12.70	0.893	0.000	0.080	4.51	-1.40	1.48	-1.62	-1.15	-0.49	-0.66	0.60	1.62	0.72	0.65
23	15.24	0.919	-0.003	0.060	3.85	-1.22	1.23	-1.44	-1.34	-0.61	-0.73	0.68	0.88	0.78	0.67
24	17.78	0.941	-0.002	0.041	3.14	-0.97	0.93	-1.26	-1.37	-0.56	-0.75	0.60	0.77	0.68	0.67
25	20.32	0.958	-0.001	0.024	2.34	-0.63	0.63	-1.07	-1.24	-0.46	-0.68	0.45	0.56	0.51	0.63
26	22.86	0.976	0.001	0.013	1.60	-0.53	0.53	-0.76	-0.85	-0.37	-0.53	0.39	0.50	0.48	0.47
27	25.40	0.984	0.002	0.006	1.08	-0.33	0.32	-0.48	-0.61	-0.22	-0.33	0.27	0.30	0.29	0.28
28	27.94	0.994	0.002	0.000	0.51	-0.15	0.18	-0.30	-0.14	-0.12	-0.13	0.10	0.25	0.17	0.10
29	30.48	0.998	0.001	-0.005	0.30	-0.06	0.06	-0.20	-0.02	-0.04	0.00	0.04	0.14	0.04	0.00
30	38.10	1.002	0.000	-0.008	0.15	0.37	0.00	-0.16	0.01	0.00	0.01	0.00	0.00	0.00	-0.03

Case Z.S1 Station= 9
x= 50.8mm Tunnel Run/= 119 Ue/Uo= 0.991 Date=1228.82 Time=18.43
No Bias Correction

LR	y (mm)	U/Ue	V/Ue	W/Ue	normalized by 0.001			normalized by 0.0001			Uet2	normalized by 0.0001			Uet3					
					uu	vv	ww	uv	vw	uw		uuu	uvv	uww		uuu	vvv	vuu	vvw	vuw
1	0.38	0.605	0.000	0.158	8.99	2.09	9.30	-1.62	-0.07	0.39	-1.98	-0.15	-0.31	0.65	0.02	0.32	-0.92	-0.02	-1.71	0.14
2	0.51	0.634	0.000	0.162	8.04	2.34	8.79	-1.52	0.19	-0.23	-1.12	-0.08	0.11	0.59	0.07	0.22	-0.38	-0.06	-1.40	0.19
3	0.63	0.650	0.000	0.166	7.83	2.40	8.61	-1.51	0.14	-0.54	-0.31	-0.08	0.11	0.34	0.06	0.27	-0.29	0.04	-0.82	0.15
4	0.76	0.669	0.000	0.167	7.61	2.61	8.60	-1.62	0.24	-0.81	-0.17	-0.08	0.51	0.34	0.18	0.32	-0.14	-0.01	-0.80	0.12
5	1.02	0.697	-0.001	0.166	7.15	2.65	8.22	-1.62	0.44	-1.18	0.02	-0.16	0.03	0.30	0.12	0.23	0.07	-0.03	0.01	0.12
6	1.27	0.720	0.000	0.161	7.11	2.81	8.13	-1.59	0.65	-1.53	-0.20	-0.15	-0.03	0.32	0.22	0.27	0.15	0.11	-0.09	0.05
7	1.52	0.739	0.000	0.164	7.09	2.87	8.06	-1.52	0.83	-1.75	-0.04	-0.14	0.07	0.28	0.08	0.17	0.12	0.07	-0.18	0.04
8	1.78	0.757	-0.001	0.157	6.81	2.86	8.10	-1.39	0.82	-1.81	-0.28	-0.29	-0.33	0.48	0.18	0.38	0.40	0.13	0.50	-0.08
9	2.03	0.770	-0.001	0.150	6.90	2.96	8.16	-1.44	1.04	-1.97	-0.51	-0.31	-0.48	0.54	0.23	0.54	0.62	0.25	0.51	-0.18
10	2.29	0.782	-0.001	0.151	6.74	2.97	8.18	-1.31	1.17	-2.14	-0.50	-0.20	-0.51	0.45	0.19	0.50	0.68	0.26	1.33	-0.20
11	2.54	0.791	-0.001	0.145	6.61	3.10	7.91	-1.34	1.28	-2.11	-0.56	-0.29	-0.69	0.56	0.18	0.47	0.67	0.25	1.27	-0.22
12	2.79	0.796	-0.001	0.143	6.69	3.30	7.88	-1.33	1.41	-2.17	-0.72	-0.47	-0.71	0.63	0.45	0.63	0.74	0.41	1.28	-0.26
13	3.30	0.799	0.003	0.153	6.41	3.54	7.61	-1.35	1.64	-2.33	-0.85	-0.26	-0.90	0.57	0.23	0.80	0.69	0.55	1.73	-0.35
14	3.81	0.814	-0.002	0.132	6.14	3.59	7.51	-1.28	1.56	-2.21	-0.74	-0.38	-0.90	0.61	0.33	0.77	0.80	0.62	1.91	-0.55
15	4.32	0.824	-0.004	0.127	6.04	3.56	7.48	-1.39	1.70	-2.26	-0.88	-0.36	-1.12	0.64	0.88	0.93	0.91	0.73	1.65	-0.49
16	4.83	0.827	-0.003	0.125	5.97	3.91	7.51	-1.39	1.70	-2.28	-0.88	-0.49	-0.85	0.62	0.71	0.96	0.87	0.73	1.53	-0.50
17	5.59	0.832	-0.005	0.121	6.00	3.85	7.33	-1.55	1.75	-2.29	-1.26	-0.53	-0.92	0.73	0.63	0.88	0.96	0.71	1.53	-0.50
18	6.35	0.840	-0.006	0.116	5.91	3.97	7.13	-1.72	1.68	-2.05	-1.30	-0.50	-0.79	0.64	1.07	0.86	0.78	0.77	1.50	-0.46
19	7.11	0.847	-0.006	0.109	5.74	4.01	6.75	-1.62	1.68	-2.08	-0.95	-0.45	-0.53	0.56	1.07	0.83	0.71	0.57	1.37	-0.34
20	8.38	0.849	-0.002	0.108	5.51	3.93	7.04	-1.64	1.78	-2.08	-0.95	-0.45	-0.53	0.56	1.07	0.83	0.71	0.57	1.37	-0.34
21	10.16	0.870	-0.002	0.093	5.13	4.06	6.47	-1.60	1.66	-1.80	-1.17	-0.48	-0.58	0.64	1.71	0.66	0.63	1.25	-0.41	
22	12.70	0.884	-0.005	0.089	4.98	3.78	6.03	-1.55	1.68	-1.73	-1.07	-0.46	-0.63	0.54	1.22	0.67	0.58	1.29	-0.38	
23	15.24	0.898	0.013	0.080	4.66	3.43	5.34	-1.40	1.51	-1.51	-1.04	-0.42	-0.38	0.48	0.83	0.55	0.44	0.53	0.94	-0.23
24	17.78	0.933	0.002	0.047	3.70	2.52	4.40	-1.13	1.15	-1.48	-1.53	-0.55	-0.82	0.65	0.80	0.82	0.81	0.68	1.69	-0.44
25	20.32	0.957	-0.001	0.026	2.89	1.92	3.26	-0.75	0.73	-1.14	-1.27	-0.49	-0.75	0.52	0.64	0.62	0.70	0.49	1.26	-0.33
26	22.86	0.971	0.003	0.014	1.87	1.59	2.54	-0.54	0.61	-0.90	-0.95	-0.38	-0.61	0.38	0.55	0.53	0.53	0.44	1.19	-0.26
27	25.40	0.984	0.004	0.004	1.31	1.33	1.83	-0.42	0.47	-0.67	-0.65	-0.30	-0.45	0.30	0.52	0.43	0.38	0.34	0.91	-0.22
28	27.94	0.992	0.004	-0.001	0.68	0.91	1.03	-0.19	0.20	-0.33	-0.22	-0.14	-0.04	0.14	0.24	0.17	0.14	0.16	0.32	-0.08
29	30.48	0.997	0.002	-0.006	0.34	0.61	0.59	-0.07	0.09	-0.22	-0.04	-0.05	-0.04	0.04	0.16	0.07	0.03	0.07	0.09	-0.03
30	33.02	0.999	0.001	-0.008	0.21	0.45	0.41	-0.03	0.04	-0.15	0.00	-0.01	0.00	0.02	0.07	0.03	0.00	0.02	0.02	-0.01
31	38.10	1.001	-0.001	-0.009	0.14	0.27	0.35	-0.01	0.01	-0.15	0.00	0.00	0.01	0.00	0.00	0.00	0.00	0.00	-0.01	0.00

Table C5. Continued.

Case Z.S1			Station= 11			Date=1228.82			Time=21.29											
x= 152.4mm			Tunnel Run# = 121			Ue/Uo= 0.985														
No Bias Correction																				
LR	y(mm)	U/Ue	V/Ue	W/Ue	normalized by 0.001 Uet2			normalized by 0.0001 Uet3			<----->									
					uu	uv	uw	uuu	uvv	uvw										
1	0.38	0.604	-0.003	0.098	9.22	1.52	7.52	-1.23	0.07	0.60	-2.08	-0.03	-0.45	0.50	-0.07	0.44	-0.27	0.03	-0.30	0.02
2	0.51	0.630	-0.003	0.098	8.38	1.70	7.43	-1.27	0.02	0.39	1.64	-0.11	-0.10	0.48	-0.04	0.26	-0.37	0.04	-0.56	0.08
3	0.63	0.651	-0.002	0.104	7.23	1.89	6.84	-1.26	0.09	0.00	-1.00	-0.14	0.04	0.41	0.06	0.27	-0.14	0.03	-0.06	0.03
4	0.76	0.665	-0.001	0.104	6.97	1.89	7.23	-1.21	0.23	-0.10	-0.66	-0.15	-0.12	0.34	0.12	0.29	-0.22	0.10	-0.05	0.01
5	1.02	0.685	-0.002	0.108	6.46	2.07	6.62	-1.24	0.26	-0.32	-0.57	-0.13	0.00	0.32	0.14	0.25	-0.07	0.10	0.16	0.06
6	1.27	0.711	-0.003	0.107	5.93	2.11	6.66	-1.14	0.25	-0.26	-0.42	-0.14	-0.04	0.24	0.12	0.25	0.06	0.13	-0.28	-0.03
7	1.52	0.730	-0.003	0.108	5.70	2.14	6.63	-1.11	0.24	-0.34	-0.08	-0.08	0.09	0.19	0.11	0.36	-0.03	0.03	0.00	0.03
8	1.78	0.741	-0.003	0.107	5.49	2.13	6.41	-1.05	0.23	-0.37	-0.29	-0.09	-0.02	0.24	0.06	0.27	0.02	0.00	-0.34	0.04
9	2.03	0.755	-0.002	0.105	5.45	2.25	6.18	-1.19	0.26	-0.48	-0.30	-0.12	-0.03	0.25	0.19	0.27	0.09	0.05	0.12	0.01
10	2.29	0.764	-0.002	0.104	5.25	2.34	6.09	-1.17	0.31	-0.52	-0.31	-0.13	-0.02	0.27	0.11	0.24	0.12	0.05	-0.15	0.04
11	2.54	0.773	-0.002	0.104	4.99	2.27	6.39	-1.08	0.36	-0.64	-0.17	-0.09	-0.10	0.20	0.10	0.31	0.07	0.04	0.25	0.02
12	2.79	0.780	-0.002	0.104	4.75	2.30	6.09	-1.05	0.35	-0.53	-0.33	-0.10	-0.28	0.27	0.06	0.32	0.03	0.02	0.16	0.03
13	3.30	0.795	-0.002	0.104	4.68	2.33	5.87	-0.99	0.35	-0.69	-0.25	-0.10	-0.13	0.26	0.09	0.30	0.16	0.04	0.01	0.00
14	3.81	0.810	-0.002	0.101	4.70	2.46	5.71	-1.00	0.48	-0.87	-0.21	-0.12	-0.11	0.26	0.07	0.32	0.13	0.08	0.17	-0.01
15	4.32	0.819	-0.002	0.099	4.36	2.52	5.68	-0.92	0.44	-0.82	-0.50	-0.17	-0.21	0.35	0.02	0.28	0.16	0.09	0.28	-0.02
16	4.83	0.830	-0.002	0.100	4.40	2.62	5.45	-0.88	0.59	-0.98	-0.21	-0.12	-0.09	0.30	0.02	0.19	0.26	0.10	0.19	-0.08
17	5.59	0.839	-0.001	0.101	4.15	2.77	5.46	-0.85	0.73	-0.88	-0.19	-0.14	-0.17	0.26	0.12	0.27	0.17	0.12	0.30	-0.05
18	6.35	0.848	-0.003	0.097	4.12	2.90	5.45	-0.93	0.94	-1.02	-0.42	-0.14	-0.30	0.31	0.20	0.27	0.21	0.17	0.58	-0.06
19	7.11	0.855	-0.003	0.094	3.99	2.99	5.31	-0.91	0.90	-0.96	-0.26	-0.10	-0.28	0.25	0.16	0.31	0.17	0.19	0.65	-0.07
20	8.38	0.866	-0.005	0.090	3.81	3.10	5.21	-0.98	1.07	-1.03	-0.39	-0.13	-0.23	0.26	0.29	0.26	0.22	0.25	0.63	-0.12
21	10.16	0.873	-0.004	0.087	3.72	3.19	5.00	-0.99	1.13	-0.91	-0.47	-0.23	-0.22	0.23	0.44	0.21	0.19	0.31	0.53	-0.05
22	12.70	0.889	-0.003	0.076	3.88	3.20	4.92	-1.11	1.25	-1.07	-0.57	-0.30	-0.28	0.33	0.71	0.36	0.23	0.39	0.74	-0.13
23	15.24	0.907	-0.003	0.064	3.52	2.80	4.81	-1.00	1.14	-1.17	-0.73	-0.38	-0.35	0.33	0.66	0.40	0.34	0.44	0.96	-0.17
24	17.78	0.925	-0.002	0.051	3.35	2.56	4.44	-0.97	1.08	-1.22	-1.05	-0.45	-0.60	0.48	0.67	0.61	0.56	0.54	1.17	-0.29
25	20.32	0.940	0.002	0.040	3.04	2.28	3.91	-0.89	0.99	-1.18	-1.18	-0.44	-0.61	0.47	0.64	0.64	0.53	0.54	1.35	-0.26
26	22.86	0.951	0.005	0.029	2.55	2.01	3.41	-0.77	0.81	-1.04	-0.99	-0.39	-0.60	0.41	0.59	0.56	0.43	0.43	1.28	-0.24
27	25.40	0.964	0.009	0.020	2.30	1.93	2.98	-0.72	0.73	-0.97	-1.12	-0.38	-0.65	0.42	0.57	0.54	0.50	0.43	1.33	-0.22
28	27.94	0.976	0.012	0.013	1.87	1.79	2.44	-0.57	0.67	-0.79	-0.88	-0.35	-0.47	0.37	0.57	0.48	0.42	0.41	0.97	-0.19
29	30.48	0.989	0.007	0.000	1.02	1.26	1.50	-0.34	0.44	-0.50	-0.44	-0.24	-0.32	0.24	0.48	0.38	0.27	0.30	0.66	-0.16
30	33.02	0.996	0.004	-0.007	0.55	0.91	0.86	-0.16	0.20	-0.26	-0.17	-0.11	-0.09	0.13	0.29	0.16	0.09	0.12	0.23	-0.05
31	35.56	0.999	0.000	-0.011	0.25	0.53	0.52	-0.05	0.06	-0.19	-0.02	-0.03	-0.03	0.03	0.12	0.06	0.02	0.04	0.05	-0.02
32	38.10	1.001	-0.001	-0.013	0.19	0.38	0.42	-0.01	0.02	-0.16	0.00	0.00	0.00	0.01	0.03	0.01	0.00	0.01	0.00	0.00

Case Z.S1 Station= 13
x= 304.8mm Tunnel Run/= 124 Ue/Uo= 0.984 Date=1229.82 Time=13.30
No Bias Correction

[illegible]

Table C5. Concluded.

Case Z.S1			Station= 14		Date=1229.82		Time=15.02													
x= 457.2mm			Tunnel Run#= 125		Ue/Uo= 1.000															
No Bias Correction																				
LR	y (mm)	U/Ue	V/Ue	W/Ue	normalized by 0.001 Uet2			normalized by 0.0001 Uet3												
					uu	uv	uw	vu	vv	ww										
1	0.38	0.564	-0.003	0.060	9.66	1.21	6.77	-1.12	0.22	0.27	-2.23	-0.04	-0.53	0.47	-0.03	0.27	-0.41	0.02	0.53	0.01
2	0.51	0.597	-0.004	0.059	8.28	1.46	6.60	-1.11	0.16	0.23	-1.63	-0.05	-0.51	0.45	-0.03	0.30	-0.26	0.02	-0.64	0.01
3	0.63	0.619	-0.003	0.061	7.47	1.60	6.29	-1.12	0.17	0.16	0.88	-0.12	-0.36	0.41	0.02	0.28	-0.10	0.07	-0.29	-0.02
4	0.76	0.635	-0.003	0.062	6.77	1.65	6.19	-1.07	0.17	0.33	-0.47	-0.08	-0.27	0.24	0.03	0.30	-0.08	0.04	-0.16	-0.03
5	1.02	0.656	-0.002	0.063	6.70	1.70	5.55	-1.11	0.11	0.17	-0.17	-0.09	-0.05	0.20	0.05	0.27	-0.04	0.05	-0.20	-0.04
6	1.27	0.679	-0.003	0.065	6.44	1.72	5.18	-1.09	0.13	0.14	-0.34	-0.13	-0.17	0.21	0.09	0.17	-0.05	0.01	-0.21	-0.05
7	1.52	0.697	-0.002	0.067	6.24	1.75	4.96	-1.05	0.05	0.18	-0.22	-0.09	-0.11	0.21	0.08	0.22	-0.09	0.04	-0.41	0.00
8	1.78	0.710	-0.002	0.067	6.09	1.82	4.77	-1.10	0.04	0.12	-0.30	-0.12	-0.21	0.21	0.11	0.17	0.01	0.02	-0.02	0.02
9	2.03	0.724	-0.002	0.068	6.03	1.82	4.61	-1.06	0.10	-0.21	-0.30	-0.09	-0.03	0.21	0.12	0.19	0.06	0.05	-0.07	-0.01
10	2.29	0.737	-0.002	0.069	5.75	1.84	4.42	-1.11	0.05	0.05	-0.58	-0.13	-0.17	0.23	0.16	0.24	-0.02	0.06	-0.08	0.01
11	2.54	0.743	-0.001	0.070	5.64	1.79	4.22	-1.09	0.08	-0.07	-0.47	-0.12	-0.13	0.27	0.12	0.14	-0.06	0.00	-0.08	0.04
12	2.79	0.753	-0.002	0.070	5.64	1.90	4.15	-1.13	0.06	-0.08	-0.75	-0.15	-0.11	0.29	0.15	0.23	-0.13	0.02	-0.09	0.03
13	3.30	0.771	-0.003	0.071	5.41	1.96	3.83	-1.24	0.14	-0.13	-0.63	-0.16	-0.07	0.31	0.12	0.15	0.01	-0.01	-0.04	0.02
14	3.81	0.781	-0.002	0.074	4.91	1.94	3.80	-1.07	0.15	-0.14	-0.71	-0.10	-0.11	0.27	0.12	0.17	-0.02	0.05	0.03	0.01
15	4.32	0.794	-0.002	0.074	4.86	2.00	3.64	-1.09	0.19	-0.13	-0.63	-0.13	-0.12	0.24	0.14	0.15	0.00	0.02	-0.22	0.04
16	4.83	0.801	-0.002	0.075	4.66	1.90	3.54	-1.02	0.16	-0.15	-0.50	-0.04	-0.13	0.20	0.08	0.18	0.01	0.03	-0.03	0.05
17	5.59	0.819	-0.003	0.075	4.48	2.00	3.52	-1.12	0.21	-0.28	-0.62	-0.13	-0.12	0.27	0.10	0.14	0.09	0.00	-0.07	0.01
18	6.35	0.832	-0.003	0.073	3.93	2.00	3.46	-1.02	0.31	-0.33	-0.53	-0.12	-0.08	0.23	0.15	0.11	0.03	0.00	-0.10	0.02
19	7.11	0.843	-0.003	0.072	3.87	2.02	3.25	-0.99	0.30	-0.30	-0.51	-0.14	-0.04	0.23	0.14	0.12	0.01	-0.01	0.01	0.06
20	8.38	0.860	-0.005	0.070	3.50	2.01	3.13	-0.94	0.33	-0.39	-0.42	-0.11	-0.10	0.19	0.12	0.10	0.06	0.00	0.01	0.02
21	10.16	0.874	-0.003	0.069	3.24	2.03	3.09	-0.84	0.41	-0.37	-0.36	-0.13	-0.07	0.21	0.16	0.13	0.04	0.04	0.00	0.01
22	12.70	0.890	0.001	0.066	2.88	1.98	3.09	-0.79	0.48	-0.40	-0.26	-0.10	-0.03	0.17	0.11	0.13	0.03	0.04	0.10	0.00
23	15.24	0.907	0.000	0.061	2.62	1.96	2.90	-0.72	0.54	-0.46	-0.18	-0.07	-0.07	0.13	0.13	0.09	0.09	0.08	0.08	-0.03
24	17.78	0.920	0.002	0.055	2.54	1.93	2.81	-0.67	0.55	-0.52	-0.32	-0.14	-0.05	0.16	0.18	0.13	0.08	0.11	0.17	-0.03
25	20.32	0.930	0.002	0.049	2.40	1.86	2.68	-0.68	0.55	-0.53	-0.32	-0.13	-0.11	0.17	0.20	0.15	0.12	0.13	0.25	-0.05
26	22.86	0.938	0.003	0.044	2.28	1.80	2.47	-0.66	0.58	-0.57	-0.43	-0.16	-0.11	0.16	0.30	0.17	0.11	0.15	0.35	-0.03
27	25.40	0.946	0.006	0.040	2.15	1.79	2.52	-0.61	0.60	-0.57	-0.38	-0.15	-0.12	0.16	0.29	0.22	0.12	0.17	0.39	-0.05
28	27.94	0.957	0.007	0.032	1.98	1.63	2.39	-0.53	0.60	-0.64	-0.51	-0.16	-0.20	0.17	0.28	0.24	0.19	0.21	0.48	-0.08
29	30.48	0.967	0.009	0.028	1.85	1.62	2.17	-0.55	0.57	-0.65	-0.52	-0.18	-0.22	0.21	0.32	0.24	0.24	0.20	0.55	-0.09
30	33.02	0.979	0.006	0.016	1.47	1.30	1.74	-0.43	0.45	-0.55	-0.54	-0.22	-0.25	0.23	0.32	0.25	0.26	0.22	0.54	-0.10
31	35.56	0.987	0.004	0.009	0.99	1.09	1.30	-0.30	0.31	-0.42	-0.36	-0.16	-0.21	0.17	0.29	0.23	0.20	0.18	0.50	-0.09
32	38.10	0.993	0.004	0.004	0.73	0.89	0.95	-0.23	0.23	-0.31	-0.24	-0.14	-0.14	0.14	0.26	0.17	0.14	0.14	0.27	-0.07
33	40.64	0.998	0.002	0.000	0.42	0.63	0.63	-0.11	0.12	-0.21	-0.11	-0.07	-0.06	0.08	0.16	0.09	0.06	0.08	0.12	-0.03
34	43.18	1.000	0.001	-0.001	0.25	0.44	0.43	-0.04	0.04	-0.15	-0.03	-0.02	-0.01	0.03	0.06	0.03	0.01	0.02	0.02	-0.01
35	50.80	1.003	0.002	-0.002	0.13	0.27	0.29	-0.01	0.02	-0.11	0.00	-0.00	0.00	0.00	0.01	0.00	0.00	0.00	0.00	0.00

Case Z.SIB		Station= 1	Date= 904.84	Time=18.25															
x=-154.0mm		Tunnel Run# = 161	Ue/Uo= 1.000																
No Bias Correction																			
LR	y(mm)	U/Ue	V/Ue	W/Ue	uu	uv	uw	uuu	uvv	uvw	uuv	uuw	uuu normalized by 0.0001	uvv normalized by 0.0001	uvw normalized by 0.0001	Uet3	WVV	WWW	UVW
1	0.38	0.622	0.022	0.332	12.06	4.54	15.58	-1.88	2.40	-4.10	-1.68	-0.77	-2.49	1.16	0.61	1.68	0.96	0.85	-1.12
2	0.51	0.642	0.025	0.311	11.65	4.68	14.74	-2.02	2.57	-4.20	-2.48	-0.73	-2.71	1.28	0.91	1.69	1.14	2.27	-1.10
3	0.63	0.658	0.026	0.302	11.07	4.47	14.18	-1.82	2.50	-3.63	-1.41	-0.55	-2.04	1.16	0.83	1.63	0.85	1.80	-0.87
4	0.76	0.674	0.024	0.285	10.73	4.44	13.74	-1.84	2.54	-3.77	-0.98	-0.59	-1.69	0.93	0.66	1.16	0.89	0.91	-0.74
5	1.02	0.699	0.022	0.259	10.48	4.37	12.98	-1.68	2.28	-3.62	-1.58	-0.68	-1.92	0.89	0.68	1.30	0.91	2.12	-0.77
6	1.27	0.715	0.019	0.240	10.25	4.37	12.31	-1.86	2.24	-3.54	-2.02	-0.83	-2.03	1.12	0.88	1.46	0.94	2.41	-0.82
7	1.52	0.736	0.014	0.223	9.33	3.94	11.82	-1.59	1.93	-3.16	-2.01	-0.51	-2.18	0.94	0.69	1.45	0.84	2.66	-0.67
8	1.78	0.748	0.014	0.205	9.62	4.10	11.74	-1.73	2.13	-3.47	-2.63	-0.80	-2.68	1.38	0.87	1.55	0.80	4.00	-0.93
9	2.03	0.759	0.012	0.194	8.81	4.01	10.74	-1.58	1.91	-3.24	-2.29	-0.84	-2.26	1.17	0.76	1.47	1.07	2.78	-0.87
10	2.29	0.768	0.012	0.188	8.59	4.10	10.34	-1.65	2.00	-2.90	-2.07	-0.66	-2.35	1.06	0.70	1.65	1.00	3.90	-0.85
11	2.54	0.773	0.011	0.183	8.44	4.07	10.32	-1.65	2.07	-3.24	-2.50	-0.91	-2.31	1.20	0.83	1.92	1.16	3.42	-0.98
12	2.79	0.779	0.014	0.178	8.54	4.09	9.82	-1.67	1.92	-2.93	-2.07	-0.70	-1.96	1.08	0.92	1.70	1.61	3.14	-0.86
13	3.30	0.792	0.013	0.166	8.18	4.30	9.62	-1.76	1.82	-3.08	-2.13	-0.91	-1.94	1.22	0.81	1.55	1.07	3.14	-0.86
14	3.81	0.794	0.013	0.165	7.56	4.46	9.04	-1.73	1.99	-2.80	-1.77	-0.81	-1.39	1.11	0.92	1.50	1.32	2.39	-0.72
15	4.32	0.799	0.012	0.161	7.71	4.66	8.92	-1.85	2.08	-2.76	-1.38	-0.67	-1.16	0.93	0.83	1.23	1.14	2.45	-0.64
16	4.83	0.806	0.011	0.153	6.97	4.44	8.38	-1.55	1.91	-2.45	-1.42	-0.62	-1.18	0.85	0.66	1.30	0.81	2.47	-0.65
17	5.59	0.813	0.012	0.145	6.82	4.53	8.10	-1.64	1.85	-2.19	-1.25	-0.63	-0.88	0.77	0.82	1.18	0.89	2.22	-0.59
18	6.35	0.816	0.016	0.145	6.82	4.79	8.10	-1.83	1.92	-2.21	-1.34	-0.64	-0.70	0.80	1.01	1.03	0.78	1.73	-

Table C6. Continued.

Case Z.S18		Station= 3		Date= 906.84		Time=10.09	
x= 6.3mm		Tunnel Run# 174		Ue/U0= 0.987			
No Bias Correction							
LR	y(mm)	U/Ue	V/Ue	W/Ue	uu	vv	ww
1	0.25	0.592	-0.015	0.373	10.25	3.64	10.22
2	0.38	0.625	-0.014	0.368	9.84	3.78	11.25
3	0.51	0.652	-0.013	0.348	10.70	4.25	11.95
4	0.63	0.678	-0.010	0.334	10.83	4.19	12.48
5	0.76	0.694	-0.008	0.314	11.00	4.05	12.64
6	1.02	0.715	-0.004	0.283	10.74	3.70	12.51
7	1.27	0.731	0.000	0.264	11.00	3.71	12.00
8	1.52	0.742	0.006	0.247	10.68	3.74	11.92
9	1.78	0.759	0.005	0.225	10.00	3.70	11.04
10	2.03	0.775	0.005	0.210	9.11	3.74	10.41
11	2.29	0.776	0.007	0.200	9.29	3.78	10.11
12	2.54	0.785	0.010	0.191	9.03	3.88	10.18
13	2.79	0.788	0.011	0.188	8.72	3.82	10.08
14	3.30	0.792	0.012	0.177	8.35	4.01	9.32
15	3.81	0.800	0.013	0.169	7.90	4.08	9.08
16	4.32	0.803	0.014	0.163	7.51	4.26	8.82
17	4.83	0.809	0.015	0.155	7.34	4.36	8.28
18	5.59	0.817	0.015	0.148	7.20	4.49	7.97
19	6.35	0.819	0.014	0.144	6.71	4.44	7.50
20	7.11	0.828	0.014	0.134	6.60	4.42	7.69
21	8.38	0.834	0.015	0.124	6.10	4.53	6.91
22	10.16	0.849	0.016	0.114	6.10	4.40	6.83
23	12.70	0.871	0.020	0.100	5.58	4.13	5.90
24	15.24	0.891	0.023	0.088	5.31	3.79	5.41
25	17.78	0.914	0.024	0.075	4.71	3.50	4.89
26	20.32	0.936	0.026	0.060	4.83	3.25	4.29
27	22.86	0.968	0.019	0.035	2.83	2.38	2.73
28	25.40	0.989	0.016	0.020	1.10	1.45	1.29
29	30.48	1.001	0.016	0.014	0.30	0.87	0.45

52

Table C6. Continued.

Case Z.S1B			Station= 5		Date= 905.84		Time=15.02													
x= 25.4mm			Tunnel Run#= 172		Ue/Uo= 1.000															
No Bias Correction																				
LR	y(mm)	U/Ue	V/Ue	W/Ue	normalized by 0.001 Uet2			normalized by 0.0001 Uet3												
					uu	uv	uw	uuu	uvv	uuv										
1	0.25	0.571	-0.005	0.257	9.67	2.40	9.76	-1.36	-0.12	-0.01	0.18	-0.06	0.70	0.21	0.06	0.29	-1.00	-0.11	-1.98	0.18
2	0.38	0.606	-0.006	0.259	9.35	2.86	10.37	-1.42	-0.03	-1.00	0.73	-0.03	0.91	0.14	-0.01	0.16	-0.92	-0.09	-1.98	0.22
3	0.51	0.634	-0.005	0.260	9.04	3.01	9.98	-1.44	0.29	-1.02	-0.05	-0.13	0.46	0.27	0.13	0.38	-0.27	-0.09	-0.96	0.33
4	0.63	0.652	-0.005	0.257	8.95	3.15	10.18	-1.49	0.42	-1.56	0.39	-0.01	0.54	0.18	0.04	0.35	-0.09	-0.04	-0.54	0.15
5	0.76	0.673	-0.007	0.250	8.92	3.17	9.89	-1.47	0.57	-1.88	0.10	-0.20	-0.11	0.25	0.20	0.14	0.03	-0.06	-0.46	0.22
6	1.02	0.705	-0.003	0.240	8.41	3.30	9.98	-1.29	0.95	-2.39	0.28	-0.18	-0.32	0.32	0.30	0.26	0.32	0.02	0.31	0.00
7	1.27	0.725	-0.003	0.230	8.65	3.28	9.82	-1.26	1.05	-2.35	-0.68	-0.22	-0.80	0.54	0.27	0.39	1.01	0.15	0.64	-0.12
8	1.52	0.743	-0.002	0.218	8.30	3.32	9.75	-1.08	1.27	-2.57	-0.66	-0.23	-0.77	0.41	0.34	0.40	1.01	0.26	0.72	-0.13
9	1.78	0.758	-0.003	0.210	8.24	3.26	9.90	-1.10	1.36	-2.61	-0.90	-0.25	-1.09	0.55	0.30	0.62	1.08	0.36	0.92	-0.29
10	2.03	0.768	0.000	0.201	8.19	3.46	9.84	-1.22	1.56	-2.79	-1.11	-0.39	-1.43	0.66	0.35	0.98	1.38	0.48	1.84	-0.46
11	2.29	0.777	0.000	0.192	8.28	3.47	9.41	-1.18	1.65	-2.91	-1.15	-0.53	-1.29	0.76	0.46	1.03	1.18	0.71	1.94	-0.56
12	2.54	0.782	0.001	0.185	8.12	3.54	9.36	-1.27	1.61	-2.83	-1.43	-0.49	-1.36	0.87	0.49	0.91	1.21	0.62	1.99	-0.49
13	2.79	0.787	0.001	0.182	7.84	3.61	9.00	-1.25	1.54	-2.83	-1.01	-0.52	-1.58	0.73	0.54	0.92	1.28	0.71	2.02	-0.46
14	3.30	0.798	-0.001	0.169	7.85	3.77	8.74	-1.33	1.70	-2.79	-1.56	-0.60	-1.47	0.99	0.48	1.24	1.33	0.78	2.36	-0.65
15	3.81	0.802	0.002	0.162	7.39	3.78	8.54	-1.32	1.73	-2.62	-1.13	-0.46	-1.03	0.72	0.59	1.10	1.14	0.65	2.14	-0.50
16	4.32	0.805	0.003	0.157	7.00	3.85	8.02	-1.41	1.64	-2.55	-1.43	-0.49	-1.21	0.81	0.43	0.92	0.95	0.66	1.75	-0.48
17	4.83	0.810	0.004	0.150	7.11	4.01	7.85	-1.46	1.61	-2.31	-1.43	-0.55	-0.80	0.77	0.72	1.04	0.84	0.66	1.52	-0.44
18	5.59	0.815	0.003	0.141	6.48	4.04	7.56	-1.47	1.59	-2.15	-1.38	-0.41	-0.72	0.62	0.65	0.72	0.75	0.61	1.45	-0.40
19	6.35	0.820	0.004	0.138	6.39	4.11	7.14	-1.60	1.69	-2.11	-1.07	-0.50	-0.71	0.65	0.71	0.69	0.69	0.61	1.39	-0.37
20	7.11	0.826	0.006	0.134	6.22	4.23	6.88	-1.58	1.65	-1.82	-0.98	-0.50	-0.60	0.43	0.66	0.81	0.82	0.76	1.24	-0.44
21	8.38	0.841	0.007	0.122	5.73	4.09	6.58	-1.46	1.52	-1.82	-0.60	-0.33	-0.51	0.30	0.74	0.62	0.41	0.41	0.92	-0.14
22	10.16	0.856	0.007	0.110	5.64	4.02	6.18	-1.49	1.45	-1.49	-0.81	-0.37	-0.17	0.28	0.62	0.41	0.24	0.41	0.92	-0.14
23	12.70	0.878	0.010	0.095	5.19	3.74	5.60	-1.53	1.45	-1.49	-0.82	-0.49	-0.51	0.35	0.74	0.53	0.34	0.52	1.28	-0.24
24	15.24	0.894	0.017	0.086	5.03	3.54	5.43	-1.34	1.26	-1.33	-0.94	-0.34	-0.41	0.36	0.63	0.35	0.35	0.38	1.09	-0.21
25	17.78	0.917	0.019	0.072	4.66	3.35	4.57	-1.33	1.04	-1.14	-1.34	-0.50	-0.44	0.52	0.66	0.47	0.35	0.45	1.22	-0.18
26	20.32	0.951	0.013	0.049	3.40	2.55	3.41	-0.98	0.77	-1.06	-1.46	-0.50	-0.71	0.53	0.71	0.55	0.67	0.49	1.37	-0.28
27	22.86	0.973	0.009	0.031	2.01	1.81	2.10	-0.59	0.43	-0.68	-1.07	-0.41	-0.60	0.42	0.57	0.38	0.44	0.33	1.02	-0.20
28	25.40	0.993	0.006	0.021	0.94	1.17	1.11	-0.25	0.22	-0.29	-0.40	-0.19	-0.25	0.18	0.31	0.23	0.23	0.18	0.49	-0.09
29	27.94	0.998	0.007	0.015	0.49	0.92	0.63	-0.13	0.10	-0.12	-0.12	-0.09	-0.06	0.10	0.22	0.09	0.05	0.10	0.12	-0.04
30	30.48	0.999	0.008	0.015	0.28	0.71	0.41	-0.05	0.03	-0.05	-0.01	-0.03	0.00	0.03	0.14	0.04	0.00	0.02	0.02	0.01
31	35.56	1.000	0.006	0.014	0.15	0.46	0.27	0.00	0.00	-0.05	0.00	0.00	0.00	0.00	0.02	0.00	0.00	0.00	0.00	0.00
32	45.72	1.000	0.006	0.015	0.12	0.40	0.26	0.00	0.01	-0.04	0.00	0.00	0.00	0.00	0.00	0.00	0.00	0.00	-0.01	0.00

Table C6. Continued.

Case Z.SIB		Station= 6		Date= 995.84		Time=14.06	
x= 50.8mm		Tunnel Run# = 171		U ₀ /U ₀₀ = 0.999			
No Bias Correction							
LR	y(mm)	U/U ₀	V/U ₀	W/U ₀	U	V	W
1	0.25	0.558	0.000	0.173	10.10	1.97	9.61
2	0.38	0.592	0.001	0.184	8.72	2.26	9.04
3	0.51	0.620	-0.001	0.189	7.60	2.61	8.59
4	0.63	0.641	0.000	0.192	7.86	2.98	8.64
5	0.76	0.660	0.001	0.192	7.48	2.98	8.52
6	1.02	0.680	0.001	0.193	7.55	3.23	8.78
7	1.27	0.702	0.002	0.192	7.49	3.17	8.38
8	1.52	0.725	0.000	0.190	7.41	3.14	7.73
9	1.78	0.740	0.000	0.185	7.24	3.12	7.65
10	2.03	0.753	0.001	0.182	7.25	3.13	7.88
11	2.29	0.767	0.001	0.176	7.11	3.22	7.74
12	2.54	0.772	0.004	0.175	7.28	3.27	7.77
13	2.79	0.783	0.001	0.168	6.73	3.32	7.62
14	3.30	0.795	0.003	0.164	6.91	3.56	7.60
15	3.81	0.799	0.005	0.159	6.38	3.56	7.69
16	4.32	0.805	0.005	0.155	6.15	3.88	7.29
17	4.83	0.811	0.005	0.151	6.25	3.90	7.42
18	5.59	0.817	0.005	0.145	6.14	4.07	7.30
19	6.35	0.824	0.007	0.141	5.91	4.35	7.07
20	7.11	0.826	0.008	0.137	5.93	4.14	7.02
21	8.38	0.835	0.009	0.128	5.86	4.27	6.69
22	10.16	0.847	0.010	0.116	5.62	4.06	6.25
23	12.70	0.869	0.009	0.097	5.28	3.94	5.76
24	15.24	0.893	0.015	0.087	4.88	3.67	5.30
25	17.78	0.914	0.016	0.073	4.57	3.29	4.57
26	20.32	0.932	0.021	0.063	3.99	3.14	4.09
27	22.86	0.949	0.023	0.052	3.63	2.86	3.56
28	25.40	0.978	0.014	0.032	2.05	2.01	2.13
29	27.94	0.994	0.008	0.019	0.80	1.16	0.97
30	30.48	0.995	0.006	0.016	0.35	0.77	0.50
31	35.56	1.001	0.006	0.015	0.17	0.51	0.32
32	45.72	0.999	0.005	0.016	0.12	0.42	0.28

Case Z.S1B Station= 7
 x= 101.6mm Tunnel Run# = 170 U_g/U₀= 0.997 Date= 905.84 Time=13.14
 No Bias Correction

55

Table C7. LDV measurements for forward-facing step with spin.

Case S.S1				Station= 1				Date= 904.84				Time=17.46						
x= -12.7mm				Tunnel Run#= 160				U ₀ /U _∞ = 1.000										
No Bias Correction																		
LR	y (mm)	U/U ₀	V/U ₀	W/U ₀	normalized by 0.001 Uot2				normalized by 0.0001 Uot3				normalized by 0.0001 Uot3					
					uu	uv	uw	vw	uuu	uvv	uuv	uuw	vuu	vuv	vuv	uvw		
1	0.25	0.651	-0.012	0.312	11.57	-1.62	1.73	-4.06	-1.91	-0.55	-1.96	0.93	0.32	1.02	2.09	0.61	1.18	-0.73
2	0.38	0.659	-0.010	0.303	10.85	-1.63	1.76	-3.93	-1.22	-0.43	-1.62	0.67	0.48	1.30	1.44	0.59	2.08	-0.53
3	0.51	0.673	-0.008	0.284	10.16	-1.45	1.69	-3.27	-1.36	-0.43	-1.19	0.71	0.55	1.10	1.55	0.55	0.82	-0.50
4	0.63	0.685	-0.008	0.270	10.29	-1.56	1.75	-3.55	-1.78	-0.46	-1.88	0.70	0.52	1.07	1.50	0.56	2.28	-0.51
5	0.76	0.701	-0.009	0.257	10.02	-1.48	1.76	-3.50	-1.77	-0.66	-1.70	0.83	0.55	0.97	1.51	0.65	1.72	-0.56
6	1.02	0.717	-0.006	0.241	9.85	-1.68	1.84	-3.57	-1.98	-0.63	-2.04	0.93	0.76	1.43	1.93	0.81	2.28	-0.70
7	1.27	0.733	-0.004	0.226	9.61	-1.57	1.95	-3.48	-1.46	-0.62	-1.24	0.82	0.66	1.00	1.22	0.73	1.69	-0.55
8	1.52	0.754	-0.008	0.202	9.10	-1.48	1.71	-3.24	-1.95	-0.57	-2.11	0.91	0.54	1.40	1.68	0.82	3.00	-0.69
9	1.78	0.765	-0.006	0.193	8.85	-1.38	1.64	-3.15	-2.31	-0.61	-2.01	1.01	0.59	1.35	1.96	0.78	2.61	-0.71
10	2.03	0.773	-0.005	0.186	8.96	-1.55	1.86	-3.37	-2.09	-0.68	-2.18	1.14	0.55	1.44	1.91	0.96	2.71	-0.79
11	2.29	0.781	-0.006	0.175	8.43	-1.50	1.59	-3.13	-2.36	-0.60	-2.12	1.12	0.58	1.49	1.96	0.82	3.21	-0.79
12	2.54	0.783	-0.003	0.173	8.45	-1.60	1.79	-3.39	-2.18	-0.74	-1.86	1.08	0.77	1.45	1.58	0.95	2.78	-0.79
13	2.79	0.785	-0.002	0.170	8.27	-1.73	1.78	-3.22	-1.94	-0.85	-1.86	1.14	0.85	1.30	1.68	1.03	2.43	-0.83
14	3.30	0.791	-0.001	0.162	7.94	-1.58	1.74	-2.97	-1.98	-0.68	-1.37	1.04	0.68	1.23	1.29	0.81	2.18	-0.72
15	3.81	0.797	0.000	0.156	7.28	-1.70	1.84	-2.57	-1.82	-0.63	-1.47	0.88	0.62	1.28	1.28	0.75	2.30	-0.67
16	4.32	0.797	0.001	0.152	7.12	-1.87	1.83	-2.85	-1.56	-0.71	-1.36	0.89	0.67	1.14	1.33	0.77	2.28	-0.74
17	4.83	0.806	0.003	0.148	7.18	-1.76	1.95	-2.63	-1.02	-0.66	-0.94	0.74	0.80	1.13	0.95	0.84	1.54	-0.61
18	5.59	0.812	0.003	0.139	6.55	-1.65	1.82	-2.30	-1.02	-0.48	-1.01	0.57	0.72	1.02	0.74	0.74	1.73	-0.55
19	6.35	0.815	0.005	0.134	6.61	-1.81	1.89	-2.36	-1.34	-0.55	-0.94	0.58	0.81	0.99	0.93	0.77	1.82	-0.49
20	7.11	0.822	0.006	0.131	6.36	-1.84	1.94	-2.18	-1.10	-0.50	-0.78	0.50	0.73	0.87	0.72	0.70	1.70	-0.44
21	8.38	0.828	0.012	0.127	5.93	-1.61	1.81	-1.80	-0.58	-0.36	-0.21	0.25	0.66	0.62	0.25	0.66	1.17	-0.20
22	10.16	0.855	0.010	0.108	5.54	-1.52	1.57	-1.62	-0.80	-0.42	-0.31	0.36	0.62	0.53	0.41	0.56	1.28	-0.19
23	12.70	0.874	0.012	0.090	5.13	-1.57	1.40	-1.66	-1.26	-0.60	-0.66	0.46	0.94	0.59	0.56	0.63	1.34	-0.36
24	15.24	0.901	0.015	0.074	4.48	-1.41	1.35	-1.44	-1.26	-0.52	-0.76	0.51	0.90	0.75	0.56	0.61	1.96	-0.30
25	17.78	0.925	0.018	0.058	3.97	-1.20	1.06	-1.17	-1.59	-0.63	-0.70	0.67	0.92	0.71	0.64	0.58	1.58	-0.36
26	20.32	0.952	0.014	0.040	2.71	-0.87	0.68	-0.98	-1.45	-0.56	-0.74	0.58	0.75	0.56	0.64	0.51	1.32	-0.31
27	22.86	0.973	0.014	0.026	1.65	-0.50	0.42	-0.52	-0.91	-0.35	-0.45	0.35	0.57	0.41	0.43	0.33	0.90	-0.20
28	25.40	0.985	0.013	0.018	0.86	-0.28	0.19	-0.29	-0.36	-0.22	-0.19	0.20	0.36	0.20	0.17	0.17	0.32	-0.09
29	27.94	0.997	0.012	0.015	0.36	-0.07	0.05	-0.12	-0.03	-0.04	-0.02	0.04	0.15	0.05	0.02	0.05	0.04	-0.01
30	30.48	0.996	0.010	0.014	0.21	-0.01	-0.01	-0.08	0.00	0.00	0.00	0.00	0.00	0.01	0.00	0.00	-0.01	0.00
31	45.72	1.000	0.011	0.016	0.12	-0.01	0.01	-0.07	0.00	0.00	0.00	0.00	0.00	0.00	0.00	0.00	0.00	0.00

Table C7. Continued.

Case S.51			Station= 2			Date= 904.84			Time=19.26						
x= 6.3mm			Tunnel Run#= 162			Ue/Uo= 0.997									
No Bias Correction															
LR	y(mm)	U/Uo	V/Uo	W/Uo	normalized by 0.001 Uot2			normalized by 0.0001 Uot3							
					uu	vv	ww	uuu	uvv	uvw					
1	0.25	0.588	-0.005	0.348	10.31	2.66	10.94	-1.20	0.48	-2.02	0.24	-0.04	-0.27	-2.16	0.25
2	0.38	0.634	-0.002	0.334	9.75	3.17	11.82	-1.04	1.06	-2.75	0.00	0.30	-0.20	-1.38	0.07
3	0.51	0.659	0.000	0.321	9.96	3.42	11.31	-1.03	1.38	-2.75	0.14	0.76	0.06	-1.10	0.01
4	0.63	0.679	0.002	0.306	9.74	3.73	12.04	-1.20	1.77	-3.00	-0.59	-0.05	-0.84	0.23	-0.05
5	0.76	0.692	0.003	0.293	9.50	4.01	12.03	-1.34	1.97	-3.11	-0.62	-0.26	-1.08	0.44	-0.25
6	1.02	0.712	0.005	0.269	9.88	4.04	11.56	-1.52	2.03	-3.30	-0.68	-0.28	-1.22	0.59	-0.44
7	1.27	0.728	0.005	0.254	9.87	4.00	11.65	-1.53	2.16	-3.47	-2.13	-0.45	-1.85	0.54	-0.54
8	1.52	0.734	0.009	0.241	9.93	4.03	11.42	-1.45	1.90	-3.50	-1.76	-0.54	-1.80	0.89	-0.54
9	1.78	0.749	0.007	0.226	9.03	3.98	10.59	-1.54	1.93	-3.63	-2.00	-0.61	-1.92	0.82	-0.62
10	2.03	0.762	0.005	0.209	8.88	3.84	10.18	-1.41	1.74	-3.28	-1.93	-0.59	-1.85	0.99	-0.75
11	2.29	0.766	0.004	0.200	8.21	3.78	9.60	-1.35	1.66	-3.07	-1.76	-0.56	-2.02	0.85	-0.70
12	2.54	0.770	0.005	0.191	8.30	3.98	9.58	-1.45	1.68	-3.00	-1.90	-0.70	-1.86	0.97	-0.65
13	2.79	0.780	0.006	0.181	8.00	3.80	8.99	-1.47	1.64	-2.75	-2.10	-0.51	-1.68	0.89	-0.72
14	3.30	0.788	0.005	0.170	7.84	3.99	8.89	-1.40	1.71	-2.97	-2.19	-0.66	-1.78	1.16	-0.64
15	3.81	0.792	0.008	0.165	7.51	3.98	8.35	-1.51	1.65	-2.64	-1.81	-0.60	-1.43	0.82	-0.64
16	4.32	0.800	0.007	0.157	6.77	3.95	7.85	-1.37	1.59	-2.40	-1.10	-0.29	-0.85	0.50	-0.40
17	4.83	0.801	0.009	0.152	6.88	4.20	7.70	-1.50	1.76	-2.58	-1.66	-0.60	-1.24	0.66	-0.59
18	5.59	0.810	0.009	0.145	6.40	4.15	7.23	-1.54	1.59	-2.15	-1.12	-0.52	-0.77	0.64	-0.50
19	6.35	0.812	0.011	0.141	6.05	4.32	7.17	-1.50	1.58	-2.16	-0.63	-0.44	-0.56	0.37	-0.31
20	7.11	0.820	0.012	0.137	6.06	4.33	6.92	-1.60	1.72	-2.20	-0.97	-0.54	-0.52	0.55	-0.37
21	8.38	0.832	0.010	0.124	5.89	4.22	6.53	-1.59	1.65	-1.81	-0.87	-0.42	-0.63	0.44	-0.37
22	10.16	0.846	0.011	0.109	5.37	4.08	6.03	-1.43	1.53	-1.59	-0.93	-0.51	-0.47	0.39	-0.28
23	12.70	0.863	0.017	0.097	5.21	3.70	5.68	-1.47	1.39	-1.52	-1.13	-0.46	-0.45	0.43	-0.29
24	15.24	0.885	0.022	0.082	4.70	3.52	5.08	-1.35	1.21	-1.26	-0.97	-0.38	-0.41	0.34	-0.12
25	17.78	0.908	0.023	0.068	4.39	3.13	4.44	-1.21	0.98	-1.20	-1.19	-0.45	-0.46	0.49	-0.23
26	20.32	0.927	0.027	0.058	3.91	3.01	3.84	-1.08	0.80	-1.09	-1.36	-0.48	-0.56	0.55	-0.24
27	22.86	0.954	0.023	0.037	2.59	2.36	2.71	-0.73	0.59	-0.72	-1.08	-0.42	-0.47	0.42	-0.16
28	25.40	0.974	0.018	0.023	1.40	1.68	1.55	-0.44	0.32	-0.44	-0.66	-0.32	-0.32	0.32	-0.13
29	30.48	0.992	0.016	0.013	0.31	0.84	0.46	-0.05	0.02	-0.10	-0.01	-0.02	-0.01	0.03	0.00
30	35.56	0.994	0.014	0.014	0.15	0.54	0.30	-0.01	0.01	-0.09	0.00	0.00	0.00	0.00	0.00
31	45.72	0.997	0.015	0.015	0.12	0.51	0.29	0.00	0.00	-0.07	0.00	0.00	0.00	0.00	0.00
					normalized by 0.001 Uot2			normalized by 0.0001 Uot3							
					uuu	uvv	uvw	uuu	uvv	uvw	uuu	uvv	uvw	uuu	uvv
					0.00	0.05	0.29	0.22	-0.15	0.29	0.14	0.06	0.09	0.19	0.03
					0.14	0.06	0.09	0.22	-0.03	-0.22	0.24	-0.03	0.22	0.07	
					-0.59	-0.05	-0.72	0.32	0.23	-0.72	-0.59	-0.05	-0.72	0.23	
					-0.62	-0.26	-1.08	0.47	0.48	-1.08	-0.62	-0.26	-1.08	0.44	
					-0.68	-0.28	-1.22	0.58	0.50	-1.22	-0.68	-0.28	-1.22	0.59	
					-1.76	-0.54	-1.85	0.89	0.54	-1.85	-2.13	-0.45	-1.85	0.54	
					-2.00	-0.61	-1.92	0.86	0.82	-1.92	-2.00	-0.61	-1.92	0.82	
					-1.93	-0.59	-1.85	0.99	0.45	-1.85	-1.93	-0.59	-1.85	0.99	
					-1.76	-0.56	-2.02	0.85	0.47	-2.02	-1.76	-0.56	-2.02	0.85	
					-1.90	-0.70	-1.86	0.97	0.69	-1.86	-1.90	-0.70	-1.86	0.97	
					-1.80	-0.51	-1.68	0.89	0.46	-1.68	-2.10	-0.51	-1.68	0.89	
					-2.19	-0.66	-1.78	1.16	0.59	-1.78	-2.19	-0.66	-1.78	1.16	
					-1.81	-0.60	-1.43	0.82	0.66	-1.43	-1.81	-0.60	-1.43	0.82	
					-1.10	-0.29	-0.85	0.50	0.36	-0.85	-1.10	-0.29	-0.85	0.50	
					-1.66	-0.60	-1.24	0.66	0.67	-1.24	-1.66	-0.60	-1.24	0.66	
					-1.12	-0.52	-0.77	0.64	0.66	-0.77	-1.12	-0.52	-0.77	0.64	
					-0.63	-0.44	-0.56	0.37	0.56	-0.56	-0.63	-0.44	-0.56	0.37	
					-0.97	-0.54	-0.52	0.55	0.60	-0.52	-0.97	-0.54	-0.52	0.55	
					-0.87	-0.42	-0.63	0.44	0.60	-0.63	-0.87	-0.42	-0.63	0.44	
					-0.93	-0.51	-0.47	0.39	0.67	-0.47	-0.93	-0.51	-0.47	0.39	
					-1.13	-0.46	-0.45	0.43	0.75	-0.45	-1.13	-0.46	-0.45	0.43	
					-0.97	-0.38	-0.41	0.34	0.59	-0.38	-0.97	-0.38	-0.41	0.34	
					-1.19	-0.45	-0.46	0.49	0.61	-0.46	-1.19	-0.45	-0.46	0.49	
					-1.36	-0.48	-0.56	0.55	0.65	-0.48	-1.36	-0.48	-0.56	0.55	
					-1.08	-0.42	-0.47	0.42	0.62	-0.42	-1.08	-0.42	-0.47	0.42	
					-0.66	-0.32	-0.32	0.32	0.51	-0.32	-0.66	-0.32	-0.32	0.32	
					-0.01	-0.02	-0.01	0.03	0.12	-0.02	-0.01	-0.02	-0.01	0.03	
					0.00	0.00	0.00	0.00	0.03	0.00	0.00	0.00	0.00	0.00	
					0.00	0.00	0.00	0.00	0.00	0.00	0.00	0.00	0.00	0.00	

Case S.S1 Station= 3
x= 12.7mm Tunnel Run#= 163 Ue/Uo= 0.997 Date= 904.84 Time=20.11
No Bias Correction

LR	y (mm)	U/Uo	V/Uo	W/Uo	normalized by 0.001			normalized by 0.001			normalized by 0.0001			Uot3	Uot3	Uot3				
					uu	vv	ww	uv	vw	uw	uuu	uvv	uww				vu	vuv	vuu	vvv
1	0.25	0.550	-0.005	0.289	10.22	2.47	11.72	-1.31	-0.09	-0.11	-0.27	0.01	1.59	-0.19	-0.07	0.51	-1.66	-0.12	-3.80	0.34
2	0.38	0.587	-0.005	0.295	9.47	2.77	10.55	-1.36	0.04	-1.05	-0.03	-0.05	0.42	0.27	0.11	0.42	-0.59	-0.11	-2.02	0.29
3	0.51	0.624	-0.003	0.292	8.70	3.06	10.43	-1.33	0.43	-2.03	0.30	-0.03	0.25	0.15	0.12	0.23	0.06	-0.15	-1.36	0.10
4	0.63	0.652	-0.004	0.281	8.77	3.27	10.69	-1.30	0.59	-2.04	0.60	-0.13	0.16	0.14	0.13	0.05	0.13	-0.11	-1.32	0.10
5	0.76	0.668	-0.005	0.273	9.27	3.36	10.67	-1.23	0.77	-2.44	0.47	-0.05	0.06	0.27	0.03	0.27	0.23	-0.06	-1.43	0.04
6	1.02	0.698	-0.001	0.262	9.05	3.43	10.77	-1.28	1.12	-2.70	-0.42	-0.15	-0.53	0.36	0.14	0.42	0.43	0.05	-0.43	0.00
7	1.27	0.718	0.000	0.246	8.74	3.66	10.56	-1.17	1.43	-2.85	-0.28	-0.25	-1.06	0.36	0.28	0.56	0.88	0.26	0.66	-0.20
8	1.52	0.734	0.000	0.233	8.87	3.70	10.44	-1.28	1.62	-2.91	-0.97	-0.37	-1.36	0.55	0.38	0.68	1.33	0.47	1.18	-0.31
9	1.78	0.745	0.002	0.221	8.73	3.83	10.49	-1.25	1.71	-3.23	-1.14	-0.42	-1.26	0.72	0.39	0.87	1.32	0.64	1.44	-0.47
10	2.03	0.754	0.001	0.210	8.57	3.76	10.17	-1.27	1.77	-2.90	-1.08	-0.51	-1.54	0.70	0.60	1.07	1.27	0.75	2.14	-0.47
11	2.29	0.763	0.002	0.200	8.57	3.82	10.05	-1.51	1.64	-3.37	-2.37	-0.61	-1.97	0.94	0.50	1.12	1.81	0.79	2.66	-0.72
12	2.54	0.765	0.005	0.195	8.13	3.89	9.64	-1.42	1.85	-3.27	-1.57	-0.69	-1.78	0.82	0.62	1.33	1.37	0.87	2.91	-0.73
13	2.79	0.771	0.005	0.188	8.47	4.15	9.40	-1.61	1.91	-3.16	-1.99	-0.61	-1.89	1.04	0.68	1.29	1.69	0.89	2.45	-0.74
14	3.30	0.781	0.005	0.179	8.26	4.17	9.14	-1.54	1.83	-3.25	-2.34	-0.61	-1.67	1.18	0.60	1.26	1.85	0.79	2.39	-0.82
15	3.81	0.787	0.005	0.168	7.46	4.14	8.61	-1.42	1.80	-2.77	-1.39	-0.69	-1.36	0.74	0.57	1.08	1.07	0.87	2.31	-0.54
16	4.32	0.798	0.003	0.157	7.10	4.14	8.44	-1.47	1.72	-2.72	-1.56	-0.57	-1.25	0.75	0.78	1.11	1.29	0.84	2.29	-0.57
17	4.83	0.808	0.003	0.147	6.53	4.00	7.78	-1.38	1.61	-2.44	-1.12	-0.54	-1.09	0.67	0.64	1.00	1.01	0.83	2.02	-0.55
18	5.59	0.813	0.003	0.142	6.42	4.28	7.49	-1.54	1.66	-2.13	-1.21	-0.57	-0.76	0.66	0.60	0.93	0.83	0.83	1.65	-0.45
19	6.35	0.816	0.006	0.136	6.46	4.38	7.19	-1.70	1.74	-2.13	-1.30	-0.63	-0.80	0.72	0.66	1.03	0.85	0.85	1.77	-0.52
20	7.11	0.825	0.005	0.128	5.99	4.32	6.79	-1.50	1.56	-2.03	-1.15	-0.60	-0.79	0.56	0.85	0.69	0.68	0.59	1.65	-0.35
21	8.38	0.829	0.011	0.126	5.09	4.42	6.58	-1.71	1.70	-1.93	-0.98	-0.53	-0.53	0.42	0.80	0.55	0.51	0.58	1.37	-0.35
22	10.16	0.841	0.013	0.116	5.74	4.26	6.42	-1.58	1.55	-1.78	-0.93	-0.39	-0.43	0.33	0.63	0.56	0.37	0.52	1.13	-0.27
23	12.70	0.867	0.013	0.096	5.51	3.94	5.87	-1.60	1.51	-1.64	-1.41	-0.53	-0.66	0.54	0.85	0.73	0.60	0.60	1.59	-0.34
24	15.24	0.893	0.014	0.076	4.66	3.39	5.02	-1.35	1.28	-1.45	-1.30	-0.56	-0.64	0.51	0.82	0.65	0.59	0.65	1.64	-0.35
25	17.78	0.922	0.011	0.053	3.67	2.72	3.84	-0.97	0.85	-1.09	-1.26	-0.53	-0.66	0.49	0.82	0.53	0.53	0.59	1.46	-0.27
26	20.32	0.946	0.012	0.037	2.72	2.21	2.81	-0.67	0.54	-0.81	-1.30	-0.46	-0.63	0.45	0.59	0.44	0.54	0.42	1.14	-0.22
27	22.86	0.959	0.017	0.028	2.11	1.99	2.18	-0.57	0.36	-0.64	-0.97	-0.39	-0.45	0.38	0.46	0.31	0.37	0.30	0.86	-0.17
28	25.40	0.976	0.017	0.019	1.19	1.50	1.32	-0.31	0.22	-0.34	-0.47	-0.20	-0.22	0.19	0.32	0.19	0.21	0.18	0.47	-0.08
29	30.48	0.990	0.014	0.012	0.23	0.73	0.40	-0.02	0.01	-0.08	0.00	0.00	0.00	0.01	0.05	0.01	0.00	0.01	0.01	0.00
30	35.56	0.994	0.014	0.013	0.16	0.57	0.31	0.00	0.00	-0.08	0.00	0.00	0.00	0.00	0.01	0.00	0.00	0.00	0.00	0.00
31	45.72	0.997	0.015	0.014	0.12	0.49	0.28	-0.01	0.01	-0.07	0.00	0.00	0.00	0.00	0.02	0.00	0.00	0.00	0.00	0.00

Table C7. Continued.

Case S.S1			Station= 4		Date= 904.84		Time=20.52													
x= 25.4mm			Tunnel Run# = 164		Ue/Uo= 0.995															
No Bias Correction																				
LR	y(mm)	U/Uo	V/Uo	W/Uo	normalized by 0.001 Uot2			normalized by 0.0001 Uot3												
					uu	uv	vw	uuu	uvv	uuv	uuu	vvv	uvw							
1	0.25	0.562	-0.005	0.248	9.43	2.21	10.20	-1.19	-0.20	0.24	-0.74	0.03	0.50	0.31	-0.08	0.54	-1.14	-0.03	-1.50	0.26
2	0.38	0.591	-0.005	0.252	8.91	2.60	9.60	-1.38	-0.07	-0.54	-0.48	-0.06	0.13	0.20	0.03	0.48	-0.17	0.00	-0.75	0.18
3	0.51	0.619	-0.005	0.250	8.47	2.90	9.62	-1.32	0.02	-1.15	-0.10	-0.05	0.08	0.33	0.13	0.26	-0.11	0.00	-0.75	0.27
4	0.63	0.640	-0.006	0.247	8.57	3.09	9.85	-1.45	0.21	-1.43	0.57	-0.17	0.06	0.22	0.20	0.31	0.00	-0.05	-0.63	0.12
5	0.76	0.657	-0.005	0.243	8.92	3.09	9.73	-1.46	0.46	-1.80	0.49	-0.15	-0.20	0.15	0.22	0.23	0.45	-0.03	-0.76	0.12
6	1.02	0.685	-0.003	0.235	8.33	3.19	10.14	-1.27	0.79	-2.41	0.11	-0.16	-0.03	0.23	0.16	0.26	0.33	0.03	-0.42	0.04
7	1.27	0.707	-0.002	0.231	8.37	3.28	9.46	-1.32	0.92	-2.45	-0.54	-0.24	0.43	0.43	0.25	0.22	0.32	0.15	0.41	0.04
8	1.52	0.723	0.001	0.221	8.22	3.24	9.63	-1.18	1.16	-2.68	-0.69	-0.34	-0.70	0.34	0.43	0.46	0.89	0.28	0.53	-0.14
9	1.78	0.738	0.001	0.211	8.02	3.19	9.57	-1.20	1.32	-2.52	-0.83	-0.37	-1.08	0.59	0.41	0.50	1.03	0.37	1.26	-0.31
10	2.03	0.747	0.000	0.204	8.00	3.49	9.75	-1.09	1.44	-2.75	-1.11	-0.28	-1.14	0.55	0.28	0.64	1.08	0.33	1.26	-0.31
11	2.29	0.759	0.001	0.191	7.71	3.41	9.41	-1.13	1.45	-2.75	-1.48	-0.36	-1.83	0.70	0.51	1.00	1.25	0.59	2.12	-0.42
12	2.54	0.763	0.002	0.191	7.82	3.65	9.55	-1.31	1.67	-2.87	-0.92	-0.39	-1.08	0.65	0.37	0.90	0.97	0.74	1.63	-0.34
13	2.79	0.768	0.002	0.184	7.66	3.58	9.32	-1.28	1.70	-2.88	-1.19	-0.47	-1.37	0.71	0.45	1.09	1.24	0.69	2.31	-0.53
14	3.30	0.778	0.003	0.175	7.37	3.70	8.62	-1.31	1.62	-2.67	-1.44	-0.47	-1.34	0.74	0.57	1.10	1.25	0.69	2.13	-0.49
15	3.81	0.786	0.004	0.166	7.35	3.85	8.11	-1.27	1.69	-2.51	-1.09	-0.54	-1.15	0.70	0.59	0.93	1.00	0.78	1.51	-0.49
16	4.32	0.790	0.005	0.160	6.80	3.96	8.06	-1.38	1.61	-2.54	-1.04	-0.52	-1.02	0.63	0.65	1.07	0.85	0.81	2.36	-0.52
17	4.83	0.794	0.004	0.153	6.78	4.00	7.87	-1.37	1.57	-2.32	-1.33	-0.50	-1.07	0.72	0.63	1.00	0.89	0.77	1.95	-0.46
18	5.59	0.803	0.006	0.146	6.48	3.97	7.35	-1.41	1.55	-2.19	-1.16	-0.50	-0.85	0.55	0.53	0.87	0.66	0.62	1.62	-0.40
19	6.35	0.807	0.007	0.141	6.40	4.20	7.13	-1.59	1.65	-2.10	-1.06	-0.50	-0.62	0.65	0.65	0.77	0.68	0.68	1.55	-0.41
20	7.11	0.815	0.008	0.135	5.88	4.11	6.73	-1.40	1.47	-1.75	-0.72	-0.45	-0.32	0.35	0.65	0.75	0.33	0.65	1.18	-0.30
21	8.38	0.829	0.005	0.122	5.71	4.10	6.30	-1.51	1.48	-1.61	-0.77	-0.30	-0.34	0.32	0.47	0.60	0.50	0.50	0.97	-0.23
22	10.16	0.849	0.004	0.100	5.21	3.66	5.90	-1.39	1.31	-1.56	-0.74	-0.45	-0.47	0.42	0.64	0.57	0.51	0.58	1.45	-0.25
23	12.70	0.872	0.004	0.082	4.69	3.38	5.08	-1.25	1.17	-1.27	-1.00	-0.52	-0.51	0.51	0.78	0.52	0.42	0.42	1.12	-0.23
24	15.24	0.886	0.015	0.078	4.74	3.26	4.98	-1.30	1.13	-1.35	-1.29	-0.53	-0.52	0.46	0.78	0.50	0.53	0.55	1.36	-0.26
25	17.78	0.906	0.018	0.065	4.12	2.94	4.16	-1.13	1.00	-1.20	-1.27	-0.46	-0.49	0.46	0.69	0.50	0.50	0.50	1.24	-0.22
26	20.32	0.925	0.026	0.054	3.83	3.78	3.78	-1.06	0.84	-1.09	-1.44	-0.48	-0.61	0.50	0.63	0.51	0.49	0.40	1.31	-0.24
27	22.86	0.946	0.026	0.038	2.88	2.42	3.01	-0.81	0.63	-0.80	-1.25	-0.44	-0.52	0.43	0.60	0.45	0.44	0.39	1.20	-0.20
28	25.40	0.970	0.020	0.022	1.39	1.54	1.57	-0.44	0.33	-0.47	-0.74	-0.34	-0.38	0.34	0.48	0.33	0.36	0.26	0.73	-0.17
29	30.48	0.988	0.018	0.012	0.30	0.73	0.43	-0.04	0.03	-0.09	-0.02	-0.02	-0.01	0.03	0.08	0.03	0.01	0.01	0.02	0.00
30	35.56	0.993	0.017	0.013	0.15	0.49	0.31	-0.01	0.00	-0.08	0.00	0.00	0.00	0.00	0.02	0.00	0.00	0.00	0.00	0.00
31	45.72	0.995	0.018	0.013	0.11	0.42	0.27	0.00	0.00	-0.07	0.00	0.00	0.00	0.00	0.00	0.00	0.00	0.00	0.00	0.00

Table C7. Continued.

Case S.51			Station= 6		Date= 905.84		Time= 9.08	
x= 76.2mm			Tunnel Run# = 166		Ue/Uo= 0.978			
No Bias Correction								
LR	y (mm)	U/Uo	V/Uo	W/Uo	uu	vv	ww	uv
1	0.25	0.498	-0.002	0.144	8.09	1.68	7.66	-1.02
2	0.38	0.526	-0.002	0.148	7.50	2.01	7.22	-1.00
3	0.51	0.544	-0.000	0.155	7.27	2.31	7.41	-1.17
4	0.63	0.556	-0.000	0.153	7.08	2.47	7.18	-1.15
5	0.76	0.567	-0.001	0.153	6.76	2.44	6.96	-1.19
6	1.02	0.594	0.002	0.155	6.76	2.73	7.21	-1.31
7	1.27	0.613	0.002	0.156	6.62	2.76	7.23	-1.31
8	1.52	0.628	0.003	0.156	6.63	2.78	7.12	-1.31
9	1.78	0.639	0.007	0.158	6.49	2.90	7.19	-1.32
10	2.03	0.657	0.006	0.152	6.50	2.93	7.32	-1.31
11	2.29	0.669	0.008	0.151	6.45	2.98	7.26	-1.28
12	2.54	0.681	0.008	0.149	6.42	3.02	7.51	-1.22
13	2.79	0.689	0.009	0.149	6.30	3.07	7.42	-1.24
14	3.30	0.706	0.011	0.144	6.26	3.08	7.16	-1.10
15	3.81	0.716	0.013	0.141	5.92	3.26	7.21	-1.05
16	4.32	0.728	0.014	0.136	5.98	3.53	6.89	-1.03
17	4.83	0.740	0.014	0.129	5.63	3.41	6.77	-0.99
18	5.59	0.747	0.015	0.128	5.57	3.49	6.84	-1.04
19	6.35	0.752	0.019	0.126	5.66	3.73	6.89	-1.12
20	7.11	0.759	0.019	0.122	5.48	3.80	6.47	-1.19
21	8.38	0.767	0.020	0.116	5.40	3.97	6.39	-1.32
22	10.16	0.776	0.026	0.110	5.56	4.04	6.33	-1.51
23	12.70	0.797	0.030	0.099	5.45	3.81	5.86	-1.52
24	15.24	0.820	0.039	0.085	5.04	3.56	5.49	-1.39
25	17.78	0.839	0.045	0.075	4.79	3.22	4.99	-1.26
26	20.32	0.863	0.051	0.062	4.14	2.98	4.28	-1.22
27	22.86	0.885	0.057	0.053	3.83	2.85	3.79	-1.06
28	25.40	0.902	0.063	0.044	3.31	2.79	3.28	-0.88
29	30.48	0.943	0.062	0.021	1.43	1.75	1.58	-0.42
30	35.56	0.963	0.056	0.011	0.30	0.79	0.46	-0.06
31	40.64	0.972	0.055	0.012	0.15	0.49	0.29	-0.01
32	45.72	0.978	0.053	0.011	0.13	0.47	0.29	-0.01

Table C7. Continued.

Case S.S1			Station= 7		Date= 905.84		Time= 9.58	
x= 101.5mm			Tunnel Run# 167		Ue/Uo= 0.981			
No Bias Correction								
LR	y(mm)	U/Uo	V/Uo	W/Uo	U	V	W	U+V+W
1	0.25	0.382	-0.002	0.119	8.79	1.51	7.48	-0.80
2	0.38	0.407	-0.001	0.124	8.24	1.93	7.05	-0.96
3	0.51	0.428	-0.001	0.129	7.95	2.07	7.29	-0.99
4	0.63	0.443	0.000	0.130	7.76	2.28	6.98	-1.08
5	0.76	0.456	0.002	0.133	7.45	2.44	6.87	-1.11
6	1.02	0.481	0.005	0.136	7.48	2.68	6.67	-1.26
7	1.27	0.499	0.007	0.136	7.71	2.79	6.66	-1.34
8	1.52	0.516	0.008	0.139	7.45	2.83	6.76	-1.36
9	1.78	0.531	0.012	0.137	7.28	2.81	7.19	-1.31
10	2.03	0.544	0.014	0.138	7.22	2.82	7.03	-1.40
11	2.29	0.557	0.017	0.137	6.78	2.93	6.86	-1.29
12	2.54	0.569	0.019	0.138	6.87	2.98	6.92	-1.37
13	2.79	0.582	0.021	0.136	6.99	3.00	7.11	-1.31
14	3.30	0.600	0.024	0.134	6.75	2.94	6.72	-1.32
15	3.81	0.614	0.028	0.134	6.23	2.92	7.01	-1.17
16	4.32	0.629	0.031	0.134	6.29	3.29	7.05	-1.20
17	4.83	0.643	0.034	0.134	6.01	3.28	7.05	-1.00
18	5.59	0.659	0.039	0.129	5.91	3.40	6.92	-1.07
19	6.35	0.671	0.041	0.127	5.70	3.67	6.97	-0.98
20	7.11	0.678	0.047	0.126	5.87	3.77	6.89	-1.08
21	8.38	0.693	0.052	0.122	5.61	4.04	6.50	-1.07
22	10.16	0.704	0.061	0.119	5.39	4.16	6.48	-1.25
23	12.70	0.727	0.067	0.106	5.70	4.40	6.23	-1.57
24	15.24	0.748	0.078	0.096	5.62	4.11	6.07	-1.50
25	17.78	0.774	0.087	0.085	5.61	3.87	5.63	-1.58
26	20.32	0.801	0.095	0.076	5.27	3.64	5.22	-1.43
27	22.86	0.823	0.107	0.065	5.11	3.45	4.83	-1.44
28	25.40	0.858	0.110	0.051	4.24	3.29	4.03	-1.30
29	30.48	0.916	0.110	0.021	1.72	1.93	1.68	-0.56
30	35.56	0.949	0.110	0.013	0.49	1.12	0.65	-0.12
31	40.64	0.967	0.107	0.010	0.22	0.73	0.34	-0.02
32	45.72	0.981	0.101	0.010	0.14	0.65	0.30	-0.01

normalized by 0.001			normalized by 0.0001			normalized by 0.0001		
U+V+W	U+V	U+V+W	U+V+W	U+V	U+V+W	U+V+W	U+V	U+V+W
0.93	0.14	0.93	0.35	0.19	0.06	0.05	-0.28	0.02
0.18	-0.22	0.37	0.25	-0.09	0.30	-0.24	0.02	-0.87
0.04	-0.10	0.41	0.27	-0.04	0.16	-0.27	0.04	-0.43
0.08	-0.11	0.18	0.25	0.13	0.06	-0.06	-0.03	-0.12
-0.01	-0.18	0.09	0.24	0.10	0.28	-0.28	0.03	-0.20
-0.35	-0.25	0.03	0.14	0.16	0.26	-0.05	-0.05	-0.49
-0.56	-0.12	0.48	0.27	0.15	0.16	-0.29	0.04	-0.74
-0.70	-0.09	0.25	0.27	0.15	0.24	-0.05	-0.01	-0.63
-0.79	0.01	0.27	0.22	0.21	0.14	-0.14	-0.13	-0.12
-0.84	0.13	0.09	0.20	0.17	0.25	0.03	0.06	-0.11
-1.05	0.20	0.16	0.29	0.27	0.19	0.08	0.07	-0.24
-1.14	0.19	0.13	0.27	0.23	0.15	-0.10	0.01	-0.44
-1.30	0.37	0.17	0.14	0.27	0.25	0.17	0.01	-0.28
-1.30	0.43	-0.19	0.08	0.36	0.24	0.33	0.07	-0.10
-1.52	0.58	-0.11	0.05	0.31	0.06	0.11	0.38	-0.19
-1.48	0.65	-0.17	0.18	0.42	0.11	0.23	0.43	0.11
-1.42	0.83	-0.15	0.05	0.34	0.08	0.17	0.10	0.14
-1.47	1.06	-0.12	0.15	0.32	0.14	0.31	0.28	0.23
-1.64	1.26	-0.07	0.07	0.35	0.11	0.22	0.09	0.22
-1.38	1.33	-0.07	0.00	0.17	0.16	0.25	0.22	0.33
-1.31	1.53	-0.01	0.27	0.10	0.27	0.19	0.02	0.33
-1.53	1.58	-0.09	0.18	0.05	0.38	0.27	0.12	0.36
-1.50	1.54	-0.64	-0.16	0.19	0.41	0.51	0.20	0.49
-1.47	1.40	-0.94	-0.38	0.33	0.70	0.52	0.37	0.48
-1.31	1.21	-1.18	-0.34	0.52	0.49	0.51	0.40	0.42
-1.34	1.11	-1.44	-0.46	0.64	0.46	0.56	0.44	0.41
-1.24	0.94	-1.49	-0.50	0.69	0.58	0.67	0.61	0.47
-0.49	0.38	-0.94	-0.40	0.41	0.40	0.51	0.34	0.32
-0.14	0.10	-0.05	-0.03	0.06	0.16	0.08	0.03	0.07
-0.09	0.01	0.00	0.00	0.01	0.03	0.01	0.00	0.01
-0.09	0.01	0.00	0.00	0.00	0.01	0.00	0.00	0.00

Case S.S1 Station= 8
x= 111.8mm Tunnel Run# = 168 Ue/Uo= 0.982 Date= 905.84 Time=11.03
No Bias Correction

63

Table C7. Continued.

Case S.S1		Station= 9	Date= 822.84		Time=15.58	
x= 115.9mm		Tunnel Run#= 155	Ue/Uo= 0.969			
No Bias Correction						
LR	y(mm)	U/Uo	V/Uo	Uot2	Uot3	Uot4
1	0.38	0.257	0.000	2.04	-1.52	0.61
2	0.51	0.278	0.002	2.43	-1.62	0.22
3	0.63	0.296	0.004	2.50	-1.73	-0.17
4	0.76	0.312	0.006	2.77	-1.82	-0.32
5	1.02	0.327	0.010	2.82	-1.69	-0.61
6	1.27	0.352	0.012	2.92	-1.81	-0.68
7	1.52	0.373	0.016	2.99	-1.80	-1.02
8	1.78	0.391	0.018	3.00	-1.77	-0.84
9	2.03	0.404	0.025	3.03	-1.78	-1.52
10	2.29	0.430	0.026	3.06	-1.91	-1.68
11	2.54	0.438	0.029	2.91	-1.86	-2.10
12	2.79	0.457	0.033	3.15	-1.95	-1.53
13	3.30	0.477	0.036	3.00	-1.85	-1.66
14	3.81	0.498	0.044	2.89	-1.84	-1.82
15	4.32	0.516	0.050	2.95	-1.82	-2.06
16	4.83	0.537	0.055	2.90	-1.60	-0.97
17	5.59	0.563	0.064	2.99	-1.59	-0.99
18	6.35	0.583	0.070	2.98	-1.52	-0.94
19	7.11	0.594	0.076	3.20	-1.44	-0.98
20	8.38	0.620	0.085	3.18	-1.29	-0.54
21	10.16	0.645	0.093	3.57	-1.43	-0.40
22	12.70	0.673	0.101	3.58	-1.49	-0.69
23	15.24	0.699	0.112	3.63	-1.71	-0.76
24	17.78	0.729	0.120	3.28	-1.71	-1.61
25	20.32	0.760	0.128	2.85	-1.45	-1.67
26	22.86	0.796	0.138	2.57	-1.39	-2.19
27	25.40	0.830	0.146	1.96	-1.07	-1.79
28	27.94	0.862	0.154	1.73	-0.83	-1.58
29	30.48	0.885	0.157	1.29	-0.58	-1.08
30	33.02	0.901	0.161	1.10	-0.46	-0.79
31	35.56	0.924	0.162	0.91	-0.34	-0.45
32	38.10	0.946	0.162	0.81	-0.24	-0.20
33	40.64	0.960	0.157	0.53	-0.13	-0.04
35	45.72	0.982	0.146	0.28	-0.07	-0.01
36	50.80	0.994	0.133	0.21	-0.05	-0.01
37	55.88	1.011	0.118	0.18	-0.03	0.00

Table C7. Continued.

Case S.S1		Station= 10		Date= 822.84		Time=15.02				
x= 122.2mm		Tunnel Run# = 154		Ue/Uo= 0.973						
No Bias Correction										
LR	y(mm)	U/Uo	V/Uo	<-- .001 Uot2 --	<-- .0001 Uot3 -->	uuu	uvv	uuu	vvv	
1	0.38	0.149	0.001	12.64	1.90	-1.17	1.78	0.32	-0.48	0.33
2	0.51	0.176	0.002	12.90	2.27	-1.41	-0.18	0.23	-0.28	-0.23
3	0.63	0.194	0.004	12.79	2.65	-1.49	-0.97	0.20	-0.01	-0.27
4	0.76	0.208	0.008	13.29	2.81	-1.52	-1.73	0.07	0.00	-0.10
5	1.02	0.234	0.010	13.94	3.24	-1.78	-1.08	0.07	-0.15	-0.06
6	1.27	0.254	0.013	13.73	3.31	-1.91	-1.02	0.24	-0.39	-0.12
7	1.52	0.280	0.018	13.66	3.41	-1.82	-2.00	-0.06	0.14	-0.02
8	1.78	0.295	0.022	13.48	3.56	-2.03	-3.33	-0.26	0.81	0.04
9	2.03	0.319	0.028	13.24	3.49	-1.95	-2.61	-0.36	0.42	0.18
10	2.29	0.321	0.034	13.02	3.55	-1.99	-2.67	-0.37	0.34	0.25
11	2.54	0.351	0.034	13.03	3.54	-2.04	-2.90	-0.25	0.37	0.24
12	2.79	0.365	0.039	12.36	3.57	-2.05	-2.83	-0.28	0.53	0.02
13	3.30	0.392	0.046	12.44	3.54	-2.08	-3.43	-0.45	0.61	0.29
14	3.81	0.415	0.055	11.11	3.48	-2.06	-2.43	-0.36	0.51	0.42
15	4.32	0.438	0.062	11.10	3.24	-2.18	-3.76	-0.47	0.86	0.31
16	4.83	0.465	0.069	9.83	3.23	-1.96	-2.82	-0.41	0.68	0.37
17	5.59	0.493	0.079	9.31	3.09	-1.96	-2.88	-0.43	0.70	0.27
18	6.35	0.520	0.088	8.15	2.95	-1.74	-1.88	-0.29	0.56	0.22
19	7.11	0.539	0.096	7.58	2.98	-1.64	-1.80	-0.35	0.85	0.31
20	8.38	0.567	0.108	7.05	3.14	-1.47	-1.00	-0.20	0.61	0.34
21	10.16	0.600	0.120	6.16	3.42	-1.51	-0.51	-0.17	0.49	0.35
22	12.70	0.632	0.133	5.76	3.57	-1.57	-0.68	-0.23	0.45	0.64
23	15.24	0.665	0.143	6.04	3.60	-1.74	-0.84	-0.44	0.47	0.68
24	17.78	0.697	0.155	5.63	3.46	-1.65	-0.90	-0.49	0.53	0.90
25	20.32	0.734	0.166	5.46	3.09	-1.64	-1.45	-0.61	0.81	0.85
26	22.86	0.770	0.174	4.99	2.73	-1.45	-1.60	-0.66	0.70	0.82
27	25.40	0.803	0.182	4.55	2.33	-1.32	-2.17	-0.63	0.84	0.67
28	27.94	0.833	0.189	3.67	2.02	-0.95	-1.83	-0.55	0.70	0.57
29	30.48	0.868	0.192	2.58	1.59	-0.75	-1.40	-0.47	0.55	0.45
30	33.02	0.897	0.196	1.75	1.20	-0.57	-0.98	-0.35	0.41	0.33
31	35.56	0.926	0.196	1.22	0.98	-0.39	-0.57	-0.19	0.24	0.24
32	38.10	0.943	0.194	0.85	0.84	-0.31	-0.29	-0.15	0.16	0.23
33	40.64	0.961	0.189	0.53	0.61	-0.17	-0.06	-0.08	0.08	0.20
35	45.72	0.987	0.174	0.29	0.29	-0.06	0.00	0.00	0.01	0.02

Table C7. Continued.

Case S.S1		Station= 11		Tunnel Run#= 153		Ue/Uo= 0.981		Date= 822.84		Time=14.31	
x= 128.6mm											
No Bias Correction											
LR	y(mm)	U/Uo	V/Uo	uu	uv	uuu	uvv	uuu	uvv	uuu	vvv
1	0.38	0.067	0.001	12.24	1.95	-0.89	2.83	0.51	-0.90	0.51	-0.55
2	0.51	0.076	0.003	13.31	2.29	-0.90	2.28	0.33	-0.65	0.33	-0.62
3	0.63	0.088	0.003	14.55	2.51	-0.88	2.67	0.33	-0.71	0.33	-0.49
4	0.76	0.098	0.003	15.01	2.88	-1.09	0.74	0.34	-0.70	0.34	-0.48
5	1.02	0.114	0.007	16.44	3.49	-1.31	-0.27	0.32	-0.91	-0.41	-0.41
6	1.27	0.132	0.013	17.03	3.62	-1.12	-0.05	0.34	-0.78	-0.24	-0.43
7	1.52	0.161	0.016	17.73	3.89	-1.41	-3.15	0.11	-0.44	-0.43	0.04
8	1.78	0.169	0.021	18.22	4.00	-1.36	-3.55	-0.09	-0.61	0.04	0.07
9	2.03	0.185	0.026	17.92	4.19	-1.31	-3.42	-0.03	-0.35	0.07	0.08
10	2.29	0.209	0.031	17.98	4.24	-1.68	-4.41	0.01	-0.33	0.04	0.07
11	2.54	0.234	0.032	18.54	4.44	-1.71	-5.77	-0.21	-0.41	0.04	0.08
12	2.79	0.252	0.038	17.05	4.56	-1.92	-5.39	-0.49	0.33	0.04	0.32
13	3.30	0.277	0.047	16.89	4.39	-1.91	-6.41	-0.49	0.00	0.08	0.21
14	3.81	0.306	0.055	16.10	4.29	-1.85	-5.24	-0.53	-0.10	0.32	0.32
15	4.32	0.332	0.066	15.50	4.23	-2.02	-5.06	-0.64	0.26	0.21	0.41
16	4.83	0.355	0.076	14.83	4.09	-2.30	-7.26	-0.77	0.81	0.41	0.49
17	5.59	0.391	0.089	13.17	3.80	-1.92	-4.38	-0.47	0.54	0.32	0.49
18	6.35	0.420	0.103	12.11	3.64	-1.84	-4.35	-0.57	0.58	0.32	0.45
19	7.11	0.440	0.115	11.25	3.57	-1.95	-4.70	-0.49	0.50	0.30	0.24
20	8.38	0.480	0.133	9.79	3.44	-1.90	-2.66	-0.23	0.55	0.42	0.13
21	10.16	0.527	0.154	7.76	3.34	-1.75	-1.77	-0.16	0.42	0.27	0.31
22	12.70	0.576	0.175	6.58	3.62	-1.55	-0.76	-0.03	0.21	0.53	0.62
23	15.24	0.609	0.191	6.20	3.76	-1.73	-0.29	-0.08	0.43	0.35	0.79
24	17.78	0.648	0.204	6.30	3.91	-2.01	-0.76	-0.32	0.43	0.35	0.80
25	20.32	0.682	0.218	6.51	3.86	-2.06	-0.98	-0.35	0.35	0.62	0.79
26	22.86	0.727	0.220	5.95	3.33	-2.03	-1.43	-0.66	0.70	0.86	0.80
27	25.40	0.767	0.225	5.23	2.82	-1.71	-2.02	-0.70	0.75	0.59	0.63
28	27.94	0.809	0.229	4.37	2.31	-1.33	-2.06	-0.69	0.61	0.63	0.60
29	30.48	0.847	0.235	3.35	1.91	-1.01	-1.71	-0.55	0.61	0.46	0.17
30	33.02	0.878	0.239	2.91	1.83	-1.01	-1.62	-0.58	0.71	0.05	0.01
31	35.56	0.904	0.239	2.35	1.55	-0.86	-1.38	-0.56	0.62	0.01	0.00
32	38.10	0.934	0.235	1.57	1.43	-0.67	-0.80	-0.42	0.48	0.30	0.45
33	40.64	0.959	0.227	1.02	1.06	-0.43	-0.48	-0.25	0.30	0.05	0.17
34	43.18	0.994	0.203	0.38	0.47	-0.12	-0.02	-0.05	0.01	0.01	0.01
35	45.72	0.994	0.203	0.38	0.47	-0.12	-0.02	-0.05	0.01	0.01	0.01
36	50.80	1.017	0.181	0.28	0.26	-0.07	-0.01	-0.01	0.01	0.01	0.01
37	55.88	1.035	0.156	0.22	0.20	-0.05	-0.01	-0.01	0.01	0.01	0.01

Table C7. Continued.

Case S.S1		Station= 12		Date= 822.84		Time=14.09							
x= 134.9mm		Tunnel Run# = 152		Ue/Uo= 1.002									
No Bias Correction													
LR	y(mm)	U/Uo	V/Uo	uu	uv	uvv	uuu	uvv	uuu	Uot3	Uot3	Uot3	Uot3
1	0.38	0.011	0.002	11.30	1.86	-0.32	2.82	0.18	-0.24	0.18	0.34	0.34	0.34
2	0.51	0.018	0.004	12.98	2.38	-0.42	4.03	0.39	-0.76	0.39	0.42	0.42	0.42
3	0.63	0.019	0.005	14.03	2.67	-0.25	3.79	0.19	-0.35	0.19	0.41	0.41	0.41
4	0.76	0.022	0.005	14.15	3.00	-0.42	4.03	0.33	-0.66	0.33	0.49	0.49	0.49
5	1.02	0.032	0.008	14.96	3.32	-0.43	3.87	0.47	-0.82	0.47	0.61	0.61	0.61
6	1.27	0.043	0.010	16.14	3.92	-0.69	4.88	0.63	-0.72	0.63	0.75	0.75	0.75
7	1.52	0.054	0.013	17.27	4.16	-0.68	5.20	0.46	-1.19	0.46	0.84	0.84	0.84
8	1.78	0.068	0.016	20.11	4.56	-0.84	5.05	0.53	-1.43	0.53	0.74	0.74	0.74
9	2.03	0.089	0.020	19.63	4.70	-0.81	2.62	0.49	-1.21	0.49	0.84	0.84	0.84
10	2.29	0.101	0.022	20.75	5.08	-0.93	1.37	0.43	-1.30	0.43	0.94	0.94	0.94
11	2.54	0.117	0.025	21.40	5.08	-1.08	0.54	0.43	-0.94	0.43	0.94	0.94	0.94
12	2.79	0.139	0.030	21.19	5.10	-1.24	-1.63	-0.16	-1.42	-0.16	0.21	0.21	0.21
13	3.30	0.176	0.043	22.05	5.34	-1.43	-4.73	-0.32	-0.68	-0.32	0.26	0.26	0.26
14	3.81	0.220	0.048	23.34	5.47	-1.53	-10.82	-0.83	-1.05	-0.83	0.01	0.01	0.01
15	4.32	0.241	0.060	21.88	5.47	-1.57	-8.75	-0.62	-0.42	-0.62	0.03	0.03	0.03
16	4.83	0.272	0.071	20.90	5.18	-1.67	-10.61	-0.81	-0.33	-0.81	0.03	0.03	0.03
17	5.59	0.301	0.084	21.25	5.04	-1.71	-14.02	-1.06	0.51	-1.06	0.10	0.10	0.10
18	6.35	0.329	0.099	18.92	4.90	-1.85	-13.28	-1.22	1.00	-1.22	0.43	0.43	0.43
19	7.11	0.371	0.112	16.18	4.51	-2.03	-8.37	-0.83	0.80	-0.83	0.44	0.44	0.44
20	8.38	0.415	0.136	13.57	4.03	-1.74	-5.13	-0.47	0.45	-0.47	0.48	0.48	0.48
21	10.16	0.461	0.167	12.07	3.75	-1.75	-6.81	-0.48	0.40	-0.48	0.27	0.27	0.27
22	12.70	0.520	0.204	8.48	3.57	-1.84	-2.13	-0.16	0.50	-0.16	0.27	0.27	0.27
23	15.24	0.569	0.229	7.01	3.82	-1.98	-1.15	-0.11	0.58	-0.11	0.26	0.26	0.26
24	17.78	0.612	0.245	6.75	3.99	-2.14	-0.66	-0.24	0.46	-0.24	0.56	0.56	0.56
25	20.32	0.641	0.273	6.71	4.04	-2.27	-0.70	-0.21	0.30	-0.21	0.46	0.46	0.46
26	22.86	0.684	0.280	6.61	4.01	-2.27	-0.63	-0.27	0.28	-0.27	0.56	0.56	0.56
27	25.40	0.736	0.277	5.46	3.32	-2.02	-1.21	-0.74	0.70	-0.74	0.98	0.98	0.98
28	27.94	0.787	0.285	5.04	2.87	-1.75	-1.89	-0.82	0.96	-0.82	0.78	0.78	0.78
29	30.48	0.833	0.288	4.41	2.49	-1.44	-2.08	-0.73	0.88	-0.73	0.79	0.79	0.79
30	33.02	0.874	0.287	3.46	2.03	-1.17	-1.98	-0.67	0.89	-0.67	0.62	0.62	0.62
31	35.56	0.917	0.284	2.44	1.55	-0.85	-1.29	-0.49	0.59	-0.49	0.53	0.53	0.53
32	38.10	0.951	0.275	1.60	1.14	-0.54	-0.75	-0.27	0.33	-0.27	0.36	0.36	0.36
33	40.64	0.976	0.266	1.09	0.99	-0.41	-0.44	-0.18	0.21	-0.18	0.31	0.31	0.31
35	45.72	1.015	0.236	0.39	0.42	-0.08	0.00	-0.01	0.02	-0.01	0.02	0.02	0.02
37	50.80	1.040	0.205	0.27	0.27	-0.08	-0.01	-0.01	0.01	-0.01	0.01	0.01	0.01
38	55.88	1.061	0.174	0.21	0.20	-0.04	0.00	0.00	0.00	0.00	0.00	0.00	0.00

Table C7. Continued.

Case S.S1		Station= 13	Date= 822.84		Time=13.41	
x= 141.8mm		Tunnel Run#= 151	Ue/Uo= 1.029			
No Bias Correction						
LR	y(mm)	U/Uo	V/Uo	uv	uuu	uvv
1	0.38	-0.044	0.005	1.67	0.40	0.16
2	0.51	-0.053	0.008	2.14	0.92	-0.02
3	0.63	-0.057	0.010	2.34	0.09	-0.25
4	0.76	-0.065	0.011	2.70	0.18	-0.16
5	1.02	-0.064	0.016	3.08	0.10	-0.13
6	1.27	-0.067	0.021	3.54	0.37	-0.24
7	1.52	-0.057	0.025	3.97	0.10	-0.32
8	1.78	-0.049	0.031	4.36	0.40	-0.36
9	2.03	-0.043	0.036	4.75	0.54	-0.45
10	2.29	-0.034	0.040	5.16	0.03	-0.45
11	2.54	-0.024	0.041	5.56	0.03	0.04
12	2.79	-0.011	0.046	5.97	0.22	0.04
13	3.30	0.020	0.057	6.19	0.23	0.06
14	3.81	0.047	0.059	6.58	0.17	-0.23
15	4.32	0.071	0.070	6.97	-0.17	-0.23
16	4.83	0.097	0.073	7.19	-0.40	-0.23
17	5.59	0.143	0.085	7.79	-0.44	-0.03
18	6.35	0.178	0.094	8.89	-1.23	-0.28
19	7.11	0.213	0.104	9.18	-1.81	0.40
20	8.38	0.257	0.125	9.70	-1.39	0.17
21	10.16	0.327	0.159	10.44	-0.11	-0.01
22	12.70	0.393	0.206	11.16	-0.76	0.48
23	15.24	0.451	0.258	11.56	-0.84	0.16
24	17.78	0.507	0.310	13.16	-1.23	0.63
25	20.32	0.558	0.344	13.71	-0.61	0.36
26	22.86	0.612	0.373	13.83	-0.32	0.31
27	25.40	0.682	0.387	13.16	-0.71	0.37
28	27.94	0.752	0.387	13.83	-0.32	0.34
29	30.48	0.817	0.382	13.16	-0.14	0.54
30	33.02	0.869	0.377	13.83	-0.07	0.34
31	35.56	0.906	0.365	13.16	-0.23	0.57
32	38.10	0.962	0.337	13.83	-0.70	0.93
33	40.64	0.995	0.323	13.16	-0.71	0.82
34	43.18	1.043	0.277	13.83	-0.95	1.02
35	45.72	1.070	0.234	13.16	-0.89	0.66
36	48.26	1.088	0.194	13.83	-0.68	0.65
37	50.80			13.16	-0.47	0.36
38	53.34			13.83	-0.04	0.18
39	55.88			13.16	0.00	0.01

Case S.S1 Station= 14
x= 147.6mm Tunnel Run# = 150 Ue/Uo= 1.067 Date= 822.84 Time=13.17
No Bias Correction

LR	y (mm)	U/Uo	V/Uo	uu	vv	uv	uuu	uuv	uu ²	Uot2	—	—	—	—	—	—	—	—	—	—	—	—	—	—	—	—	—	—	—	—	—	—	—	—	—	—	—	—	—	—	—	—	—	—	—	—	—	—	—	—	—	—	—	—	—	—	—	—	—	—	—	—	—	—	—	—	—	—	—	—	—	—	—	—	—	—	—	—	—	—	—	—	—	—	—	—	—	—	—	—	—	—	—	—	—	—	—	—	—	—	—	—	—	—	—	—	—	—	—	—	—	—	—	—	—	—	—	—	—	—	—	—	—	—	—	—	—	—	—	—	—	—	—	—	—	—	—	—	—	—	—	—	—	—	—	—	—	—	—	—	—	—	—	—	—	—	—	—	—	—	—	—	—	—	—	—	—	—	—	—	—	—	—	—	—	—	—	—	—	—	—	—	—	—	—	—	—	—	—	—	—	—	—	—	—	—	—	—	—	—	—	—	—	—	—	—	—	—	—	—	—	—	—	—	—	—	—	—	—	—	—	—	—	—	—	—	—	—	—	—	—	—	—	—	—	—	—	—	—	—	—	—	—	—	—	—	—	—	—	—	—	—	—	—	—	—	—	—	—	—	—	—	—	—	—	—	—	—	—	—	—	—	—	—	—	—	—	—	—	—	—	—	—	—	—	—	—	—	—	—	—	—	—	—	—	—	—	—	—	—	—	—	—	—	—	—	—	—	—	—	—	—	—	—	—	—	—	—	—	—	—	—	—	—	—	—	—	—	—	—	—	—	—	—	—	—	—	—	—	—	—	—	—	—	—	—	—	—	—	—	—	—	—	—	—	—	—	—	—	—	—	—	—	—	—	—	—	—	—	—	—	—	—	—	—	—	—	—	—	—	—	—	—	—	—	—	—	—	—	—	—	—	—	—	—	—	—	—	—	—	—	—	—	—	—	—	—	—	—	—	—	—	—	—	—	—	—	—	—	—	—	—	—	—	—	—	—	—	—	—	—	—	—	—	—	—	—	—	—	—	—	—	—	—	—	—	—	—	—	—	—	—	—	—	—	—	—	—	—	—	—	—	—	—	—	—	—	—	—	—	—	—	—	—	—	—	—	—	—	—	—	—	—	—	—	—	—	—	—	—	—	—	—	—	—	—	—	—	—	—	—	—	—	—	—	—	—	—	—	—	—	—	—	—	—	—	—	—	—	—	—	—	—	—	—	—	—	—	—	—	—	—	—	—	—	—	—	—	—	—	—	—	—	—	—	—	—	—	—	—	—	—	—	—	—	—	—	—	—	—	—	—	—	—	—	—	—	—	—	—	—	—	—	—	—	—	—	—	—	—	—	—	—	—	—	—	—	—	—	—	—	—	—	—	—	—	—	—	—	—	—	—	—	—	—	—	—	—	—	—	—	—	—	—	—	—	—	—	—	—	—	—	—	—	—	—	—	—	—	—	—	—	—	—	—	—	—	—	—	—	—	—	—	—	—	—	—	—	—	—	—	—	—	—	—	—	—	—	—	—	—	—	—	—	—	—	—	—	—	—	—	—	—	—	—	—	—	—	—	—	—	—	—	—	—	—	—	—	—	—	—	—	—	—	—	—	—	—	—	—	—	—	—	—	—	—	—	—	—	—	—	—	—	—	—	—	—	—	—	—	—	—	—	—	—	—	—	—	—	—	—	—	—	—	—	—	—	—	—	—	—	—	—	—	—	—	—	—	—	—	—	—	—	—	—	—	—	—	—	—	—	—	—	—	—	—	—	—	—	—	—	—	—	—	—	—	—	—	—	—	—	—	—	—	—	—	—	—	—	—	—	—	—	—	—	—	—	—	—	—	—	—	—	—	—	—	—	—	—	—	—	—	—	—	—	—	—	—	—	—	—	—	—	—	—	—	—	—	—	—	—	—	—	—	—	—	—	—	—	—	—	—	—	—	—	—	—	—	—	—	—	—	—	—	—	—	—	—	—	—	—	—	—	—	—	—	—	—	—	—	—	—	—	—	—	—	—	—	—	—	—	—	—	—	—	—	—	—	—	—	—	—	—	—	—	—	—	—	—	—	—	—	—	—	—	—	—	—	—	—	—	—	—	—	—	—	—	—	—	—	—	—	—	—	—	—	—	—	—	—	—	—	—	—	—	—	—	—	—	—	—	—	—	—	—	—	—	—	—	—	—	—	—	—	—	—	—	—	—	—	—	—	—	—	—	—	—	—	—	—	—	—	—	—	—	—	—	—	—	—	—	—	—	—	—	—	—	—	—	—	—	—	—	—	—	—	—	—	—	—	—	—	—	—	—	—	—	—	—	—	—	—	—	—	—	—	—	—	—	—	—	—	—	—	—	—	—	—	—	—	—	—	—	—	—	—	—	—	—	—	—	—	—	—	—	—	—	—	—	—	—	—	—	—	—	—	—	—	—	—	—	—	—	—	—	—	—	—	—	—	—	—	—	—	—	—	—	—	—	—	—	—	—	—	—	—	—	—	—	—	—	—	—	—	—	—	—	—	—	—	—	—	—	—	—	—	—	—	—	—	—	—	—	—
----	--------	------	------	----	----	----	-----	-----	-----------------	------	---	---	---	---	---	---	---	---	---	---	---	---	---	---	---	---	---	---	---	---	---	---	---	---	---	---	---	---	---	---	---	---	---	---	---	---	---	---	---	---	---	---	---	---	---	---	---	---	---	---	---	---	---	---	---	---	---	---	---	---	---	---	---	---	---	---	---	---	---	---	---	---	---	---	---	---	---	---	---	---	---	---	---	---	---	---	---	---	---	---	---	---	---	---	---	---	---	---	---	---	---	---	---	---	---	---	---	---	---	---	---	---	---	---	---	---	---	---	---	---	---	---	---	---	---	---	---	---	---	---	---	---	---	---	---	---	---	---	---	---	---	---	---	---	---	---	---	---	---	---	---	---	---	---	---	---	---	---	---	---	---	---	---	---	---	---	---	---	---	---	---	---	---	---	---	---	---	---	---	---	---	---	---	---	---	---	---	---	---	---	---	---	---	---	---	---	---	---	---	---	---	---	---	---	---	---	---	---	---	---	---	---	---	---	---	---	---	---	---	---	---	---	---	---	---	---	---	---	---	---	---	---	---	---	---	---	---	---	---	---	---	---	---	---	---	---	---	---	---	---	---	---	---	---	---	---	---	---	---	---	---	---	---	---	---	---	---	---	---	---	---	---	---	---	---	---	---	---	---	---	---	---	---	---	---	---	---	---	---	---	---	---	---	---	---	---	---	---	---	---	---	---	---	---	---	---	---	---	---	---	---	---	---	---	---	---	---	---	---	---	---	---	---	---	---	---	---	---	---	---	---	---	---	---	---	---	---	---	---	---	---	---	---	---	---	---	---	---	---	---	---	---	---	---	---	---	---	---	---	---	---	---	---	---	---	---	---	---	---	---	---	---	---	---	---	---	---	---	---	---	---	---	---	---	---	---	---	---	---	---	---	---	---	---	---	---	---	---	---	---	---	---	---	---	---	---	---	---	---	---	---	---	---	---	---	---	---	---	---	---	---	---	---	---	---	---	---	---	---	---	---	---	---	---	---	---	---	---	---	---	---	---	---	---	---	---	---	---	---	---	---	---	---	---	---	---	---	---	---	---	---	---	---	---	---	---	---	---	---	---	---	---	---	---	---	---	---	---	---	---	---	---	---	---	---	---	---	---	---	---	---	---	---	---	---	---	---	---	---	---	---	---	---	---	---	---	---	---	---	---	---	---	---	---	---	---	---	---	---	---	---	---	---	---	---	---	---	---	---	---	---	---	---	---	---	---	---	---	---	---	---	---	---	---	---	---	---	---	---	---	---	---	---	---	---	---	---	---	---	---	---	---	---	---	---	---	---	---	---	---	---	---	---	---	---	---	---	---	---	---	---	---	---	---	---	---	---	---	---	---	---	---	---	---	---	---	---	---	---	---	---	---	---	---	---	---	---	---	---	---	---	---	---	---	---	---	---	---	---	---	---	---	---	---	---	---	---	---	---	---	---	---	---	---	---	---	---	---	---	---	---	---	---	---	---	---	---	---	---	---	---	---	---	---	---	---	---	---	---	---	---	---	---	---	---	---	---	---	---	---	---	---	---	---	---	---	---	---	---	---	---	---	---	---	---	---	---	---	---	---	---	---	---	---	---	---	---	---	---	---	---	---	---	---	---	---	---	---	---	---	---	---	---	---	---	---	---	---	---	---	---	---	---	---	---	---	---	---	---	---	---	---	---	---	---	---	---	---	---	---	---	---	---	---	---	---	---	---	---	---	---	---	---	---	---	---	---	---	---	---	---	---	---	---	---	---	---	---	---	---	---	---	---	---	---	---	---	---	---	---	---	---	---	---	---	---	---	---	---	---	---	---	---	---	---	---	---	---	---	---	---	---	---	---	---	---	---	---	---	---	---	---	---	---	---	---	---	---	---	---	---	---	---	---	---	---	---	---	---	---	---	---	---	---	---	---	---	---	---	---	---	---	---	---	---	---	---	---	---	---	---	---	---	---	---	---	---	---	---	---	---	---	---	---	---	---	---	---	---	---	---	---	---	---	---	---	---	---	---	---	---	---	---	---	---	---	---	---	---	---	---	---	---	---	---	---	---	---	---	---	---	---	---	---	---	---	---	---	---	---	---	---	---	---	---	---	---	---	---	---	---	---	---	---	---	---	---	---	---	---	---	---	---	---	---	---	---	---	---	---	---	---	---	---	---	---	---	---	---	---	---	---	---	---	---	---	---	---	---	---	---	---	---	---	---	---	---	---	---	---	---	---	---	---	---	---	---	---	---	---	---	---	---	---	---	---	---	---	---	---	---	---	---	---	---	---	---	---	---	---	---	---	---	---	---	---	---	---	---	---	---	---	---	---	---	---	---	---	---	---	---	---	---	---	---	---	---	---	---	---	---	---	---	---	---	---	---	---	---	---	---	---	---	---	---	---	---	---	---	---	---	---	---	---	---	---	---	---	---	---	---	---	---	---	---	---	---	---	---	---	---	---	---	---	---	---	---	---	---	---	---	---	---	---	---	---	---	---	---	---	---	---	---	---	---	---	---	---	---	---	---	---	---	---

Table C8. LDV measurements for zero pressure gradient, no spin.

[illegible]

Table C8. Continued.

Case Z.50		Station=	Date=		Time=	
x=-12.7mm		2	810.84		12.36	
No Bias Correction		Tunnel Run#	0.994			
		135	Ue/Uo=			
LR	y(mm)	U/Ue	V/Ue	uv	uu	vv
0	0.51	0.567	-0.005	1.53	-1.28	-0.10
1	0.76	0.606	-0.005	1.83	-1.19	-0.14
2	1.02	0.632	-0.004	1.89	-1.07	-0.10
3	1.27	0.654	-0.004	1.94	-1.21	-0.15
4	1.52	0.668	-0.003	1.92	-1.07	-0.48
5	1.78	0.679	-0.002	2.01	-1.32	-0.44
6	2.03	0.697	-0.002	2.06	-1.26	-0.63
7	2.29	0.708	-0.002	1.97	-1.24	-0.50
8	2.54	0.721	-0.002	2.04	-1.25	-0.69
9	2.79	0.731	-0.001	2.10	-1.32	-0.58
10	3.30	0.745	-0.001	1.97	-1.16	-0.59
11	3.81	0.763	0.000	1.94	-1.23	-0.66
12	4.32	0.775	0.000	1.91	-1.20	-0.91
13	4.83	0.790	0.001	1.91	-1.16	-0.69
14	5.59	0.814	0.001	1.83	-1.10	-0.87
15	6.35	0.830	0.002	1.78	-1.04	-0.80
16	7.11	0.856	0.002	1.69	-0.98	-1.04
17	8.38	0.876	0.004	1.50	-0.84	-0.92
18	10.16	0.911	0.004	1.18	-0.60	-0.67
19	12.70	0.957	0.005	0.80	-0.33	-0.53
20	15.24	0.977	0.006	0.53	-0.13	-0.21
21	17.78	0.992	0.006	0.21	0.00	-0.02
22	20.32	0.999	0.006	0.20	0.00	0.00
23	22.86	0.998	0.006	0.19	0.00	0.00
24	25.40	0.997	0.005	0.19	0.00	0.00
25	38.10	1.006	0.000	0.17	0.00	0.00

Table C8. Concluded.

Case Z.50			Station= 3	Date= 807.84 Time=12.50						
x= 304.8mm			Tunnel Run# = 134	Ue/Uo= 1.003						
No Bias Correction										
LR	y (mm)	U/Ue	V/Ue	<— .001 Ue12 —	<— .0001 Ue13 —>	vuv				
1	0.51	0.587	-0.001	7.59	1.63	-1.08	uuu	uvv	vvv	
2	0.76	0.614	0.000	7.25	1.77	-1.07	-0.96	-0.03	0.22	0.00
3	1.02	0.640	0.000	6.72	1.92	-1.11	-0.40	-0.07	0.26	0.10
4	1.27	0.652	0.000	6.53	1.88	-1.12	-0.37	-0.03	0.15	0.07
5	1.52	0.675	0.001	6.38	1.92	-1.04	-0.49	-0.06	0.24	0.07
6	1.78	0.687	0.001	6.03	2.00	-1.13	-0.45	-0.04	0.13	0.05
7	2.03	0.694	0.001	6.20	1.99	-1.04	-0.30	0.02	0.11	0.11
8	2.29	0.701	0.004	6.09	2.01	-1.17	-0.10	-0.03	0.13	-0.04
9	2.54	0.717	0.001	5.59	2.00	-1.08	-0.20	-0.06	0.15	0.09
10	2.79	0.729	0.003	5.89	2.00	-1.18	-0.16	-0.02	0.04	0.03
11	3.30	0.738	0.003	5.57	1.92	-1.00	-0.53	-0.07	0.25	0.10
12	3.81	0.750	0.003	5.25	2.00	-1.07	-0.62	-0.07	0.15	0.10
13	4.32	0.767	0.003	5.10	1.91	-1.12	-0.38	-0.04	0.08	0.05
14	4.83	0.779	0.004	4.94	1.93	-1.19	-0.48	-0.06	0.16	0.04
15	5.59	0.800	0.003	4.90	1.98	-1.09	-0.50	-0.12	0.20	0.10
16	6.35	0.812	0.003	4.33	1.91	-0.98	-0.64	-0.11	0.20	0.02
17	7.11	0.835	0.002	4.29	1.77	-0.93	-0.51	-0.14	0.08	0.14
18	8.38	0.857	0.003	3.76	1.72	-0.93	-0.80	-0.20	0.28	0.13
19	10.16	0.885	0.002	3.11	1.48	-0.72	-0.70	-0.21	0.23	0.18
20	12.70	0.920	0.004	2.41	1.20	-0.61	-0.81	-0.18	0.24	0.13
21	15.24	0.957	0.005	1.48	0.86	-0.38	-0.79	-0.19	0.23	0.16
22	17.78	0.980	0.005	0.79	0.61	-0.18	-0.54	-0.14	0.16	0.14
23	20.32	0.994	0.003	0.30	0.37	-0.06	-0.26	-0.08	0.08	0.07
24	22.86	0.996	0.002	0.14	0.25	-0.01	-0.04	-0.02	0.03	0.05
25	25.40	1.002	0.001	0.12	0.19	0.00	0.00	0.00	0.00	0.02
26	38.10	1.002	-0.002	0.11	0.17	0.00	0.00	0.00	0.00	0.01

Table C9. LDV measurements for forward-facing step, no spin.

Case S.50		Station= 1		Date= 815.84		Time=22.38	
x= -11.1mm		Tunnel Run#= 145		Ue/Uo= 1.000			
No Bias Correction							
LR	y(mm)	U/Uo	V/Uo	<-.001 Uot2 -	<-.0001 Uot3 ->	uuu	uvv
1	0.13	0.501	0.000	11.76	0.00	0.00	0.00
2	0.19	0.538	0.000	10.63	0.00	0.00	0.00
3	0.25	0.550	0.000	9.14	0.00	0.00	0.00
4	0.32	0.572	0.000	8.84	0.00	0.00	0.00
1	0.38	0.570	-0.005	9.87	-2.13	0.00	0.00
2	0.51	0.592	-0.004	8.19	-1.32	0.00	0.00
3	0.63	0.606	-0.003	7.72	-1.14	0.00	0.00
4	0.76	0.620	-0.002	7.35	-0.65	0.00	0.00
5	1.02	0.647	-0.001	6.95	-0.67	0.00	0.00
6	1.27	0.664	0.000	6.56	-0.55	0.00	0.00
7	1.52	0.687	0.001	6.25	-0.63	0.00	0.00
8	1.78	0.701	0.002	6.59	-0.75	0.00	0.00
9	2.03	0.710	0.002	6.35	-0.82	0.00	0.00
10	2.29	0.728	0.002	6.37	-0.79	0.00	0.00
11	2.54	0.731	0.003	5.87	-0.48	0.00	0.00
12	2.79	0.744	0.003	5.64	-0.62	0.00	0.00
13	3.30	0.763	0.003	5.39	-0.82	0.00	0.00
14	3.81	0.778	0.006	5.10	-0.55	0.00	0.00
15	4.32	0.801	0.005	5.00	-0.96	0.00	0.00
16	4.83	0.811	0.006	4.93	-1.02	0.00	0.00
17	5.59	0.834	0.006	4.17	-0.91	0.00	0.00
18	6.35	0.851	0.007	3.97	-1.07	0.00	0.00
19	7.11	0.873	0.008	3.57	-0.90	0.00	0.00
20	8.38	0.902	0.008	2.87	-0.75	0.00	0.00
21	10.16	0.933	0.010	2.04	-0.49	0.00	0.00
22	12.70	0.972	0.011	0.94	-0.25	0.00	0.00
23	15.24	0.990	0.011	0.33	-0.06	0.00	0.00
24	17.78	0.990	0.013	0.21	-0.03	0.00	0.00
25	20.32	0.992	0.013	0.19	-0.03	0.00	0.00
26	22.86	0.992	0.012	0.18	-0.03	0.00	0.00
27	25.40	0.996	0.011	0.17	-0.03	0.00	0.00
28	27.94	0.996	0.009	0.17	-0.03	0.00	0.00
29	30.48	0.996	0.008	0.17	-0.03	0.00	0.00
30	35.56	0.998	0.008	0.16	-0.03	0.00	0.00
31	40.64	0.999	0.010	0.16	-0.03	0.00	0.00
32	45.72	1.000	0.010	0.17	-0.03	0.00	0.00
33	50.80	0.999	0.010	0.20	-0.03	0.00	0.00
34	55.88	1.000	0.011	0.20	-0.03	0.00	-0.01

74

Table C9. Continued.

Case S.50			Station= 3	Date= 815.84			Time=21.44
x= 79.1mm			Tunnel Run# 143	U _e /U _o = 1.009			
No Bias Correction							
LR	y(mm)	U/U _o	V/U _o	uu	uv	uvv	vvv
15	0.13	0.350	0.000	13.88	0.00	0.00	0.00
16	0.19	0.382	0.000	12.45	0.00	0.00	0.00
17	0.25	0.415	0.000	11.92	0.00	0.00	0.00
18	0.32	0.446	0.000	10.36	0.00	0.00	0.00
1	0.38	0.470	0.000	9.96	-1.38	-0.14	-0.09
2	0.51	0.489	0.002	9.23	-1.35	-0.25	0.00
3	0.63	0.502	0.003	8.70	-1.47	-0.51	0.13
4	0.76	0.523	0.004	8.39	-1.42	-0.41	0.16
5	1.02	0.543	0.005	8.42	-1.55	-0.22	0.21
6	1.27	0.560	0.007	8.06	-1.60	-0.12	0.14
7	1.52	0.585	0.006	7.59	-1.46	-0.64	0.13
8	1.78	0.595	0.009	7.84	-1.55	-1.00	0.17
9	2.03	0.614	0.011	7.86	-1.63	-0.93	0.16
10	2.29	0.622	0.011	7.92	-1.63	-0.93	0.09
11	2.54	0.628	0.013	7.71	-1.53	-0.87	0.17
12	2.79	0.643	0.014	7.58	-1.54	-0.85	0.20
13	3.30	0.665	0.016	7.33	-1.57	-1.21	0.19
14	3.81	0.686	0.017	6.77	-1.41	-1.33	0.23
15	4.32	0.707	0.018	6.43	-1.39	-1.55	0.21
16	4.83	0.719	0.022	6.42	-1.38	-1.66	0.21
17	5.59	0.752	0.023	5.61	-1.29	-1.27	0.19
18	6.35	0.768	0.027	5.15	-1.23	-1.35	0.23
19	7.11	0.777	0.030	4.71	-1.08	-1.21	0.21
20	8.38	0.814	0.032	4.17	-1.59	-0.28	0.21
21	10.16	0.847	0.038	3.15	-1.28	-0.77	0.16
22	12.70	0.893	0.045	1.95	-0.91	-0.49	0.14
23	15.24	0.926	0.050	1.05	-0.60	-0.42	0.09
24	17.78	0.944	0.054	0.42	-0.32	-0.07	0.02
25	20.32	0.949	0.057	0.25	-0.21	0.00	0.01
26	22.86	0.959	0.059	0.21	-0.16	0.00	0.00
27	25.40	0.961	0.058	0.18	-0.14	0.00	0.00
28	30.48	0.974	0.057	0.15	-0.11	0.00	0.00
29	35.56	0.984	0.057	0.16	-0.11	0.00	0.00
30	40.64	0.990	0.057	0.15	-0.11	0.00	0.00
31	45.72	0.997	0.057	0.17	-0.14	0.00	0.00
32	50.80	1.006	0.053	0.18	-0.16	0.00	0.00
33	55.88	1.009	0.050	0.17	-0.16	0.00	0.00

Case S.S0 Station= 4
x= 103.2mm Tunnel Run# = 142 Ue/Uo= 1.024 Date= 815.84 Time=21.22
No Bias Correction

LR	y(mm)	U/Uo	V/Uo	uu	vv	uv	uuu	uvv	uuu	uvv	Uot3	→
21	0.13	0.229	0.000	11.88	0.00	0.00	0.00	0.00	0.00	0.00	0.00	vuv
22	0.19	0.230	0.000	10.90	0.00	0.00	0.00	0.00	0.00	0.00	0.00	0.00
23	0.25	0.273	0.000	11.13	0.00	0.00	0.00	0.00	0.00	0.00	0.00	0.00
24	0.32	0.318	0.000	10.98	0.00	0.00	0.00	0.00	0.00	0.00	0.00	0.00
1	0.38	0.330	0.001	11.47	1.64	-1.33	0.49	0.11	0.13	0.13	-0.14	0.00
2	0.51	0.351	0.002	10.61	1.87	-1.31	0.26	0.06	0.30	0.30	-0.08	0.00
3	0.63	0.367	0.003	10.26	2.11	-1.44	-0.15	0.03	0.14	0.14	-0.04	0.00
4	0.76	0.383	0.005	9.55	2.25	-1.44	-0.39	-0.07	0.23	0.23	0.08	0.00
5	1.02	0.410	0.007	9.69	2.44	-1.44	-0.05	-0.10	0.17	0.17	0.13	0.00
6	1.27	0.429	0.010	9.88	2.41	-1.55	0.15	-0.05	0.08	0.08	0.14	0.00
7	1.52	0.443	0.013	9.69	2.58	-1.51	-0.22	-0.06	0.17	0.17	0.09	0.00
8	1.78	0.459	0.014	9.73	2.58	-1.57	-0.88	-0.05	0.32	0.32	0.11	0.00
9	2.03	0.479	0.017	9.76	2.55	-1.65	-0.94	-0.16	0.35	0.35	0.08	0.00
10	2.29	0.493	0.019	9.66	2.55	-1.66	-1.34	-0.19	0.38	0.38	0.13	0.00
11	2.54	0.503	0.020	9.60	2.63	-1.64	-0.70	-0.21	0.30	0.30	0.22	0.00
12	2.79	0.519	0.024	9.65	2.56	-1.56	-1.31	-0.30	0.42	0.42	0.18	0.00
13	3.30	0.542	0.026	9.82	2.62	-1.72	-1.35	-0.12	0.28	0.28	0.12	0.00
14	3.81	0.564	0.031	8.98	2.48	-1.58	-1.10	-0.24	0.41	0.41	0.17	0.00
15	4.32	0.581	0.035	8.96	2.47	-1.54	-1.60	-0.21	0.35	0.35	0.17	0.00
16	4.83	0.599	0.040	8.79	2.38	-1.61	-1.92	-0.21	0.36	0.36	0.16	0.00
17	5.59	0.623	0.044	8.04	2.26	-1.49	-1.79	-0.28	0.30	0.30	0.27	0.00
18	6.35	0.652	0.051	7.44	2.20	-1.37	-1.93	-0.39	0.39	0.39	0.27	0.00
19	7.11	0.678	0.056	6.50	2.07	-1.30	-1.63	-0.34	0.43	0.43	0.21	0.00
20	8.38	0.713	0.062	5.80	1.85	-1.23	-2.15	-0.36	0.54	0.54	0.29	0.00
21	10.16	0.753	0.074	4.48	1.48	-0.94	-1.36	-0.19	0.27	0.27	0.16	0.00
22	12.70	0.801	0.088	3.18	1.21	-0.69	-1.09	-0.18	0.26	0.26	0.15	0.00
23	15.24	0.853	0.099	1.91	0.82	-0.43	-0.83	-0.16	0.21	0.21	0.12	0.00
24	17.78	0.885	0.108	1.00	0.54	-0.24	-0.41	-0.09	0.11	0.11	0.07	0.00
25	20.32	0.905	0.114	0.37	0.31	-0.08	-0.07	-0.02	0.02	0.02	0.03	0.00
26	22.86	0.921	0.118	0.22	0.20	-0.05	0.00	0.00	0.00	0.00	0.01	0.00
27	25.40	0.932	0.119	0.18	0.15	-0.04	0.00	0.00	0.00	0.00	0.00	0.00
28	27.94	0.941	0.118	0.18	0.14	-0.03	0.00	0.00	0.00	0.00	0.00	0.00
29	30.48	0.951	0.117	0.16	0.11	-0.03	0.00	0.00	0.00	0.00	0.00	0.00
30	33.02	0.959	0.116	0.16	0.12	-0.03	0.00	0.00	0.00	0.00	0.00	0.00
31	35.56	0.970	0.114	0.16	0.11	-0.03	0.00	0.00	0.00	0.00	0.00	0.00
32	38.10	0.977	0.112	0.16	0.10	-0.03	0.00	0.00	0.00	0.00	0.00	0.00
33	40.64	0.985	0.111	0.15	0.10	-0.03	0.00	0.00	0.00	0.00	0.00	0.00
34	43.72	0.999	0.106	0.16	0.11	-0.03	0.00	0.00	0.00	0.00	0.00	0.00
35	50.80	1.011	0.099	0.18	0.15	-0.03	0.00	0.00	0.00	0.00	0.00	0.00
36	55.88	1.024	0.090	0.18	0.16	-0.02	0.00	0.00	0.00	0.00	0.00	0.00

Table C9. Continued.

Case S.50			Station= 5	Date= 815.84			Time=20.29
x= 114.6mm			Tunnel Run#= 141	Ue/Uo= 1.040			
No Bias Correction							
LR	y(mm)	U/Uo	V/Uo	uu	uv	uuu	uvv
27	0.13	0.055	0.000	4.19	0.00	0.00	0.00
28	0.19	0.155	0.000	10.06	0.00	0.00	0.00
29	0.25	0.180	0.000	11.10	0.00	0.00	0.00
30	0.32	0.199	0.000	12.20	0.00	0.00	0.00
1	0.38	0.224	0.000	11.59	1.65	0.34	0.19
2	0.51	0.242	0.002	12.27	1.87	0.08	0.20
3	0.63	0.257	0.004	11.99	2.10	-0.48	0.14
4	0.76	0.275	0.006	12.29	2.26	-0.96	0.16
5	1.02	0.294	0.009	11.99	2.67	-0.87	-0.01
6	1.27	0.321	0.011	11.94	2.78	-0.88	-0.07
7	1.52	0.332	0.015	12.25	2.85	-1.64	-0.01
8	1.78	0.352	0.017	12.43	2.89	-1.56	-0.05
9	2.03	0.370	0.020	12.26	3.03	-1.15	-0.04
10	2.29	0.386	0.025	12.49	2.96	-1.47	-0.21
11	2.54	0.399	0.028	12.18	3.00	-2.32	-0.20
12	2.79	0.413	0.032	12.03	2.86	-1.76	-0.16
13	3.30	0.433	0.037	12.86	3.05	-2.84	-0.36
14	3.81	0.466	0.042	11.81	2.84	-2.43	-0.33
15	4.32	0.483	0.049	12.04	2.94	-2.69	-0.24
16	4.83	0.510	0.053	11.34	2.75	-3.15	-0.33
17	5.59	0.534	0.061	10.38	2.68	-2.87	-0.32
18	6.35	0.565	0.068	9.53	2.52	-2.87	-0.34
19	7.11	0.591	0.075	8.96	2.43	-3.19	-0.42
20	8.38	0.617	0.089	8.16	2.26	-2.42	-0.31
21	10.16	0.677	0.102	6.21	1.92	-2.16	-0.35
22	12.70	0.735	0.121	4.74	1.60	-1.79	-0.29
23	15.24	0.789	0.136	3.14	1.14	-1.23	-0.26
24	17.78	0.834	0.149	2.12	0.84	-1.10	-0.19
25	20.32	0.868	0.159	0.96	0.53	-0.40	-0.09
26	22.86	0.895	0.165	0.37	0.31	-0.09	-0.02
27	25.40	0.909	0.168	0.22	0.21	0.00	0.00
28	27.94	0.927	0.169	0.20	0.17	0.00	0.00
29	30.48	0.937	0.166	0.17	0.14	0.00	0.00
30	33.02	0.953	0.163	0.16	0.12	0.00	0.00
31	35.56	0.967	0.159	0.17	0.12	0.00	0.00
32	38.10	0.978	0.156	0.16	0.11	0.00	0.00
33	40.64	0.988	0.150	0.17	0.11	0.00	0.00
34	45.72	1.008	0.141	0.16	0.11	0.00	0.00
35	50.80	1.025	0.128	0.17	0.13	0.00	0.00
36	55.88	1.040	0.116	0.17	0.15	0.00	0.00

Table C9. Continued.

Case S.50		Station= 6	Date= 815.84		Time=20.03	
x= 122.2mm		Tunnel Run#= 140	Ue/Uo= 1.049			
No Bias Correction						
LR	y (mm)	U/Uo	V/Uo	uv	uu	uvv
33	0.13	0.087	0.000	0.00	0.00	0.00
34	0.19	0.116	0.000	0.00	0.00	0.00
35	0.25	0.141	0.000	0.00	0.00	0.00
36	0.32	0.156	0.000	0.00	0.00	0.00
1	0.38	0.167	0.001	0.84	-0.91	-0.14
2	0.51	0.190	0.004	2.10	-1.18	-0.23
3	0.63	0.201	0.004	2.41	-1.32	-0.30
4	0.76	0.212	0.007	2.64	-1.27	-0.26
5	1.02	0.236	0.010	2.95	-1.46	-0.24
6	1.27	0.255	0.014	3.11	-1.45	-0.16
7	1.52	0.277	0.017	3.32	-1.68	-0.22
8	1.78	0.295	0.021	3.40	-1.64	-0.16
9	2.03	0.306	0.025	3.44	-1.61	-0.25
10	2.29	0.328	0.028	3.46	-1.76	-0.23
11	2.54	0.342	0.031	3.45	-1.77	-0.20
12	2.79	0.351	0.035	3.40	-1.67	-0.15
13	3.30	0.381	0.042	3.26	-1.65	-0.29
14	3.81	0.404	0.047	3.40	-1.68	-0.09
15	4.32	0.420	0.054	3.38	-1.78	-0.05
16	4.83	0.451	0.060	3.12	-1.69	-0.28
17	5.59	0.477	0.071	3.07	-1.72	-0.60
18	6.35	0.498	0.082	2.83	-1.49	-0.30
19	7.11	0.523	0.091	2.82	-1.77	-0.48
20	8.38	0.567	0.103	2.60	-1.59	-0.48
21	10.16	0.621	0.121	2.28	-1.34	-0.48
22	12.70	0.680	0.145	2.02	-1.37	-0.38
23	15.24	0.737	0.163	1.47	-0.87	-0.49
24	17.78	0.798	0.179	1.10	-0.68	-0.26
25	20.32	0.840	0.192	0.75	-0.38	-0.35
26	22.86	0.876	0.200	0.61	-0.18	-0.32
27	25.40	0.894	0.203	0.44	-0.18	-0.13
28	27.94	0.917	0.203	0.27	-0.08	-0.06
29	30.48	0.933	0.201	0.17	-0.04	-0.01
30	33.02	0.948	0.197	0.14	-0.04	0.00
31	35.56	0.966	0.192	0.12	-0.04	0.00
32	38.10	0.978	0.186	0.11	-0.02	0.00
33	40.64	0.992	0.179	0.13	-0.02	0.00
34	45.72	1.014	0.165	0.18	-0.03	0.00
35	50.80	1.034	0.150	0.13	-0.03	0.00
36	55.88	1.049	0.132	0.14	-0.02	0.00

Table C9. Continued.

Case S.00			Station= 7	Date= 815.84			Time=19.37
x= 127.3mm			Tunnel Run# = 139	Ue/Uo= 1.065			
No Bias Correction							
LR	y(mm)	U/Uo	V/Uo	uu	uv	uuu	uvv
39	0.13	0.046	0.000	6.86	0.00	0.00	0.00
40	0.19	0.053	0.000	9.45	0.00	0.00	0.00
41	0.25	0.062	0.000	12.17	0.00	0.00	0.00
42	0.32	0.069	0.000	13.07	0.00	0.00	0.00
1	0.38	0.077	0.001	14.88	2.09	1.84	0.27
2	0.51	0.086	0.002	16.26	2.33	1.33	0.08
3	0.63	0.099	0.004	17.77	2.79	0.48	0.02
4	0.76	0.101	0.006	17.98	2.93	0.02	0.05
5	1.02	0.116	0.008	18.42	3.39	-1.18	0.07
6	1.27	0.155	0.012	19.87	3.70	-2.25	-0.05
7	1.52	0.155	0.015	21.56	4.17	-4.38	-0.16
8	1.78	0.177	0.015	21.75	4.36	-6.64	-0.22
9	2.03	0.202	0.022	21.21	4.30	-7.40	-0.38
10	2.29	0.216	0.026	20.24	4.49	-6.81	-0.64
11	2.54	0.235	0.029	20.99	4.46	-6.26	-0.40
12	2.79	0.249	0.031	19.59	4.52	-6.43	-0.47
13	3.30	0.284	0.039	19.05	4.60	-7.54	-0.54
14	3.81	0.307	0.047	18.76	4.38	-7.26	-0.66
15	4.32	0.333	0.054	18.37	4.28	-6.59	-0.72
16	4.83	0.359	0.063	18.13	4.21	-6.06	-0.70
17	5.59	0.394	0.077	17.82	3.79	-6.96	-0.81
18	6.35	0.419	0.087	16.50	3.87	-7.77	-0.82
19	7.11	0.458	0.097	14.71	3.64	-6.99	-0.64
20	8.38	0.489	0.115	14.73	3.36	-7.32	-0.73
21	10.16	0.544	0.140	11.17	2.96	-4.88	-0.55
22	12.70	0.614	0.166	9.07	2.44	-4.61	-0.54
23	15.24	0.681	0.191	6.38	1.87	-2.90	-0.43
24	17.78	0.738	0.213	4.49	1.42	-1.94	-0.27
25	20.32	0.793	0.230	2.99	1.08	-1.58	-0.25
26	22.86	0.836	0.243	1.43	0.72	-0.65	-0.13
27	25.40	0.874	0.251	0.65	0.44	-0.22	-0.06
28	27.94	0.902	0.251	0.27	0.26	-0.01	-0.01
29	30.48	0.920	0.248	0.22	0.20	0.00	0.00
30	33.02	0.940	0.242	0.19	0.14	0.00	0.00
31	35.56	0.963	0.234	0.16	0.12	0.00	0.00
32	38.10	0.981	0.225	0.16	0.11	0.00	0.00
33	40.64	0.998	0.215	0.16	0.11	0.00	0.00
34	45.72	1.026	0.196	0.17	0.11	0.00	0.00
35	50.80	1.046	0.173	0.17	0.13	0.00	0.00
36	55.88	1.065	0.151	0.18	0.16	0.00	-0.01

Table C9. Continued.

Case S.50			Station= 8	Date= 815.84 Time=19.16		
x= 134.9mm			Tunnel Run#= 138	Ue/Uo= 1.085		
No Bias Correction						
LR	y(mm)	U/Uo	V/Uo	uu	uv	vv
57	0.13	0.020	0.000	6.14	0.00	0.00
47	0.19	0.019	0.000	8.08	0.00	0.00
48	0.25	0.016	0.000	10.40	0.00	0.00
49	0.32	0.016	0.000	12.34	0.00	0.00
1	0.38	0.009	0.001	15.12	2.98	-0.35
2	0.51	0.007	0.001	16.50	3.43	-0.83
3	0.63	0.017	0.000	17.26	3.90	-0.28
4	0.76	0.014	0.001	18.20	4.28	-0.54
5	1.02	0.019	0.003	20.19	4.71	-0.61
6	1.27	0.021	0.006	22.16	5.07	-0.37
7	1.52	0.038	0.012	25.98	5.91	-0.50
8	1.78	0.053	0.014	28.05	5.91	-0.33
9	2.03	0.055	0.018	27.22	-4.37	-0.14
10	2.29	0.084	0.021	29.10	-8.86	0.78
11	2.54	0.090	0.027	30.01	-9.07	-0.48
12	2.79	0.108	0.032	32.35	-12.00	1.61
13	3.30	0.140	0.042	30.20	-13.85	2.88
14	3.81	0.162	0.051	31.91	-15.38	3.62
15	4.32	0.206	0.060	30.18	-22.72	0.10
16	4.83	0.223	0.071	30.32	-19.24	4.69
17	5.59	0.275	0.080	26.99	-26.05	4.11
18	6.35	0.318	0.095	23.25	-20.63	4.51
19	7.11	0.339	0.104	22.07	-14.23	3.24
20	8.38	0.387	0.122	20.45	-12.53	2.98
21	10.16	0.447	0.147	17.95	-13.08	1.27
22	12.70	0.524	0.180	14.03	-12.13	1.46
23	15.24	0.597	0.215	10.05	-7.64	1.28
24	17.78	0.658	0.244	7.34	-5.37	0.69
25	20.32	0.721	0.270	4.86	-3.37	0.63
26	22.86	0.774	0.291	3.56	-3.37	0.35
27	25.40	0.831	0.306	1.87	-2.12	0.29
28	27.94	0.874	0.310	0.74	-1.91	0.46
29	30.48	0.911	0.309	0.50	-1.05	0.17
30	33.02	0.942	0.300	0.29	-0.28	0.31
31	35.56	0.970	0.288	0.15	-0.09	0.11
32	38.10	0.992	0.271	0.12	-0.03	0.02
33	40.64	1.013	0.257	0.11	0.00	0.00
34	45.72	1.045	0.227	0.12	0.00	0.00
35	50.80	1.067	0.197	0.15	0.00	0.00
36	55.88	1.085	0.170	0.20	0.00	0.00

Table C9. Continued.

Case S.50		Station= 9	Tunnel Run# = 137		Ue/Uo = 1.108	Date = 815.84	Time = 18.53
x = 141.3mm		No Bias Correction					
LR	y(mm)	U/Uo	V/Uo	uv	uu	uvv	vvv
58	0.13	0.000	0.000	0.00	0.00	0.00	0.00
59	0.19	-0.052	0.000	0.00	0.00	0.00	0.00
60	0.25	-0.091	0.000	0.00	0.00	0.00	0.00
61	0.32	-0.128	0.000	0.00	0.00	0.00	0.00
1	0.38	-0.156	0.020	3.32	-0.90	5.40	-0.29
2	0.51	-0.186	0.028	30.33	4.08	-1.55	12.02
3	0.63	-0.204	0.035	29.62	4.62	-1.89	19.46
4	0.76	-0.220	0.044	28.80	5.29	-2.09	25.87
5	1.02	-0.230	0.056	26.07	6.36	-3.30	26.34
6	1.27	-0.233	0.069	24.09	7.40	-2.89	28.94
7	1.52	-0.223	0.079	25.35	8.67	-4.27	33.69
8	1.78	-0.218	0.087	22.17	9.34	-3.72	27.94
9	2.03	-0.202	0.097	22.94	9.89	-3.96	27.69
10	2.29	-0.188	0.099	22.56	10.23	-3.12	28.37
11	2.54	-0.154	0.106	27.31	10.97	-4.14	35.41
12	2.79	-0.139	0.112	26.71	11.51	-3.80	30.90
13	3.30	-0.089	0.118	30.05	12.26	-3.56	32.13
14	3.81	-0.033	0.128	34.91	13.54	-4.71	24.18
15	4.32	0.029	0.138	34.53	13.12	-4.87	13.77
16	4.83	0.081	0.139	33.94	12.73	-3.81	-0.31
17	5.59	0.186	0.147	31.30	12.29	-6.54	-7.39
18	6.35	0.254	0.146	25.42	10.71	-5.56	-9.21
19	7.11	0.280	0.144	26.02	10.45	-3.86	-11.62
20	8.38	0.340	0.143	24.17	8.53	-2.84	-11.76
21	10.16	0.408	0.153	20.71	7.07	-2.84	-11.76
22	12.70	0.478	0.176	18.33	5.06	-1.95	-10.01
23	15.24	0.532	0.218	14.74	3.82	-1.35	-8.18
24	17.78	0.600	0.259	10.57	2.94	-1.53	-6.01
25	20.32	0.660	0.301	7.91	2.14	-1.37	-4.85
26	22.86	0.722	0.339	5.65	1.60	-1.16	-3.38
27	25.40	0.799	0.366	3.05	1.23	-0.84	-1.37
28	27.94	0.865	0.379	1.50	0.81	-0.47	-0.16
29	30.48	0.918	0.380	0.58	0.47	-0.21	-0.15
30	33.02	0.960	0.368	0.28	0.27	-0.08	-0.02
31	35.56	0.995	0.347	0.21	0.17	-0.03	0.00
32	38.10	1.019	0.324	0.19	0.13	-0.02	0.00
33	40.64	1.042	0.300	0.19	0.13	-0.03	0.00
35	45.72	1.076	0.255	0.18	0.13	-0.03	0.00
36	50.80	1.090	0.215	0.20	0.12	-0.03	0.00
37	55.88	1.108	0.182	0.19	0.15	-0.02	0.00

Table C9. Concluded.

Case S.50			Station= 10		Date= 815.84		Time=18.26	
x= 147.6mm			Tunnel Run# 136		Ue/Uo= 1.135			
No Bias Correction								
LR	y(mm)	U/Uo	V/Uo	uu	uv	uvv	uuu	uvv
75	0.13	-0.304	0.000	14.78	0.00	0.00	0.00	0.00
76	0.19	-0.340	0.000	13.16	0.00	0.00	0.00	0.00
77	0.25	-0.352	0.000	12.13	0.00	0.00	0.00	0.00
78	0.32	-0.360	0.000	11.87	0.00	0.00	0.00	0.00
1	0.38	-0.353	-0.013	10.77	4.55	-0.54	-3.13	-0.04
2	0.51	-0.352	-0.015	10.37	5.70	-0.61	-2.36	-0.45
3	0.63	-0.341	-0.014	10.39	6.60	-0.64	-2.36	-0.32
4	0.76	-0.333	-0.017	9.17	7.10	-0.49	-1.44	-0.42
5	1.02	-0.323	-0.027	9.33	8.19	-0.91	-0.87	-0.56
6	1.27	-0.296	-0.031	8.90	9.03	-0.76	0.27	-0.49
7	1.52	-0.284	-0.042	9.10	9.81	-0.92	0.36	-0.40
8	1.78	-0.265	-0.048	9.27	10.55	-0.49	-0.08	-0.39
9	2.03	-0.248	-0.056	10.08	11.08	-0.78	1.47	-0.17
10	2.29	-0.234	-0.062	10.65	12.49	-0.75	1.15	-0.56
11	2.54	-0.214	-0.071	11.71	12.58	-0.46	2.07	-0.51
12	2.79	-0.196	-0.077	12.42	13.38	0.09	2.49	-0.07
13	3.30	-0.156	-0.087	17.01	14.83	0.34	5.69	0.38
14	3.81	-0.119	-0.096	20.36	16.11	0.83	10.46	1.31
15	4.32	-0.068	-0.102	26.18	16.70	0.81	13.64	1.50
16	4.83	-0.013	-0.099	31.92	17.30	2.37	16.23	0.75
17	5.59	0.060	-0.096	37.44	17.23	3.67	-10.61	-3.09
18	6.35	0.132	-0.085	39.17	16.64	5.33	-27.80	-5.15
19	7.11	0.189	-0.067	38.21	14.85	4.89	-21.75	-4.99
20	8.38	0.264	-0.030	30.06	12.40	4.26	-10.27	-2.55
21	10.16	0.323	0.024	23.63	8.59	2.32	-10.44	-1.80
22	12.70	0.367	0.091	21.40	6.43	0.66	-12.98	-1.67
23	15.24	0.399	0.163	18.97	5.20	0.20	-9.95	-1.33
24	17.78	0.439	0.245	16.46	4.12	-0.41	-7.99	-0.81
25	20.32	0.499	0.336	13.83	3.19	-1.26	-6.17	-0.62
26	22.86	0.586	0.425	11.29	2.81	-1.67	-4.50	-0.64
27	25.40	0.704	0.484	7.42	2.23	-1.70	-2.54	-0.41
28	27.94	0.820	0.501	4.51	1.66	-1.20	-1.10	-0.28
29	30.48	0.929	0.492	2.16	1.11	-0.76	-0.20	-0.11
30	33.02	0.994	0.460	0.74	0.58	-0.30	-0.03	-0.03
31	35.56	1.035	0.420	0.37	0.32	-0.12	0.00	0.00
32	38.10	1.064	0.381	0.24	0.18	-0.05	0.00	0.00
33	40.64	1.087	0.345	0.21	0.14	-0.03	0.00	0.00
34	45.72	1.111	0.282	0.21	0.11	-0.03	0.00	0.00
35	50.80	1.129	0.231	0.19	0.12	-0.02	0.00	0.00
36	55.88	1.135	0.188	0.20	0.14	-0.03	0.00	0.00

REFERENCES

1. Johnston, J. P.: Experimental Studies in Three Dimensional Turbulent Boundary Layers. Report MD-34, Thermosciences Div., Dept. Mechanical Engineering, Stanford Univ., July 1976.
2. Anderson, S.; and Eaton, J.: An Experimental Investigation of Pressure Driven Three-Dimensional Turbulent Boundary Layers. Report MD-49, Thermosciences Div., Dept. Mechanical Engineering, Stanford Univ., June 1987.
3. Elsenaar, A.; and Boelsma, S.: Measurements of the Reynolds Stress Tensor in a Three-Dimensional Turbulent Boundary Layer under Infinite Swept-Wing Conditions. National Aerospace Laboratory, The Netherlands, NRL TR 74095 U, 1974.
4. Muller, U.: Measurements of the Reynolds Stresses and the Mean Flow Field in a Three-Dimensional Pressure Driven Boundary Layer. *J. Fluid Mech.*, vol. 119, June 1982, pp. 121-153.
5. Pontikos, N.; and Bradshaw, P.: The Structure of Three- Dimensional Turbulent Boundary Layers. Ph.D. Thesis, Dept. Aeronautics, Imperial College, London, England, Sept. 1982.
6. Bradshaw, P.; and Pontikos, N.: Measurements in the Turbulent Boundary Layer on an Infinite Swept Wing. *J. Fluid Mech.*, vol. 159, Oct. 1985, pp. 105-130.
7. Furuya, Y.; Nakamura, I.; and Kawachi, H.: The Experiment on the Skewed Boundary Layer on a Rotating Body. *Bull. Japan Society of Mechanical Engineers*, vol. 9, no. 36, 1966, pp. 702-710.
8. Bissonnette, L. R.; and Mellor, G. L.: Experiments on the Behavior of an Axisymmetric Turbulent Boundary Layer with a Sudden Circumferential Strain. *J. Fluid Mech.*, vol. 63, part 2, Apr. 1974, pp. 369-413.
9. Lohmann, R.: The Response of a Developed Turbulent Boundary Layer to Local Transverse Surface Motion. *J. Fluids Engineering*, vol. 98, Sept. 1976, pp. 354-363.
10. Higuchi, H.; and Rubesin, M. W.: An Experimental and Computational Investigation of the Transport of Reynolds Stress in an Axisymmetric Swirling Boundary Layer. AIAA Paper 81-0416, Jan. 1981.
11. Higuchi, H.; and Rubesin, M. W.: Behavior of a Turbulent Boundary Layer Subjected to Sudden Transverse Strain. *AIAA J.*, vol. 17, no. 9, Sept. 1979, pp. 931-941.
12. Nakamura, I.; and Yamashita, S.: Boundary Layers on Bodies of Revolution Spinning in Axial Flows. IUTAM Symposium on Three-Dimensional Turbulent Boundary Layers, Berlin, West Germany, Mar. 29-Apr. 1, 1982.
13. Driver, D. M.; and Hebbar, S. K.: Experimental Study of a Three-Dimensional, Shear-Driven, Turbulent Boundary Layer. *AIAA J.*, vol. 25, no. 1, Jan. 1987, pp. 35-42.

14. Furuya, Y.; Nakamura, I.; Yamashita, S.; and Ishii, T.: Experimental Investigation of the Relatively Thick Turbulent Boundary Layers on a Rotating Cylinder in Axial Flows: 2nd Report, Flows under Pressure Gradients. *Bull. JSME*, vol. 20, no. 140, Feb. 1977, pp. 191-200.
15. Johnston, J.: Measurements in a Three-dimensional Turbulent Boundary Layer Induced by a Swept, Forward-Facing Step. *J. Fluid Mech.*, vol. 42, part 4, May 1970, pp. 823-844.
16. Driver, D. M.; and Hebbar, S. K.: Three-Dimensional, Shear-Driven, Boundary-Layer Flow with Streamwise Adverse Pressure Gradient. *AIAA J.*, vol. 27, no. 12, Dec. 1989, pp. 1689-1697.
17. Hebbar, S. K.; and Driver, D. M.: A Three-Dimensional Turbulent Boundary Layer Undergoing Transverse Strain and Streamwise Pressure Gradient. NASA TM-86768, 1985.
18. Wilcox, D. C.: Recent Improvements to the Spinning Body Version of the EDDYBL Computer Program. Report DCW-R-24-01, DCW Industries Inc., Studio City, CA, Nov. 1979.
19. Launder, B. E.; Reece, G. J.; and Rodi, W.: Progress in the Development of a Reynolds-Stress Turbulence Closure. *J. Fluid Mech.*, vol. 68, part 3, Apr. 1975, pp. 537-566.
20. Wilcox, D. C.; and Rubesin, M. W.: Progress in Turbulence Modeling for Complex Flow Fields Including Effects of Compressibility. NASA TP-1517, 1980.
21. Jones, W. P.; and Launder, B. E.: The Prediction of Laminarization with a 2-Equation Model of Turbulence. *International Journal of Heat and Mass Transfer*, vol. 15, Feb. 1972, pp. 301-314.
22. Cebeci, T.: Calculation of Three-Dimensional Boundary Layers I. Swept Infinite Cylinders and Small Cross Flow. *AIAA J.*, vol. 12, no. 6, June 1974, pp. 779-786.
23. Simpson, R.; Chew, Y.; and Shivaprasad, B.: The Structure of a Separating Turbulent Boundary Layer. Part 1. Mean Flow and Reynolds Stresses. *J. Fluid Mech.*, vol. 113, Dec. 1981, pp. 23-51.
24. Yanta, W. J.: A Three-Dimensional Laser Doppler Velocimeter for Use in Wind Tunnels. IEEE Publication 79CH 1500-8 AES, Sept. 1979.
25. Ausherman, D. W.; and Yanta, W. J.: The 3-D Turbulent Transport Properties in the Boundary Layers of Conical Body Configurations at Mach 3. AIAA Paper 84-1528, June 1984.
26. Meyers, J. F., ed.: Proceedings of the International Symposium on Applications of Laser Doppler Anemometry to Fluid Mechanics. Lisbon, Portugal, July 5-7, 1982.
27. Orloff, K. L.; and Snyder, P. K.: Laser Velocimetry in the Low-Speed Wind Tunnels at Ames Research Center. NASA TM-85855, 1984.
28. Bell, J.; Rodman, L.; and Mehta, R.: Aspects of the Design and Performance of a 3-Component LDV System. 11th ICIASF Meeting on Instrumentation, Stanford University, Aug. 1985.

29. Acharya, M.: Effects of Compressibility on Boundary-Layer Turbulence. AIAA Paper 76-334, July 1976.
30. Bradshaw, P.: Effects of Streamline Curvature on Turbulent Flow. NATO, AGARDograph No. 169, Aug. 1973.

REPORT DOCUMENTATION PAGEForm Approved
OMB No. 0704-0188

Public reporting burden for this collection of information is estimated to average 1 hour per response, including the time for reviewing instructions, searching existing data sources, gathering and maintaining the data needed, and completing and reviewing the collection of information. Send comments regarding this burden estimate or any other aspect of this collection of information, including suggestions for reducing this burden, to Washington Headquarters Services, Directorate for Information Operations and Reports, 1215 Jefferson Davis Highway, Suite 1204, Arlington, VA 22202-4302, and to the Office of Management and Budget, Paperwork Reduction Project (0704-0188), Washington, DC 20503.

1. AGENCY USE ONLY (Leave blank)		2. REPORT DATE December 1991	3. REPORT TYPE AND DATES COVERED Technical Memorandum	
4. TITLE AND SUBTITLE Three-Dimensional Turbulent Boundary Layer Flow over a Spinning Cylinder			5. FUNDING NUMBERS 505-60-11	
6. AUTHOR(S) David M. Driver and Sheshagiri K. Hebber (Naval Postgraduate School, Monterey, California)				
7. PERFORMING ORGANIZATION NAME(S) AND ADDRESS(ES) Ames Research Center Moffett Field, CA 94035-1000			8. PERFORMING ORGANIZATION REPORT NUMBER A-89258	
9. SPONSORING/MONITORING AGENCY NAME(S) AND ADDRESS(ES) National Aeronautics and Space Administration Washington, DC 20546-0001			10. SPONSORING/MONITORING AGENCY REPORT NUMBER NASA TM-102240	
11. SUPPLEMENTARY NOTES Point of Contact: David M. Driver, Ames Research Center, MS 229-1, Moffett Field, CA 94035-1000 (415) 604-5396 or FTS 464-5396				
12a. DISTRIBUTION/AVAILABILITY STATEMENT Unclassified-Unlimited Subject Category - 34			12b. DISTRIBUTION CODE	
13. ABSTRACT (Maximum 200 words) <p>Two sets of experiments are reported for a three-dimensional turbulent boundary-layer flow over a spinning cylinder, with and without a pressure gradient, which was produced by a forward-facing-step obstruction. Additional measurements are reported for two-dimensional flow over the same cylinder (non-spinning), with and without a pressure gradient. The data are presented in tables. The cylinder, which is axially aligned with the flow, contains three sections: an upstream stationary section, a central spinning section (where the flow develops a lateral component), and a downstream stationary section (where the flow's lateral component decays). Measurements were acquired primarily on the downstream stationary section and include all 3 components of mean velocity, all 6 Reynolds stresses, and 10 triple-velocity-product correlations. Surface pressure and skin friction were also measured. The data indicate that Reynolds shear stress is not simply proportional to mean-flow strain rate and that significant anisotropies develop in eddy viscosities. Also, the streamwise pressure gradient is seen to alter streamwise velocity and Reynolds stress without significantly affecting transverse velocity and Reynolds stress. Calculations using a Reynolds-stress-equation model predict the mean flow reasonably well.</p>				
14. SUBJECT TERMS Three-dimensional boundary layer, Turbulence, Pressure gradient			15. NUMBER OF PAGES 86	
			16. PRICE CODE A05	
17. SECURITY CLASSIFICATION OF REPORT Unclassified	18. SECURITY CLASSIFICATION OF THIS PAGE Unclassified	19. SECURITY CLASSIFICATION OF ABSTRACT Unclassified	20. LIMITATION OF ABSTRACT	